CAPE BABOON CYTOCHROME P450 11β-HYDROXYLASES: THE CHARACTERIZATION OF TWO FUNCTIONAL ENZYMES

by

Natasja Brown

Dissertation presented in partial fulfillment of the requirements for the Degree of Doctor of Philosophy (Biochemistry) at the University of Stellenbosch

Supervisor: Dr. A. C. Swart

Co-Supervisor: Prof. P. Swart

March 2007

DECLARATION

I, the undersigned, hereby declare that the work contained in this dissertation is my own original work and that I have not previously in its entirety or in part submitted it at any university for a degree.

…….. ……..

Signature Date

SUMMARY

This study:

1. Describes the localization of CYP11B1 in the Cape baboon adrenal gland using Western blot analysis. CYP11B1 was localized to the adrenal cortex and medulla.

2. Describes the catalytic activity of CYP11B1 towards 11-deoxycorticosterone and corticosterone in adrenal cortical- and medullary tissue homogenates. Aldosterone formation in the adrenal medulla was identified using an atmospheric pressure chemical ionization-mass spectrometry method, which was developed in our department.

3. Compares the catalytic activity of three recombinant Cape baboon CYP11B1 cDNAs, expressed in COS-1 cells, towards 11-deoxycorticosterone and 11-deoxycortisol.

4. Describes the determination of the Michaelis-Menten constants and maximum reaction rates of 11-deoxycorticosterone and 11-deoxycortisol utilization by two functional recombinant Cape baboon CYP11B1 cDNAs, respectively. 11-Deoxycorticosterone metabolites were quantified using an enzyme immunoassay kit. 11-Deoxycortisol metabolites were quantified using a liquid chromatography-mass spectrometry method, which was developed in our department.

5. Describes the homology modeling of two isoforms of Cape baboon CYP11B1 using CYP102 and CYP2C5 as structural templates. The influence of three amino acid residue substitutions, located in the predicted D-E helix, on the catalytic activity of the two CYP11B1 isoforms was examined.

OPSOMMING

Hierdie studie:

1. Beskryf die lokalisering van CYP11B1 in die bynier van die Kaapse bobbejaan deur gebruik te maak van die Western kladtegniek. CYP11B1 is gelokaliseer tot die adrenale korteks en medulla.

2. Beskryf die metabolisme van 11-deoksikortikosteroon en kortikosteroon in adrenale korteks- and medulla weefsel preparate, onderskeidelik. Die produksie van aldosteroon in die medulla is geïdentifiseer deur gebruik te maak van ‘n atmosferiese druk chemiese ionisasie-massa spektrometrie metode wat in ons departement ontwikkel is.

3. Vergelyk die katalitiese aktiwiteit van drie rekombinante Kaapse bobbejaan CYP11B1 cDNAs, getransfekteer in COS-1 selle, ten opsigte van 11-deoksikortikosteroon en 11-deoksikortisol metabolisme.

4. Beskryf die bepaling van die Michaelis-Menten konstantes en maksimum snelhede van twee funksionele rekombinante Kaapse bobbejaan CYP11B1 cDNAs, getransfekteer in COS-1 selle, ten opsigte van 11-deoksikortikosteroon en 11-deoksikortisol metabolisme. 11-Deoksikortikosteroon metaboliete is gekwantifiseer deur gebruik te maak van ‘n ensiem immunotoets. 11-Deoksikortisol metaboliete is gekwantifiseer deur middel van ‘n vloeistofchromatografie-massaspektrometrie metode, ontwikkel in ons departement.

5. Beskryf die modelering van drie-dimensionele strukture van twee funksionele Kaapse bobbejaan CYP11B1 isoensieme deur CYP102 en CYP2C5 as template te gebruik. Die effek van drie aminosuurresiduveranderinge in die voorspelde D-E heliks op die katalitiese aktiwiteit van die twee CYP11B1 isoforme is bepaal.

Dedicated to the ones I love...

ACKNOWLEDGEMENTS

I hereby would like to express my sincere gratitude and appreciation to everyone that has contributed to this study in any form or manner, and in particular, I would like to thank:

Both of my supervisors, Dr. Amanda Swart and Prof. Pieter Swart, for the opportunity to work in their laboratory and for all that they have imparted to me during my studies.

Dr. Amanda Swart for her patience in teaching me techniques, for her advice, supervision, support and encouragement throughout this study and for her expert guidance during the preparation of this thesis.

Prof. Pieter Swart also for his guidance, advice and financial support.

Dr. Carine Smith for her kindness, encouragement and dissecting the baboon adrenals.

Dr. Thinus van der Merwe for developing an APcI-MS method used to identify steroid metabolites.

Dr. Marietjie Stander for her friendliness, willingness to help and for developing a LC-MS method used to quantify steroid metabolites.

Karl-Heinz Storbeck for his help with the modeling of Cape baboon CYP11B1 and especially his help with Figure 5.13.

Mr. Edward Foster for all his help, academic guidance and for inspiring me to go the extra mile.

Ms. Ralie Louw for her encouragement and help during this study.

Anita Februarie, Welma Maart, Kerneels Botha and Ghalieb Damonse for their encouragement and assistance.

Mrs. Lynnette Eygelaar for her encouragement.

The University of Stellenbosch, the Harry Crossley Trust and the FRD for financial support.

Floris, Gloria, Rumacques, Rhaändi, Glireska, Mark, Danielle, Nathanael-Mark and Maliika for their unconditional love, support and encouragement.

Prof. Alf Botha, Prof. Janet Hapgood, Drs. Ann Louw, Lydia Joubert and Karin Jacobs, Heidi, Trudy, Angela, Karin C, Jo-Marié, Vuyiswa, Etienne and Cobus for your support and encouragement during tough times.

Dave, Jubelian, Natalie, Michelle, Pris, Berenice, Willie, Samantha, Jessica, Debbie, Zainoe, Donita, Schalk, Sareanne, Erna, Christie, Cornelia, Norbert, Bronwyn, Adri and Vera-Marié for their friendship and encouragement.

Arrie-Paul, for his kindness, patience, encouragement, love and most of all, his friendship, which means the world to me.

TABLE OF CONTENTS

ABBREVIATIONS

11-DOC	11-Deoxycorticosterone
3β-HSD	3β-Hydroxysteroiddehydrogenase
ACTH	Adrenocorticotropin hormone
AdR	Adrenoredoxin reductase
AdX	Adrenoredoxin
Amu/s	Atomic mass units per second
ANG II	Angiotensin II
APcI-MS	Atmospheric pressure chemical ionization mass spectrometry
AT1	Angiotensin II receptor 1
ATCC	American Type Culture Collection
ATF	Activating transcription factor
BSA	Bovine serum albumin
bp	Base pairs
CAH	Congenital adrenal hyperplasia
CaM	Calmodulin
cAMP	cyclic AMP
CRE	cAMP response element
CREB	cAMP response element binding protein
CYP17	Cytochrome P450 17α-hydroxylase
CYP11A1	Cytochrome P450 side chain cleavage
CYP11B1	Cytochrome P450 11β-hydroxylase
CYP11B2	Cytochrome P450 aldosterone synthase
CYP21	Cytochrome P450 21-hydroxylase
DAG	1,2-Diacylglycerol
DEAE-dextran	Diethylaminoethyl-dextran
DHEA	Dehydroepiandrosterone
DMEM	Dulbecco's modified eagle's medium
EDTA	Ethylenediaminetetra-acetic acid
ELISA	Enzyme-linked immunoassay

ER	Endoplasmic reticulum
FAD	Flavin adenine dinucleotide
FCS	Fetal calf serum
FMN	Flavin mononucleotide
HPLC	High pressure liquid chromatography
IgG	Immunoglobulin G
IP_3	Inositol 1,4,5-triphosphate
Kb	Kilo bases
kDa	Kilodaltons
LC-MS	Liquid chromatography mass spectrometry
Mr	Relative molecular weight
NADPH	Nicotinamide adenine dinucleotide phosphate
NBRE-1	Nerve growth factor-induced clone B response element
NGFIB	Nerve growth factor-induced clone B
PBS	Phosphate buffered saline
Pen-strep	Penicillin-Streptomycin
PKA	Protein kinase A
PKC	Protein kinase C
PdR	Putidaredoxin
RT-PCR	Reverse transcriptase polymerase chain reaction
SCP-2	Sterol carrier protein-2
SCR	Structurally conserved region
SDS-PAGE	Sodium dodecyl sulphate polyacrylamide gel electrophoresis
SF-1	Steroidogenic factor-1
SRS	Substrate recognition site
StAR	Steroidogenic acute regulatory protein
SVR	Structurally variable region
TLC	Thin layer chromatography
TMB	Tetramethylbenzidine
zF	Zona fasciculata
zG	Zona glomerulosa

zR	Zona reticularis

CHAPTER ONE

INTRODUCTION

In nature cytochromes P450 (P450 enzymes) are highly complex and ubiquitously distributed enzymes. These enzymes display a broad field of activity and catalyze a variety of reactions, which include the oxidative transformation of a number of endogenous substrates. P450 enzymes are hemoproteins encoded by a superfamily of genes, which are involved in the biosynthesis of physiologically important compounds including steroid hormones.

Steroid hormones mediate a wide variety of vital physiological functions in the mammalian body. This unique group of hormones is synthesized and secreted into the bloodstream by three endocrine organs, of which the adrenal cortex produces essential corticoids. These corticoids exert numerous actions in the mammalian body.

The most active corticosteroids are those that are 11β-hydroxylated. The key enzymes in the biosynthesis of these corticoids are CYP11B1 and CYP11B2, which catalyze the final steps in the synthesis of cortisol and aldosterone, respectively. In humans, cortisol acts as the major glucocorticoid and exerts numerous actions, which include the mobilization of energy resources by glycogenolysis and gluconeogenesis, increasing heart rate, altering brain physiology and acts as an anti-inflammatory agent. Aldosterone is the primary mineralocorticoid in man and its function is to promote sodium reabsorption and potassium excretion in the distal tubuli of the kidney. The mean daily secretion of cortisol is between 15 mg and 30 mg compared to 0.05-0.15 mg of aldosterone secretion and is therefore the most prominent adrenocortical steroid hormone.

Mutations or deficiencies in the CYP11B1 and CYP11B2 genes together with abnormally increased plasma levels of cortisol and aldosterone are the cause of a variety of diseases in humans such as congenital adrenal hyperplasia, corticosterone methyl oxidase I, II or glucocorticoid suppressible hyperaldosteronism. Congenital adrenal hyperplasia is characterized by a severe decline in cortisol secretion, resulting in a compensatory increase in adrenocorticotropin hormone and the consequent adrenal growth (hyperplasia), signs of androgen excess and hypertension. The mutations in CYP11B1 are distributed over the entire coding region, but cluster in exons two, six, seven, and eight. All defects in the CYP11B1

gene have been found to be due to nonsense, missense or splice site mutations. The lack of aldosterone impedes renal reabsorption of Na^+ and excretion of K^+ and H^+, with a characteristic massive urinary salt loss, and causes hyponatremia, hyperkalemia and hypovolemic shock in infancy. The affected enzyme can be totally or partially impaired. The severity of the condition is determined by the degree of enzyme insufficiency.

The adrenal cortex is the primary site of CYP11B1 and CYP11B2 gene expression. However, numerous reports have shown that these enzymes also occur in the brain, the spinal cord, cardiac tissue and peripheral nervous system of humans, mice and rats.

The number of genes encoding these CYP11B-related enzymes differs significantly among species. Some species have two isozymes involved in the formation of either glucocorticoids or mineralocorticoids, while others possess a single enzyme, which is responsible for the biosynthesis of these corticoids.

Cape baboon CYP11B1 cDNA was cloned from baboon adrenals and successfully expressed in COS-1 cells, for the first time in our laboratory [1, 2]. Genomic studies identified the baboon CYP11B1 gene in an open reading frame of 1509 bases, containing nine exons, similar to that found in humans [1]. As the number of CYP11B genes differs between species, research was undertaken in our laboratory to determine if the Cape baboon, like the rat, had more than two CYP11B genes. Utilizing RT-PCR, three CYP11B1 genes, sharing 99% homology, were cloned from Cape baboon adrenal tissue. The cloned CYP11B1 genes shared 96% and 94.6% sequence homology to human CYP11B1 and CYP11B2, respectively. One of the genes contained a termination codon in exon one and was therefore termed CYP11B1S [2]. Sequence analysis showed that one of the genes had two Sma1 sites in the same position as human CYP11B1 and was subsequently termed CYP11B1 wild-type while the other, which contained a single Sma1 site, was termed CYP11B1a.

The aims of the work presented in this thesis were to: (a) to establish if the two CYP11B genes cloned from the Cape baboon adrenals were enzymatically distinct and to characterize the enzymes with respect to their kinetic parameters and structure function relationships and (b) to localize the two enzymes in the adrenal through enzyme activity studies. To achieve these aims:

1. The catalytic activity of CYP11B1 towards 11-deoxycorticosterone and corticosterone in baboon adrenal cortical- and medullary- tissue homogenates was investigated.
2. The catalytic activity of three recombinant Cape baboon CYP11B1 cDNAs, expressed in COS-1 cells, towards 11-deoxycorticosterone and 11-deoxycortisol was determined.
3. The Michaelis-Menten constants and maximum reaction rates of 11-deoxycorticosterone and 11-deoxycortisol utilization by two functional recombinant baboon CYP11B1 cDNAs, expressed in COS-1 cells, were determined.
4. The effects of three amino acid residue substitutions on the catalytic activity of the two functional CYP11B1 isoforms were investigated using homology modeling.

In chapter two a broad overview of cytochromes P450 and the role played by these enzymes in adrenal steroidogenesis is presented. Particular reference is given to steroid hormone biosynthesis, the adrenal cortex zonation and regulation of adrenocorticoid biosynthesis.

Immunohistochemistry and *in situ* hybridization studies carried out in our laboratory showed that Cape baboon CYP11B1 is present in the histologically distinct regions of the adrenal cortex and medulla. Tissue distribution of CYP11B1 in adrenal tissue homogenates was investigated using Western blot analysis and is presented in chapter three. The findings demonstrated the presence of a protein corresponding to the molecular mass of human CYP11B1 in the adrenal cortical tissue homogenates and two proteins, corresponding to the molecular masses of human CYP11B1 and CYP11B2 in the medullary tissue homogenates. A subsequent study into the catalytic activity of CYP11B was carried out in the adrenal tissue homogenates. Different catalytic activity towards 11-deoxycorticosterone and corticosterone was observed in the tissue homogenates.

Three genes encoding Cape baboon CYP11B have previously been cloned in our laboratory. Since sequence analysis revealed that the nucleotide sequence of these genes were 96.5% and 94.6% homologous to human CYP11B1 and CYP11B2, respectively, it was assumed that they encoded the CYP11B1 isoform of the enzyme. In chapter four the results obtained from the subsequent investigations of the catalytic activity of these recombinant proteins expressed in non-steroidogenic cells are presented. The proteins were expressed in COS-1 cells and a study of 11-deoxycorticosterone and 11-deoxycortisol metabolism was performed. Two of the

genes encoded an active enzyme and a comparative enzyme activity study of the isoforms of Cape baboon CYP11B1, expressed in COS-1 cells with 11-deoxycorticosterone and 11-deoxycortisol as substrates, followed. Results obtained revealed that the isoforms bind both substrates, but hydroxylate them with different efficiencies and selectivities. The apparent Km- and V-values for the expressed enzymes were subsequently determined for each of the abovementioned substrates. There was a marked difference between the kinetics of 11-deoxycorticosterone metabolism by the two CYP11B1 isoforms of the Cape baboon.

Sequence analysis of the amino acid residues showed that Cape baboon CYP11B1a and CYP11B1wt differed by three amino acid substitutions in exon three. An investigation into the structural and functional implication of the three amino acid substitutions, in order to compare the kinetic parameters for the CYP11B1a and CYP11B1wt, followed. The three-dimensional structures of both CYP11B1 isoforms were investigated using homology modeling to better understand the differences in the 11β-hydroxylation of the substrates. Chapter five gives an overview of the contribution made by crystallized structures of bacterial cytochromes P450 and the microsomal CYP2C5, with reference to the common structural features to structure/function elucidation of P450 enzymes. Homology modeling of human CYP11B1, CYP11B2 and ADX are discussed. This chapter presents the predicted three dimensional structures of the two isoforms of Cape baboon CYP11B1, obtained with homology modeling using CYP102 and CYP2C5 as templates.

Chapter six discusses the research presented in this thesis.

CHAPTER TWO

CYTOCHROMES P450

2.1 INTRODUCTION

In the mammalian endocrine system cytochrome P450 enzymes (P450 enzymes) catalyze the biosynthesis of steroid hormones in the adrenal cortex, ovaries and testis. The placenta develops as an additional major source of steroid hormones during the course of pregnancy. Steroid hormone concentrations in the blood vary due to a specific response to physiological or pathological modifications in order to maintain various processes in the body. These endocrine organs produce and secrete steroid hormones under the regulation of specific extracellular hormones and factors that stimulate a sequence of intracellular processes to ultimately alter the steroid output [3, 4]. Steroid hormone biosynthesis originates in the mitochondria with cholesterol and proceeds *via* a number of P450 enzymes in the endoplasmic reticulum (ER) and mitochondria [5].

In 1958, Garfinkel and Klingenberg identified a carbon monoxide-binding pigment in liver microsomes of pigs and rats, which was reducible by either NADPH or dithionite and exhibited a distinctive absorption maximum of the reduced CO-bound complex at 450 nm [6, 7]. Six years later, in 1964, Omura and Sato reported that this CO-binding pigment was indeed a hemoprotein. They named the enzyme cytochrome P450, due to the characteristic absorption peak obtained at 450 nm after saturating the reduced form of the enzyme with CO. The unique spectral properties of the newly discovered cytochrome P450 could be attributed to a thiolate anion which acts as the fifth ligand to the heme moiety [8, 9].

P450 enzymes are ubiquitously distributed in the biosphere and comprise a superfamily of heme-thiolate enzymes. Up to date the genes of approximately 2500 distinct members of the P450 superfamily have been sequenced [10]. This diverse group of enzymes catalyzes the oxidation of a wide variety of substrates in microorganisms, plants and animals. The principal catalytic cycle of these enzymes has been characterized and is the same for all P450 enzymes [9, 11, 12]. These membrane-associated enzymes function as monooxygenases, activating molecular oxygen and incorporating a hydroxyl group into a hydrophobic substrate,

increasing the polarity, with the concomitant formation of a water molecule as shown in the following scheme [9].

$$\text{Steroid-H} + \text{NADPH} + \text{H}^+ + \text{O}_2 \rightarrow \text{Steroid-OH} + \text{NADP}^+ + \text{H}_2\text{O}$$

NADPH provides two reducing equivalents during electron transfer, which is mediated by one or two redox partners depending on the P450 system [11]. The adrenal P450 systems can be grouped into two categories, Class I and Class II, based on their electron transport mechanisms and their subcellular location as illustrated in Figure 2.1.

Class I P450 enzymes comprise mitochondrial hemoproteins and also include bacterial P450 enzymes [13]. Eukaryotic Class I P450 enzymes are expressed on the matrix side of the inner mitochondrial membrane and constitute a three-component system including two redox transporter proteins, a flavin adenine dinucleotide (FAD)- containing reductase, namely adrenodoxin reductase (AdR), and an iron-sulfur protein (ferredoxin), namely adrenodoxin (AdX), which mediates the channeling of reducing equivalents from NAD(P)H to the terminal electron acceptor, a P450 enzyme. Although the prokaryotic class I P450 enzymes share the same three-component system, CYP102 from *Bacillus megaterium* and its homologs, CYP102A2 and CYP102A3 from *Bacillus subtilis,* differ in that its NADPH-dependent, FAD/FMN-containing oxidoreductase is covalently joined to the class II hemoprotein, yielding a self-sufficient flavocytochrome [14, 15, 16].

In the Class II P450 enzymes, which include the microsomal P450 system, the above two redox carrier proteins are replaced by a single flavoprotein, NADPH-P450 oxidoreductase. This reductase consists of a two-part structure, which constitutes an FAD-containing, flavin mononucleotide (FMN)-containing NADPH-dependent P450 reductase. The NADPH specific P450 reductase and the microsomal P450 enzymes are located on the cytoplasmic side of the endoplasmic reticulum membrane and are affixed to the membrane by their hydrophobic amino termini, which are inserted into the membrane during translation [17].

The substrate pocket of P450 enzymes contains an iron protoporphyrin IX, which is located in a relatively large hydrophobic groove on the surface of the enzyme, and is bound in part by hydrophobic forces. The fifth ligand is formed by a thiolate anion, which is supplied by a

cysteine residue, a characteristic that contributes to the unusual spectral and catalytic properties of P450 enzymes. An exchangeable water molecule may engage the sixth coordination site, which functions as the binding site for the molecular oxygen throughout the reduction of the heme iron. Following the reduction of the iron, oxygen or, in a competitive fashion, carbon monoxide can be bound in the sixth position. The capacity of a potential substrate to bind in the active site of the enzyme and shift the spin state equilibrium, consequently promoting electron transfer to the heme iron, determines the substrate specificity of P450 enzymes. A further contribution is made by the degree to which completion of the catalytic cycle occurs without uncoupling of NADPH and oxygen utilization from substrate oxidation [9].

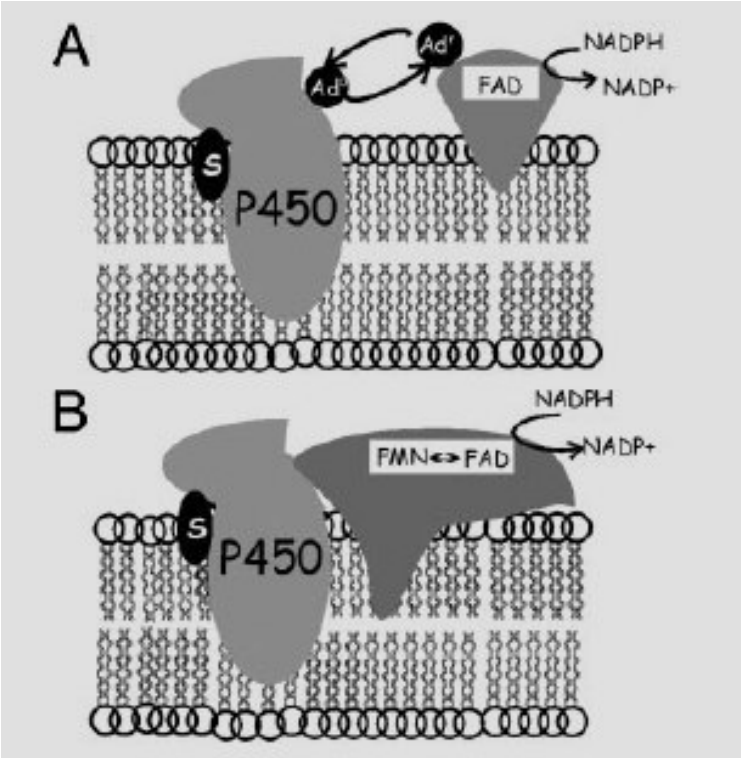

Figure 2.1. Schematic representation of the (A) Class I mitochondrial electron transfer system and (B) Class II microsomal electron transfer system. FAD, flavin adenine dinucleotide; FMN, flavin mononucleotide; Ad^r, reduced adrenodoxin reductase; Ad^o, oxidized adrenodoxin; S, substrate [18].

The general catalytic cycle of P450 enzymes has been extensively studied and the essential features are well characterized. The seven crucial steps in the monooxygenation reactions involve the following steps (Figure 2.2): (1) binding of the substrate to the low-spin ferric form of the enzyme, converting the heme iron to the high-spin ferric form; (2) transfer of the

first electron, reducing the ferric resting P450 enzyme to the ferrous state; (3) binding of molecular oxygen to the reduced heme iron to produce a ferrous cytochrome P450-dioxygen complex; (4) transfer of the second electron to this complex gives rise to a peroxoiron(III) complex; (5) protonation and cleavage of the O-O bond with the concurrent incorporation of the distal oxygen atom into a molecule of water and the formation of a reactive iron-oxo species; (6) oxygen atom transfer from this oxo complex to the bound substrate and (7) dissociation of the product [9].

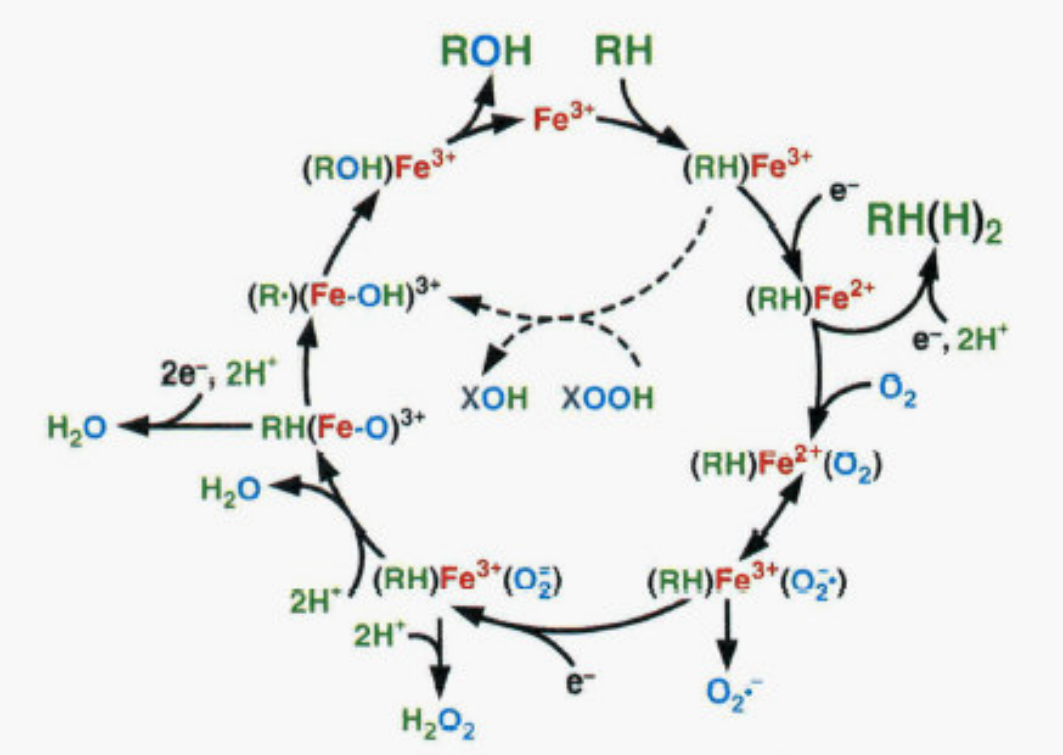

Figure 2.2. Scheme for mechanism of action of cytochromes P450. *Fe* represents the heme-iron atom at the active site; *RH* the substrate; *RH(H)₂* a reduction product; *ROH* a monooxygenation product; and *XOOH* a peroxy compound that can serve as an alternative oxygen donor [9].

2.2 ADRENAL STEROIDOGENESIS

P450 enzymes play a vital role in the synthesis of adrenocortical steroids, classified as glucocorticoids, mineralocorticoids and androgens. Glucocorticoids are essential in the regulation of energy mobilization, stress response and are also involved in the immune response of the human body. The mineralocorticoids are important for the regulation of sodium/potassium homeostasis, which participates in the control of blood pressure [19]. The

androgens affect sexual development and function by maintaining sexual differentiation, secondary sex characteristics and sexual behavior patterns. Biosynthesis of these corticoids entails four P450 enzymes, which belong to a large family of heme-bound mixed function oxidases, and 3β-hydroxysteroid dehydrogenase (3 β-HSD) (Figure 2.3) [20, 21].

In mammals, cholesterol serves as the common precursor of all steroid hormones. Biosynthesis of the adrenal corticoids is initiated by the first and rate-limiting step, which is the transport of free cholesterol from the cytoplasm into the mitochondria, after which a series of P450-mediated transformations follows. This sequential processing by the P450 enzymes involves the shuttling of steroids between the mitochondria and the ER of the adrenal cortex (Figure 2.3) [22, 23].

The mobilization of cholesterol from the outer to the inner mitochondrial membrane, where CYP11A1 is located, is regulated by the phosphoprotein, Steroidogenic Acute Regulatory protein (StAR), under the rapid stimulation of adrenocorticotropin hormone (ACTH) and various other factors including the sterol-carrier protein 2 (SCP-2) and the peripheral benzodiazepine receptor. SCP-2 enhances cholesterol transfer and stimulates cholesterol metabolism by CYP11A1.

2.2.1. CYP11A1

In 1984 Morohashi *et al.* and John *et al.* cloned the gene encoding CYP11A1 from bovine adrenals [24, 25]. In 1986 Chung *et al.* cloned and sequenced full-length human CYP11A cDNA and located the gene to chromosome 15 [26]. Chung *et al.* also established that primary cultures of human placental tissue showed an accumulation of CYP11A1 mRNA in response to cyclic AMP (cAMP) and concluded that the human CYP11A1 gene is expressed in the placenta in early and mid-gestation. The structure of the CYP11A1 gene has been determined in various species.

Studies by Morohashi *et al.* demonstrated that the CYP11A1 gene is approximately 20 kb long and is split into nine exons by eight introns [27]. The human and rat CYP11A1 genes have an unusual exon/intron junctional sequence that begins with GC in the sixth intron.

Sparkes *et al.* mapped the human CYP11A gene to 15q23-q24 using *in situ* hybridization [28]. Mouse CYP11A1 is located on chromosome 9 at 31 cM [18].

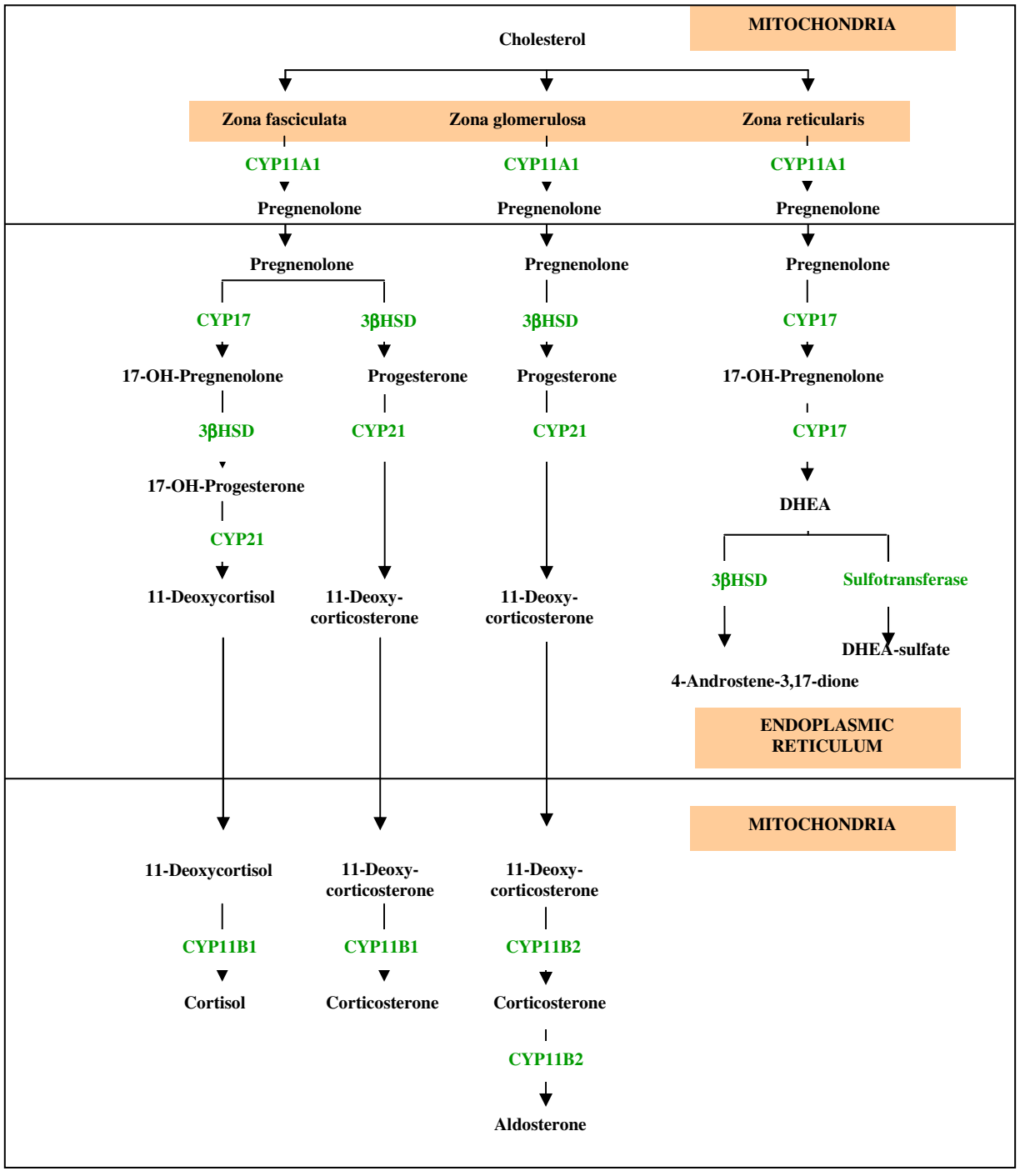

Figure 2.3. Schematic representation of mammalian adrenocortical steroidogenesis.

The amino acid sequence homology of CYP11A1 between various species is approximately 71%. The open reading frame of human cDNA encodes a peptide containing 521 amino acid residues. The amino terminus consists of the N-terminal leader sequence, which contains 39

amino acid residues, and is important for translocation of the protein to the inner mitochondrial membrane. The molecular mass of the mature protein is 56kDa [18].

CYP11A1 cDNA, cloned from Cape baboon adrenals in our laboratory, was shown to be 97% homologous to human CYP11A1 with the putative 39 amino acid pre-sequence being 85% homologous to the human mitochondrial targeting sequence. The pre-sequence, 98% homologous to that of human CYP11A1, comprises various basic and hydroxylated amino acid residues. The deduced amino acid sequence of mature baboon and human CYP11A1 differ by eight amino acid residues [29, 30].

CYP11A1 catalyzes three successive monooxygenations reactions of cholesterol where each reaction requires one molecule of O_2 and one molecule of NADPH (Figure 2.4). The first reaction is a 22-hydroxylation, followed by a 20-hydroxylation to produce 20,22R-dihydroxycholesterol, which is subsequently cleaved between C20 and C22, yielding the C21 steroid, pregnenolone and isocaproaldehyde [18, 31, 32].

Studies on purified CYP11A1 and recombinant proteins from CYP11A1 cDNAs revealed that a single protein catalyzes all three reactions at a single active site. The hydroxylated intermediates bind tightly to the active site of CYP11A1 and do not show significant dissociation from the enzyme. In contrast, pregnenolone exhibits a dissociation constant 40-600 fold higher than the intermediates, facilitating its release from the enzyme [10, 18, 33].

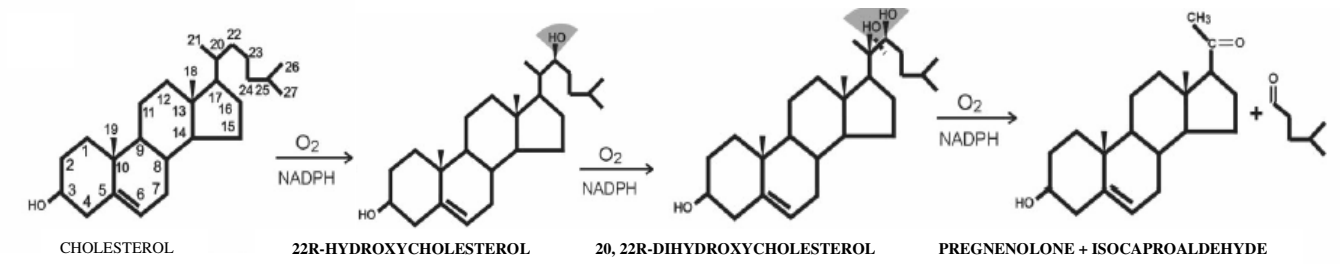

Figure 2.4. Reaction sequence catalyzed by CYP11A for the conversion of cholesterol to pregnenolone. CYP11A catalyzes three sequential oxidation reactions followed by cleavage of the six carbon side-chain. Each oxidation reaction requires one molecule of oxygen and one molecule of NADPH and uses the mitochondrial electron transfer system [18].

Pregnenolone is shuttled to the endoplasmic reticulum of the adrenal cortex where it serves as a substrate for two different enzymes. Pregnenolone may act as a substrate for CYP17, which

is at a strategic position and plays a key role in conducting the flow of pregnenolone to either glucocorticoid- or androgen biosynthesis, and 3 β-HSD.

2.2.2. CYP17

A single gene, encoding this enzyme, has been isolated from various species and is approximately 6 kb in length. The gene comprises eight exons with the location of intron-exon boundaries conserved among species. The promoter region of the human, mouse and rat CYP17 gene is highly homologous in the first 550 base pairs (bp). The human and mouse CYP17 genes have been mapped to chromosome 10q24-25 and chromosome 19 at 46 cM, respectively [18, 28, 34].

The human protein encoded by this gene, comprises 508 amino acid residues resulting in an estimated molecular mass of 57 kDa, while the mouse and rat CYP17 proteins contain 507 amino acid residues. Mouse and rat CYP17 share 83% homology in their amino acid sequence, while that of mouse and human is 66% homologous [18]. Cape baboon CYP17 encodes a protein of 508 amino acid residues, which shares 96% sequence homology with human CYP17. Studies showed that baboon CYP17 exhibited higher 17α-hydroxylase activity towards progesterone than CYP21, whereas human fetal CYP17 and CYP21 displayed similar hydroxylase activities towards this substrate. Furthermore, human CYP17 exhibited 16α-hydroxylase activity towards progesterone, yielding 16-hydroxyprogesterone, while baboon CYP17 displayed no 16-hydroxylase activity towards progesterone. Both baboon and human CYP17 showed no lyase activity towards 17-hydroxyprogesterone [35].

CYP17 has two well-defined activities, which mediate the 17α-hydroxylation of C21 steroids, required in cortisol biosynthesis, and the cleavage of the C17-20 carbon bond of the side-chain, a reaction essential for androgen biosynthesis (Figure 2.5).

In a two-step reaction, CYP17 hydroxylates pregnenolone and progesterone, which is formed *via* the actions of 3 β-HSD, at the C17-position yielding the intermediates, 17α-hydroxypregnenolone and 17α-hydroxyprogesterone. The side-chains of the 17α-hydroxylated products are subsequently cleaved to generate dehydroepiandrosterone (DHEA)

and androstenedione, respectively [33]. The 17α-hydroxylation and lyase of the steroid at the 17, 20-bond requires one molecule of NADPH and one molecule of O_2 each.

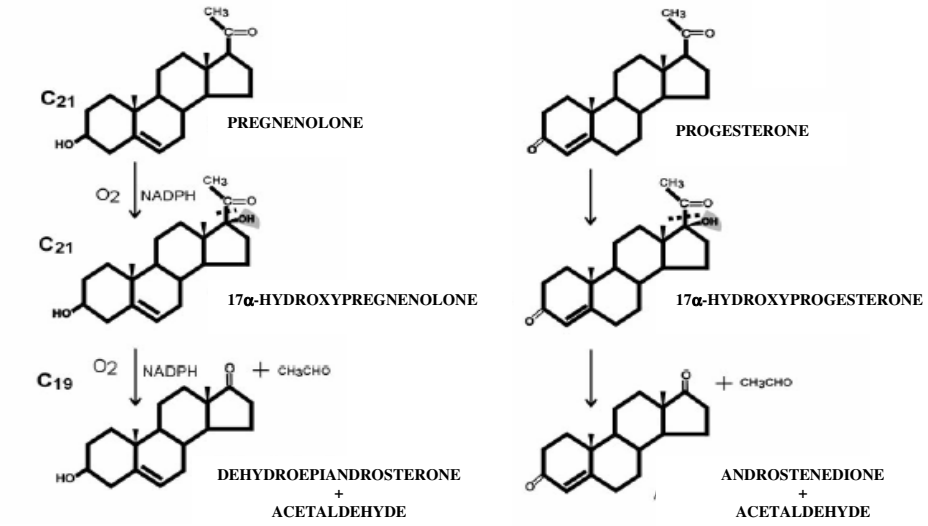

Figure 2.5. Reaction sequence of CYP17. CYP17 catalyzes two mixed-function oxidase reactions, 17α-hydroxylation and C17–C20 cleavage. Each reaction requires one molecule of oxygen and one molecule of NADPH and uses the microsomal electron transfer system [18].

Progesterone and 17α-hydroxyprogesterone is further metabolized by CYP21 in the endoplasmic reticulum.

2.2.3. CYP21

Humans and mice express two genes encoding CYP21 and CYP21P, respectively. In both species, the two genes are arranged in tandem in the major histocompatibility locus. The human CYP21 gene encodes an active enzyme. Human CYP21P has an eight-base deletion, a one-base insertion, and a transition mutation, which results in the premature termination of translation. The two human genes comprise ten highly homologous exons; the introns and flanking regions are also highly homologous. The human genes are mapped to chromosome 6p21.3. The mouse *Cyp21a* gene encodes the active enzyme, while the *Cyp21b* gene has a 215-nucleotide deletion in exon two and a few other nucleotide changes, which results in frame shifts and premature termination codons. The mouse genes are located on chromosome 17 at 18.77 cM. The open reading frame of the human and mouse cDNA encode proteins consisting of 495 and 487 amino acid residues, respectively, resulting in an estimated

molecular mass of 56 kDa for human and 55.3 kDa for mouse. In all other species investigated thus far, CYP21 is encoded by a single gene [18].

CYP21 catalyzes the 21-hydroxylation of progesterone and its 17α-hydroxylated intermediate, 17α-hydroxyprogesterone, yielding 11-deoxycorticosterone (11-DOC) and 11-deoxycortisol, respectively (Figure 2.6) [16, 33]. This reaction requires one molecule of NADPH and one molecule of O_2. 11-DOC and 11-deoxycortisol are shuttled back to the mitochondria where it undergoes further metabolism by the CYP11B enzymes.

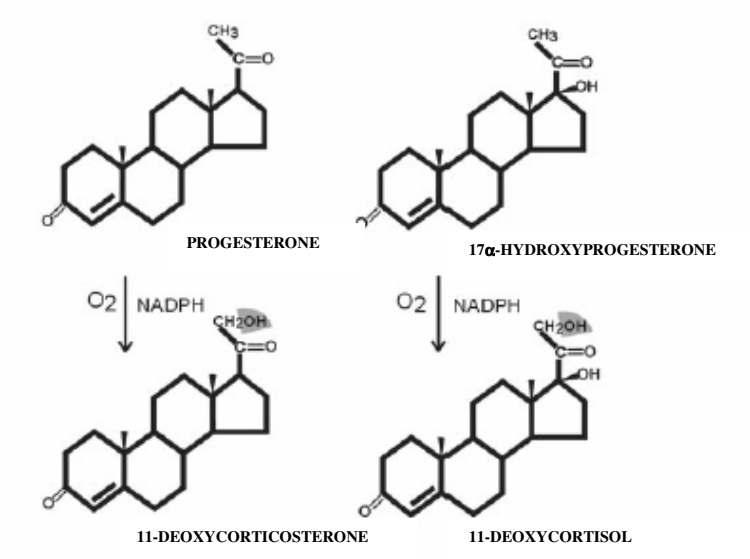

Figure 2.6. Reaction catalyzed by CYP21. This enzyme uses the microsomal electron transfer system and catalyzes the 21-hydroxylation of either progesterone or 17α-hydroxyprogesterone [18].

2.2.4. CYP11B1 and CYP11B2

CYP11B1 and CYP11B2 play a key role in the biosynthesis of mineralo- and glucocorticoids. In 1987 White *et al.* isolated human CYP11B1 cDNA and established, through *in situ* hybridization and Southern blot analysis of DNA from human-mouse somatic cell hybrids, that the structural gene is a single copy on the long arm of chromosome eight [36]. Chua *et al.* localized the two CYP11B isozyme genes, CYP11B1 and CYP11B2, to chromosome 8q21 and showed that the genes are arranged in tandem approximately 45 kb apart from each other [37, 38]. Mornet and White determined that the human CYP11B genes are 6.5 kb long from the onset of transcription to the polyadenylation site and contains nine exons, with eight

introns that are identical in location to the introns of the CYP11A gene. The genes encoding the two human isozymes of CYP11B are approximately 95% identical in their coding regions and 90% identical in their introns. Mornet and White showed that the 5' upstream region of CYP11B2 diverged considerably from that of CYP11B1 and suggested that the enzymes might be regulated differently [39, 40]. The number of genes encoding these isozymes differs among species. In addition to human CYP11B, species such as rat, mouse, guinea pig and hamster possess two distinct CYP11B isoforms, namely CYP11B1 and CYP11B2. In the rat and guinea pig more than two CYP11B genes have been identified. In species such as cows, pigs, sheep and frogs a single enzyme, namely CYP11B1, catalyzes the synthesis of the vital corticoids [41, 42].

Human CYP11B1 and CYP11B2 are situated in the inner mitochondrial membrane and share 93% homology in their amino acid sequences. The divergent amino acid residues are located outside the substrate recognition sites and are spread throughout the protein. The pro-enzymes contain 503 amino acid residues, which include a leader sequence of 24 amino acid residues. The 24-residue N-terminal targeting sequence is cleaved off after translocation into the mitochondria, yielding a mature protein consisting of 479 amino acid residues, resulting in apparent molecular masses of 51 kDa and 49 kDa for human CYP11B1 and CYP11B2, respectively [18].

Sequence analysis of genomic DNA, previously isolated from Cape baboon blood [1] identified a single gene with an open reading frame of 1509 bp, containing nine exons. To ascertain whether the Cape baboon, like the rat, has more than two CYP11B genes, recombinant cDNAs were cloned from baboon adrenal tissue [2]. The characterization of the expressed enzymes, from the recombinant CYP11B cDNAs, is described in this thesis.

CYP11B1 catalyzes the 11β-hydroxylation of 11-DOC and 11-deoxycortisol to produce corticosterone and cortisol, respectively (Figure 2.7). This enzyme also has the ability to 18-hydroxylate 11-DOC and corticosterone yielding 18-hydroxy-DOC and 18-hydroxycorticosterone, respectively, but lacks 18-oxidase activity and thus cannot synthesize aldosterone [18]. In some species, CYP11B1 also exhibits 19-hydroxylase activity towards 11-DOC, producing 19-hydroxy-DOC [41, 43, 44].

CYP11B2 catalyzes aldosterone synthesis from 11-DOC *via* three sequential reactions, which use one molecule of NADPH and O_2 each (Figure 2.8). The first reaction is the 11β-hydroxylation of 11-DOC, followed by the 18-hydroxylation of corticosterone. The last reaction is the 18-oxidation of 18-hydroxy-corticosterone, yielding aldosterone. The additional 18-hydroxylase and 18-oxidase activities of CYP11B2, but not of CYP11B1, are probably due to the presence of a subset of 36 amino acid differences, which differentiate the two enzymes. Experiments carried out *in vitro*, showed that only 2 of the 36 amino acid differences, i.e. Ser288Gly and Val320Ala, distinguishing the CYP11B1 and CYP11B2 enzymes, are responsible for the additional 18-hydroxylase and 18-oxidase activities of CYP11B2 when 11-DOC is used as substrate. Further studies revealed that the Val320Ala substitution is sufficient to enable CYP11B1 to catalyze limited aldosterone synthesis [18, 41, 42].

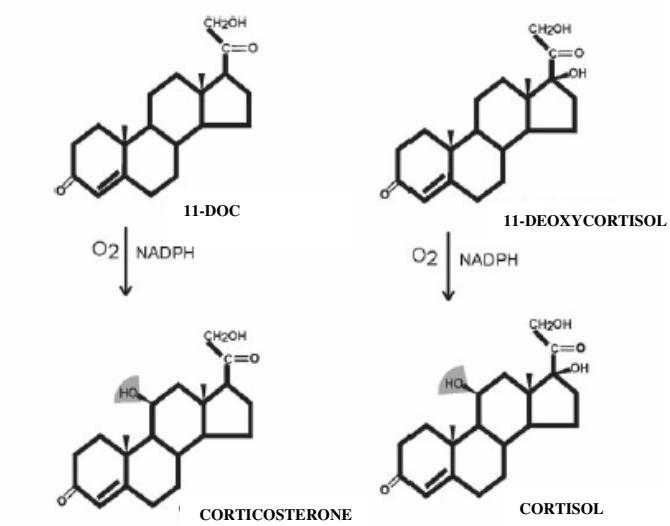

Figure 2.7. Reactions catalyzed by CYP11B1. This enzyme utilizes the two mitochondrial electron transfer system (adrenodoxin and adrenodoxin reductase), and requires one molecule of oxygen and one molecule of NADPH [18].

Valuable data with regards to enzyme activity, i.e. 11β-hydroxylase-, 18-hydroxylase- and 18-oxidase activities, came from the analyses of natural mutations and crossing-over in patients suffering from genetic deviations in the CYP11B1 and CYP11B2 genes, respectively. These studies identified amino acid residues which are important for the specific hydroxylation reactions. Although the crystal structures of these isozymes have not been resolved yet, homology modeling of the two isozymes revealed important information about these amino acids with regards to their structure/function relationships. CYP11B, with 18-

hydroxylase and 18-oxidase activities, were investigated and demonstrated that specific amino acid residue substitutions could be ascribed to the CYP11B2-like activities. This showed the presence of functionally important amino acid residues in CYP11B1 and CYP11B2 and could be used to elucidate structure/function relationship [42].

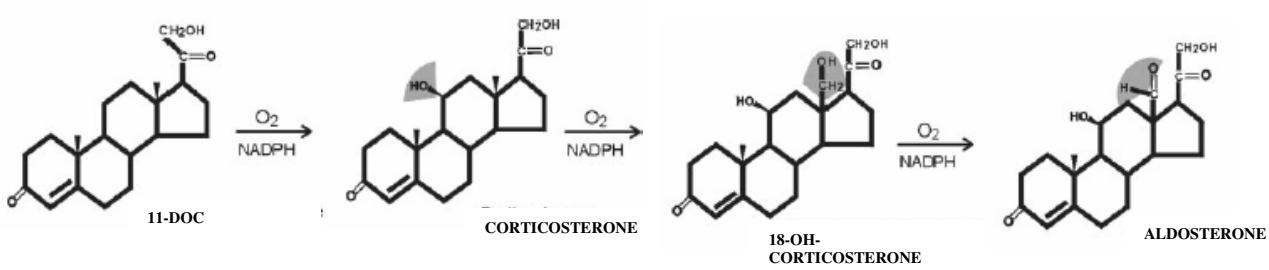

Figure 2.8. Reaction catalyzed by CYP11B2. The enzyme catalyzes three sequential reactions, each requiring one molecule of oxygen and one molecule of NADPH. This enzyme uses the mitochondrial electron transfer system. [18].

It has been proposed that the tandem-type arrangement of CYP11B1 and CYP11B2 on chromosome eight may lead to mutations in these genes, causing various human diseases. Within the steroidogenic pathway, the CYP21 gene and its pseudogene, CYP21P, are also tandemly arranged on chromosome six. Most of the mutations existing in patients with 21-hydroxylase deficiencies are the consequence of recombination between the active gene and the pseudogene. Recombination of these genes usually results in partial or complete loss of function. These types of mutations add to making deficiencies of the 21-hydroxylase activities one of the most common of the inherited disorders. It is therefore expected that genetic recombination between the isozymes of CYP11B could be an important source of mutation of these genes. In contrast to the loss of CYP21 activity due to mutations, recombinant CYP11B genes remain functional and therefore have the ability to produce genes encoding enzymes with novel activities or inappropriately regulated activities [55].

Abnormalities caused by gene conversions, insertions or deletions lead to changes in the production of these corticoids, manifesting in clinical abnormalities and various diseases. A defective CYP11B1 gene does not have the ability to convert the precursors, 11-deoxycortisol and 11-DOC, to cortisol and corticosterone, respectively. The levels of these precursors in the blood are thus elevated in the untreated state. The accumulated precursors are subsequently shunted into the androgen biosynthesis pathway and cause symptoms of androgen excess, which include disordered sexual differentiation and increased somatic

growth. The elevated levels of 11-deoxycortisol or the metabolites with mineralocorticoid activity may cause hypokalemia and hypertension. In contrast, deficiencies in aldosterone biosynthesis are caused by defects in the CYP11B2 gene, leading to elevated plasma levels of aldosterone precursors. Disorders arising from this insufficiency are characterized by salt wasting, hyponatremia, hyperkalemia, and in infants, the inability to thrive [45].

Deficiencies in CYP11B1 and CYP11B2 cause three known Mendelian diseases in humans. Inactivating mutations in CYP11B1 lead to a type of virilizing congenital adrenal hyperplasia (CAH), which is distinguished clinically from the more general CYP21 deficiency by the lack of salt-wasting. Patients with this form of CAH develop hypertension, probably due to elevated levels of the mineralocorticoid, 11-DOC, and characteristically have suppressed secretion of renin and aldosterone. Inactivating mutations in CYP11B2 cause a deficiency in this enzyme, which is characterized by salt-wasting during childhood with normal cortisol biosynthesis. These patients typically have elevated renin and 11-DOC, with very low levels of aldosterone. Unequal crossing-over between CYP11B1 and CYP11B2 leads to glucocorticoid suppressible hyperaldosteronism where the transcriptional regulatory region of CYP11B1 is juxtaposed to coding sequences from CYP11B2. This recombination leads to the formation of a chimeric enzyme with CYP11B2 activity, which is due to the 3′ CYP11B2 coding sequences, and is expressed at high levels in the *zona fasciculata* under the control of ACTH due to the presence of the CYP11B1 promoter and regulatory elements. An excess of aldosterone is produced and causes hypertention in patients suffering from this disease. Chimeric CYP11B1-CYP11B2 enzymes have similar enzymatic activity if the cross-over breakpoint is between exons one and four, but are incapable of synthesizeing aldosterone if the breakpoint is after exon five [46].

Figure 2.9 illustrates several mutations, obtained from clinical mutation studies in CYP11B1 and CYP11B2, causing these diseases. Some of these mutations in CYP11B1 result in the premature termination of the coding sequence, being either nonsense mutations (Lys174End, Gln338, 374→End, Trp116End, Trp247End) or frameshift mutations (a deletion mutation at position 32, insertion of 2 bp at codon 394, a 28 bp deletion in exon two and a 5 bp duplication in exon 2). *In vitro* expression studies revealed that the missense mutations (Arg448His, Arg448Cys, Thr318Met, Arg374Gln, Arg384Gln, Arg384Gly, Val441Gly, Glu371Gly, Ala331Val, Val129Met, Gly267Arg, Gly267Asp, Arg427His, Cys494Phe) and

the insertion of Leu at position 464 destroy the 11β-hydroxylase activity of CYP11B1 completely [47, 48, 49].

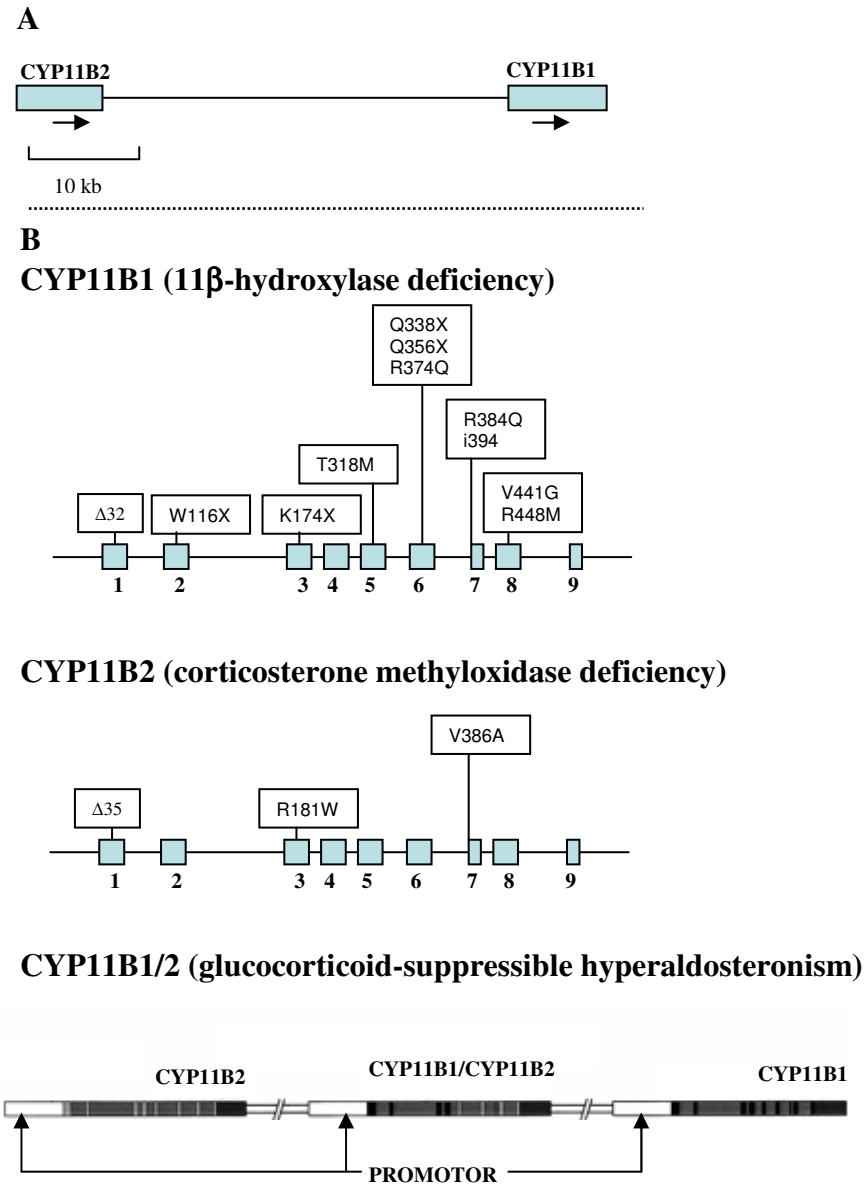

Figure 2.9. Mutations involving CYP11B1 and CYP11B2. (A) Relative positions of CYP11B1 and CYP11B2 on chromosome 8q22 are illustrated. Arrows indicate direction of transcription. (B) The exons of each gene are depicted as shaded bars; introns, untranslated and flanking regions are represented by thin lines. Mutations causing CYP11B1 or CYP11B2 deficiency are marked. Frameshift mutations, Δ32 and i394, are a small deletion and insertion in codon 32 and 394, respectively. Other CYP11B1 deficiency mutations are: W116X, Trp-116End (*i.e.* a nonsense mutation); K174X, Lys-174End; T318M, Thr318Met; Q338 and Q356X. Gln→End; R374Q and R384Q, Arg→Gln; V441G, Val441Gly; R448H, Arg448His. Δ32 (a deletion of 5 base pairs) is a type I CYP11B2 deficiency mutation. R181W and V386A are type II CYP11B2 deficiency mutations. In glucocorticoid suppressible hyperaldosteronism, an intergenic recombination juxtaposes the 5′ end of CYP11B1, including regulatory sequences, with the 5′ end of CYP11B2, yielding a hybrid gene that is regulated like CYP11B1 [48].

In expression studies, the mutations, Arg181Trp and Val386Ala, were introduced individually into human CYP11B2 cDNA. Arg181Trp reduced the 18-hydroxylase and eliminated the 18-oxidase activities of this enzyme. However, the 11β-hydroxylase activity was left intact. The CYP11B2 cDNA constructs containing the Val386Ala mutation, encoded an enzyme that was able to catalyze aldosterone synthesis, however, with reduced efficiency. A combination of these mutations in the human cDNA resulted in the loss of both the 18-hydroxylase and 18-oxidase activities. Expression studies of the human CYP11B2, carrying the point mutations, Arg384Pro and Leu461Pro, demonstrated that the encoded enzymes were inactive [47, 48, 49].

Unequal crossovers result in a CYP11B1/CYP11B2 duplication and are associated with glucocorticoid suppressible hyperaldosteronism, which is a form of hypertension inherited in an autosomal dominant manner. This disease is characterized by moderate hypersecretion of aldosterone and suppressed plasma renin activity. The steroids, 18-hydroxycortisol and 18-oxocortisol, are characteristically elevated in this disorder and are 17α-hydroxylated analogues of 18-hydroxycorticosterone and aldosterone, respectively. Since CYP17 is not expressed in the *zona glomerulosa*, the presence of large quantities of 17α-hydroxy-, 18-oxo-steroids suggests that an enzyme with 18-oxidase activity is abnormally expressed in the *zona fasciculata*. Patients with glucocorticoid suppressible hyperaldosteronism have a chromosome that carries three CYP11B genes instead of the normal two. The middle gene on this chromosome contains a chimera with 5' and 3' ends corresponding to CYP11B1 and CYP11B2, respectively, and is flanked by normal CYP11B2 and CYP11B1 genes [47, 48, 49].

Deficiencies of the P450 enzymes participating in adrenal steroidogenesis, affect the early development of the adrenal cortex, interfering with both differentiation and zonation. The functional zonation of the adrenal cortical zones is coupled to the onset of expression of the steroidogenic enzymes during embryogenesis and fetal development.

2.3. ZONATION OF THE ADRENAL GLAND

The adrenal gland is located atop each kidney and is encased in a connective tissue capsule. This gland's most distinctive feature is its partitioning into two histologically different areas, namely the cortex and medulla, which are responsible for the synthesis and secretion of important hormones in the mammalian body. The inner medulla, which is fairly homogeneous, produces catecholamines, while the outer cortex contains cells that produce the three major classes of steroid hormones. The outer cortex is divided into three distinct concentric zones, which produces specific steroid hormones depending on the enzymes present in the cells of each zone [43]. The adrenal cortex can be distinguished, from the surface inwards, as the *zonae glomerulosa* (zG), *fasciculata* (zF) and *reticularis* (zR). The zG is responsible for the biosynthesis of the major mineralocorticoid, aldosterone, which is produced and secreted in response to the stimulation by Angiotensin II (ANG II). Cells of the zF/R produce the main glucocorticoid, cortisol, which is synthesized and secreted under the stimulation of ACTH. The zR is further responsible for the production of the androgens. The location of the adrenals and the partitioning of the significantly different zones of the adrenal gland are shown in Figure 2.10.

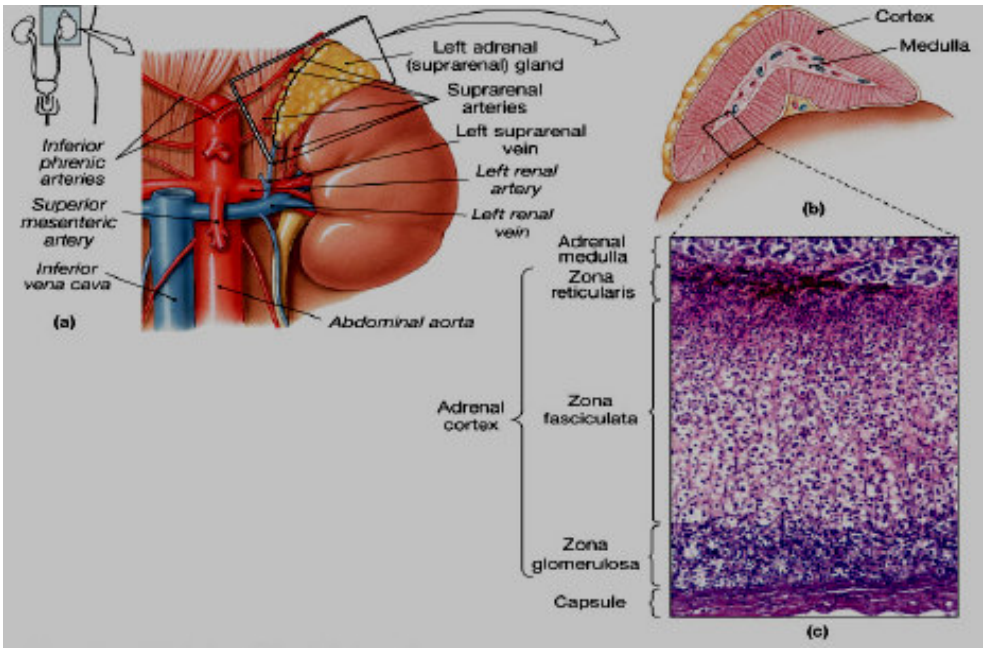

Figure 2.10. (a) Presentation of the location of the adrenal glands. (b) Characteristic partitioning of the adrenal gland into the adrenal cortex and medulla. (c) Three distinct concentric zones of the adrenal cortex [50].

2.3.1. Development of the adrenal cortex

The human adrenal cortex appears as a blastema of undifferentiated cells of mesodermal origin from a condensation of coelomic epithelial cells on the urogenital ridge at the 25th day after conception. Mesothelial cells begin to reproduce and invade the underlying mesenchyme during the fifth week of fetal development. During week six to eight, a second layer of cells from the mesoderm penetrates and surrounds the original cell mass, developing the first evidence of zonation. These cells are smaller than those of the first migration and form what will later become the definitive zone. The earlier mesothelial cells will develop into the fetal zone. Another cell type develops from the mesonephron, originating from the region of Bowman's capsule. Thus, the adrenal cortex stems from three embryologically distinct mesodermal cell lineages, two from the coelomic epithelium and one from the mesonephron [47].

During the 9th and 12th week of embryonic development the sinusoidal vascularization of the glands forms the framework for the zonation of the adrenal cortex. In the fourth month of gestation the fetal cortex reaches its maximum size and becomes larger than the kidney. During this period, the fetal cortex comprises the thin definitive zone, which remains undifferentiated, and the prominent fetal zone that expresses the steroidogenic enzymes. The fetal zone is lipid-rich and contains large eosiniphilic cells with the characteristics of steroid-secreting cells. These cells contain large numbers of tubular smooth endoplasmic reticulum, mitochondria with tubulovesicular cristae and Golgi complexes. In the outer regions of the fetal zone, the cells are positioned in tightly packed chords while in the central region the cells are more widely spaced. The undifferentiated definitive zone subsequently develops into the adult adrenal cortex. After the fourth month the fetal cortex reduces in size, cells from the definitive zone start to differentiate and replace the fetal cells. In the 28th week, the definitive zone, which consists of tightly packed basophilic cells arranged in a narrow band with columns of cells reaching into the outer rim of the fetal zone, begins to differentiate into the zG. The cells of the definitive zone have a small cytoplasmic volume and consist of free ribosomes, small mitochondria and small amounts of lipid. With increasing age the cells in this zone begin to resemble steroidogenically active cells. After birth, the fetal cortex rapidly degenerates, resulting in a dramatic reduction in adrenal mass. By the end of the first year of life, the transition zone between the definitive and fetal zones, which by this time is reduced

to largely fibrous tissue between the adult cortex and medulla, is still present. At 30 weeks the transition zone takes on the appearance of the zF. By late gestation the fetal adrenal cortex starts to resemble the adult adrenal cortex. Although there are immunohistochemical data, indicating that the zR appears at the end of the third year of life, there is little conclusive evidence to support this view [36, 47].

2.3.2. Functional zonation in steroidogenic expression

Functional zonation of the adrenal gland contributes towards the regulation of the synthesis of glucocorticoids, mineralocorticoids and adrenal androgens and relies, in part, on the zone-specific expression of the P450 and 3β-HSD enzymes.

CYP11A1 is expressed in all three zones of the adult adrenal cortex. Investigations of primate fetal adrenal glands revealed that the human adrenal gland expresses CYP11A1 in the fetal and transitional zones of the adrenal cortex only between 14 and 22 weeks of gestation. CYP11A1 is detectable in the definitive zone after 23 weeks. Studies on the expression of steroidogenic enzyme mRNA in human fetal adrenal glands revealed that CYP11A1 was most abundant in the adrenal gland between 20 and 21 weeks. In mouse primordium, CYP11A1 expression was observed as early as embryonic day 11 and in rat fetal adrenal glands at embryonic day 12. In the monkey, adrenal expression of CYP11A1 was observed in all three zones in late gestation [18, 36].

The expression of CYP17 in the adrenal gland is specie specific. CYP17 is expressed in the zF/R in the adrenals of human, bovine, macaque monkey and guinea pig. The zG, which is the site of aldosterone synthesis, lacks this enzyme. Furthermore, CYP17 is not expressed in mouse or rat adrenal glands. Investigations into the expression of CYP17 in human and monkey fetal adrenal glands showed that CYP17 mRNA and protein was detected in the transitional and fetal zones throughout gestation, but not in the definitive zone. CYP17 mRNA was detected in the mouse fetal adrenal gland between embryonic days 12.5 and 14.5, after which expression disappeared [18, 36].

CYP21, which is essential for the synthesis of the glucocorticoids and mineralocorticoids, is expressed in all three zones of the adrenal cortex. Immunohistochemistry of human fetal adrenal glands detected little CYP21 expression in the definitive zone, while all the cells of the transitional and fetal zones expressed this enzyme between weeks 13 and 24. In the adult adrenal gland, CYP21 expression is more intense in the zG/F, with little expression in the zR. The fetal adrenal gland of the rhesus monkey expressed CYP21 in all three zones between 109 days and term. However, CYP21 expression was markedly reduced in the fetal zone relative to the definitive and transitional zones [18, 36].

Human, rat and mouse CYP11B1 is expressed in the zF/R of the adrenal gland, while CYP11B2 is exclusively expressed in the zG. The expression of CYP11B1 is 100 times higher than that of CYP11B2 [51]. Rat CYP11B3 mRNA is expressed in the zF/R, but not in the zG. In the human fetal adrenals CYP11B1 and CYP11B2 are present in the transitional and fetal zones, but not in the definitive zone between 13 and 24 weeks of gestation. The expression of these enzymes is higher in the fetal zone than in the transitional zone. In the fetal rhesus monkey CYP11B1 and CYP11B2 was detected in all cells of the transitional and fetal zones between 109 days and term. These enzymes were absent in the definitive zone until near term. The developmental expression of rat CYP11B1, CYP11B2 and CYP11B3 in rat adrenal glands differs from that in adult rat adrenals. Studies with adrenal glands from neonatal day 2 rats revealed that a relatively large amount of CYP11B1 mRNA was expressed, with little detectable CYP11B2 and no detectable CYP11B3 mRNA. At day 10, CYP11B1 mRNA was significantly reduced and CYP11B3 became the main CYP11B mRNA until postnatal day 18. In the adult adrenal glands CYP11B3 expression is considerable less than CYP11B1 [18, 36].

Appropriate development of the steroidogenic ability of the primate fetal adrenal gland is vital for the maintenance of intrauterine homeostasis, the development of enzyme systems that are important for extrauterine life, and in some species, the timing of parturition. Studies performed with primate fetal adrenal glands showed that this gland consists of three functional zones: the outer definitive zone, which is believed to function as a reservoir of precursor stem cells that facilitate the secretion of mineralocorticoids from this zone until close to term; the middle transitional zone, which introduces steroidogenic cability by 24-28 weeks of human pregnancy and contains the enzymes that are important for the production of

de novo cortisol; and the inner fetal zone, which starts to function early in pregnancy and possesses the enzymes that are necessary for DHEA synthesis. These studies also demonstrated that glucocorticoid synthesis by the human fetal adrenal is possible early in intrauterine life. Studies in the human and rhesus monkey fetal adrenal gland showed that the definitive zone expresses CYP11A1, but not CYP17. The transitional zone expresses CYP11A1, CYP17, CYP21 and CYP11B1 during the last trimester. The localization and expression of CYP21 and CYP11B enzymes in the human and non-human primate fetal adrenal gland were studied using immunocytochemical techniques. CYP21 was identified in the transitional and fetal zones of the human adrenal gland between 13 and 24 weeks. In the fetal rhesus monkey CYP21 was present throughout the definitive-, transitional and fetal zones between 109 days and term. In the human fetal adrenal CYP11B1 was present in the transitional zone and the fetal zone between 13 and 24 weeks [52, 53].

Neonatal human males synthesize high levels of DHEA, which decline within a few months of birth as a result of deterioration of the adrenal fetal zone. Adult male humans and rhesus monkeys produce large quantities of these C19 steroids from the adrenal zR due to its high expression of CYP17 in combination with low expression of 3β-HSD. It is interesting to note that, in contrast to humans and other primates such as the rhesus monkey, the neonatal male marmoset monkey exhibits a C19 steroid-secreting fetal zone which is similar to humans and synthesizes DHEA at birth. However, the adult male fails to develop a functional zR and therefore does not produce large amounts of DHEA in adulthood [52, 53].

2.4. REGULATION OF ADRENAL STEROIDOGENESIS

The optimal synthesis and secretion of the essential gluco- and mineralocorticoids and adrenal androgens by the adrenal cortex depends on different mechanisms. The two principal effectors of glucocorticoid- and mineralocorticoid biosynthesis are ACTH and ANG II, while the adrenal androgen-stimulating hormone regulates androgen synthesis.

The temporary and immediate control of adrenal steroidogenesis is determined by the rate of cholesterol uptake into the mitochondria mainly *via* the action of StAR [54, 55]. The long-term regulation of steroidogenesis by these trophic hormones takes place principally through

changes in the expression levels of the various mitochondrial enzymes concerned in the conversion of cholesterol into hormonally active steroids, of which the initial step is catalyzed by the CYP11A1 [25].

Both short and long term stimulation of steroidogenesis depend essentially on the availability of cholesterol substrate. Upon binding to its cell-surface receptors, ACTH activates adenylyl cyclase and subsequently increases the cAMP concentration. The elevated cAMP levels further activate the cAMP-dependent protein kinase A (PKA) and phosphorylation of several proteins, including the cAMP response element binding protein (CREB). The phosphorylation of CREB takes place rapidly after stimulation of the cells with cAMP and leads to functional CREB activity. As the promoter area of the StAR gene lacks an identifiable cAMP response element (CRE), inactive (unphosphorylated) CREB does not act directly on the StAR promoter. However, the phosphorylated CREB can act indirectly, through an as yet unknown mechanism, on the StAR promoter and thus transactivates gene expression [56, 57]. Extracellular calcium is required for optimal ACTH binding and ACTH-induced steroidogenesis (Figure 2.11) [25].

The effects of ACTH on steroidogenesis can be divided into acute effects, which occur within minutes, and the chronic effects, which require hours or days.

2.4.1. The acute ACTH response

The acute response of ACTH takes place swiftly and has short-term effects on the steroidogenic process. The main purpose of this response is to increase the conversion of cholesterol to pregnenolone. The principal site of this regulation is at the delivery of free cholesterol to the mitochondria. This response is characterized by the rapid mobilization and transport of cholesterol through the steroidogenic system, leading to a quick production of corticoids.

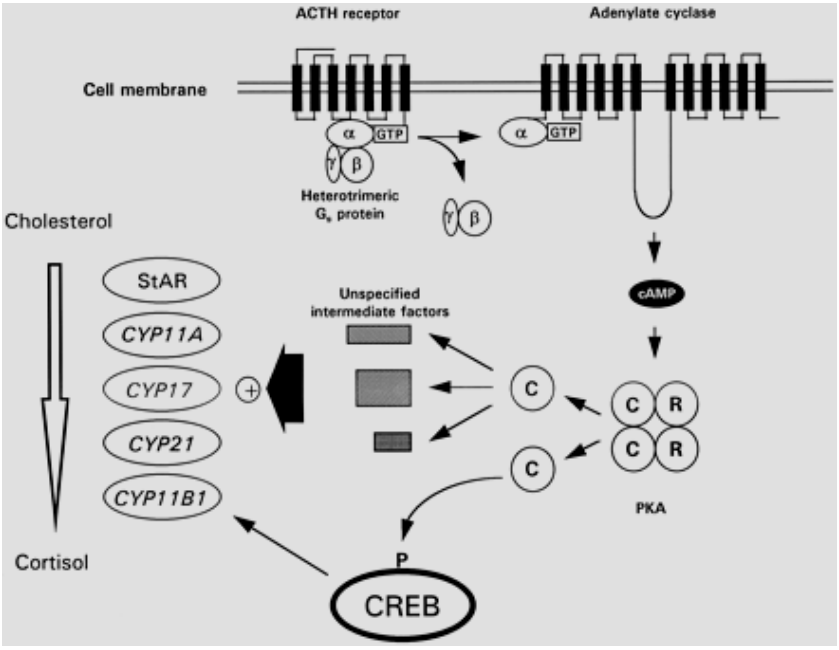

Figure 2.11. Mechanism of action of ACTH in stimulating steroidogenesis in the adrenal zF/R. ACTH binds to and stimulates its cognate seven-transmembrane domain receptor at the cell surface. The heterotrimeric G-protein is activated by exchanging GTP for GDP and the dissociation of the α-subunit from the ß?-subunits. Gsα stimulates the membrane-bound adenylate cyclase to synthesize cAMP, thus activating PKA in the cytosol. The catalytic subunits of PKA dissociate and phosphorylate target factors, including the cAMP response element binding protein (CREB). CREB and other factors, possibly substrates for PKA, activate StAR, inducing the transcription of CYP11A, CYP17, CYP21 and CYP11B, resulting in increased glucocorticoid synthesis [25].

The mobilization of cholesterol is mediated by the binding of ACTH to its receptors on the adrenal membrane, activating adenylate cyclase with a resulting increase in intracellular cAMP. The increased cAMP levels further activate cholesterol-esterase, *via* a cAMP-mediated phosphorylation, leading to the translocation of cholesterol from lipid droplets to the inner mitochondrial membrane. Steroidogenesis commences under the regulation of StAR, which can function as a sterol transfer protein, enhancing sterol desorption from the outer membrane to the inner membrane (Figure 2.12) [54, 55, 58]. Although the exact mechanism of StAR action is still unknown, it is assumed that the N-terminus of StAR is directed towards the mitochondria and presumably, by using C-terminal sequences, modifies the outer mitochondrial membrane resulting in the transfer of cholesterol from the outer to the inner membrane. This increase in cholesterol ultimately leads to an increase in the activity of CYP11A1, with the subsequent increase in the activities of the steroidogenic enzymes [22].

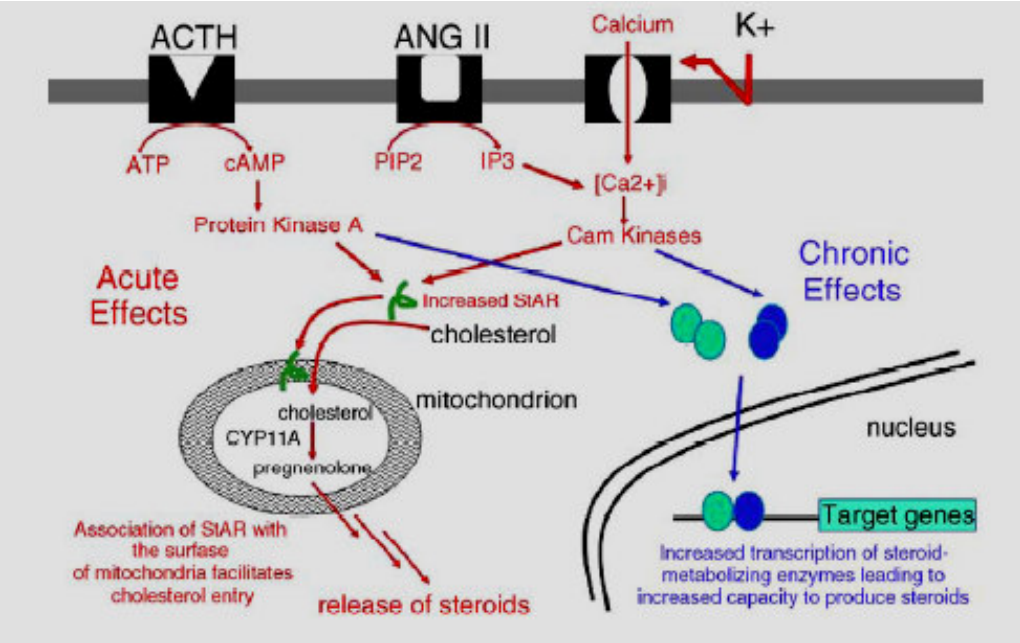

Figure 2.12. Signalling pathways that regulate steroid production in human adrenal cells. The primary regulators of adrenal steroid hormone biosynthesis are ACTH, ANG II and K^+, which are active at the level of the cell membrane. Both the CaM kinases and PKA pathways are able to activate acute and chronic steroid hormone biosynthesis. The green circles represent PKA, while the blue circles represent CaM kinases [58].

2.4.2. The chronic ACTH response

The chronic response in the regulation of glucocorticoid synthesis takes place progressively and has long-term effects on steroidogenesis. It takes place primarily at the level of gene transcription, leading to the manufacturing of more steroidogenic machinery and therefore increasing the cellular capability for steroidogenesis. Under normal physiological conditions the adrenal cortex is stimulated by ACTH in a pulsitile fashion, leading to optimal levels of steroidogenic enzymes present in the cells and the consequent diurnal rhythm of corticoid production (Figure 2.12) [54, 55, 58].

Extensive studies on the chronic response of ACTH in bovine adrenocortical cells showed that this peptide hormone leads to an increase in the levels of the adrenal steroid hydroxylases, CYP11A1, CYP17, CYP21 and CYP11B. This increase in enzyme levels was due to increased levels of mRNA in the adrenal cells, indicating that the chronic response of ACTH entails the regulation of the biosynthesis of the steroidogenic enzymes. ACTH binds to its specific receptor on the adrenal cell membrane and subsequently causes an increase in

the intracellular cAMP levels *via* the activation of adenylate cyclase. This activation stimulates the synthesis of the steroid hydroxylase inducing protein, which is involved in this process as a transcriptional factor and is responsible for the transcriptional activation of the genes encoding the steroidogenic cytochromes P450 (Figure 2.13). It further increases the mRNA levels for AdX and AdR and consequently lead to the transcription of both of the genes encoding these steroidogenic electron transport proteins. The elevated levels of steroidogenic components lead to an overall increase in steroidogenesis. It is evident that the primary function of ACTH in the regulation of optimal steroidogenic capacity is at the transcriptional level [54, 55, 58].

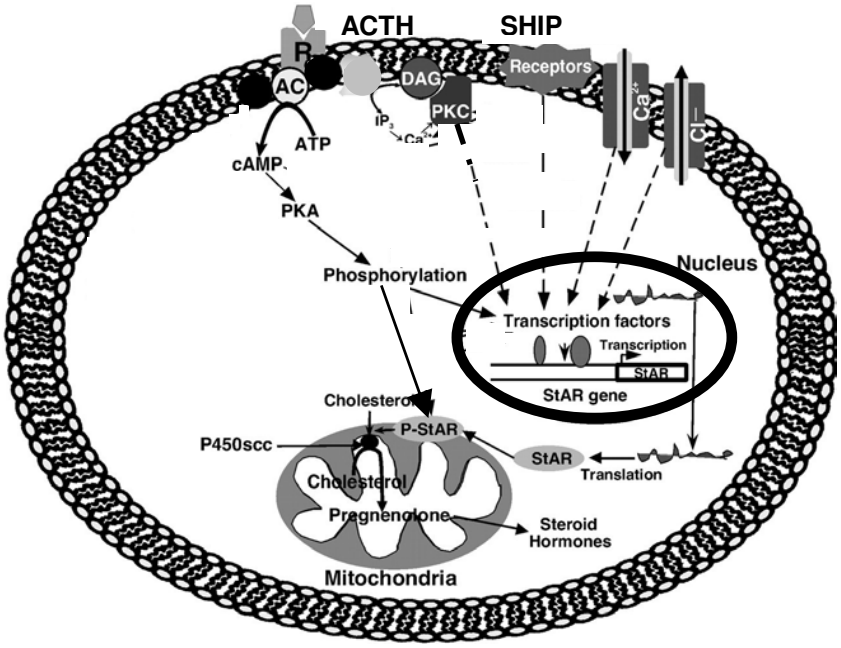

Figure 2.13. Illustration of signaling pathways in the regulation of StAR expression and steroidogenesis. ACTH interaction with specific membrane receptors results in the activation of G proteins, which, in turn, activate membrane-associated adenylyl cyclases (AC) that catalyzes cAMP formation from ATP. cAMP then activates PKA, which results in the phosphorylation of transcription factors regulating StAR gene transcription. CAMP-mediated signaling mechanisms predominantly regulate StAR expression and steroid biosynthesis in steroidogenic cells. The StAR protein regulates steroidogenesis by controlling the transport of cholesterol from the outer to the inner mitochondrial membrane, the site of CYP11A1. Conversion of cholesterol to pregnenolone is the first enzymatic step in steroid hormone biosynthesis. Ca^{2+} messenger system and Cl^{-} ions have been demonstrated to be effectively involved in potentiating trophic hormone-stimulated steroidogenesis and StAR expression. The PKC pathway is also involved in regulating the steroidogenic response. Activation of the PKC pathway results in an increase in the transcription and translation of StAR, but not its phosphorylation. Thus, StAR induced through the PKC pathway is inactive in cholesterol transfer. SHIP binds to specific membrane receptors and can stimulate the steroidogenic response *via* different signaling pathways [59].

2.4.3. Regulation of zone-specific expression of CYP11B isozymes by *cis*-elements

In humans, the capability of the adrenal cortex to differentially synthesize glucocorticoids and mineralocorticoids mainly relies on the zonal expression of the CYP11B isozymes, which in turn, ultimately depends upon several *cis*-elements and *trans*-acting factors that control gene transcription. The first 400 bases, located in the promoter regions of the human CYP11B isozymes, display a relatively high extent of sequence similarity. Regulation of the zone-specific expression of the CYP11B isozymes is performed by *cis*-elements, which is mainly located in the 5'-flanking regions of these genes. Numerous conserved *cis*-elements have been identified in the 5'-flanking region of CYP11B genes of various species. Studies with bovine CYP11B revealed the existence of several *cis*-element regions, namely Ad1 to Ad6, which bind nuclear proteins.

Equivalent sequences have been identified in human CYP11B1 and CYP11B2 genes. The *cis*-acting regulatory elements in the 5'-flanking regions of CYP11B1 and CYP11B2 were defined using luciferase reporter constructs and the NCI-H295R adrenocortical cell line, which expresses both isozymes under the control of the presumptive physiological signaling systems, namely cAMP, ANG II and K^+. Deletion and mutation studies of the 5'-flanking region of human CYP11B1 showed that steroidogenic factor-1 (SF-1) plays a crucial role in transcription of this gene *via* the interactions with an Ad4 element/SF-1 element at -249. This *cis*-regulatory element is similar to the Ad4 elements observed in other CYP11B1 genes. This study also revealed that a cAMP response element (CRE), which shows substantial sequence homology to the Ad1/CRE site in CYP11B2 genes and bovine CYP11B at position -78, was essential for cAMP stimulation of the reporter activity. Human CYP11B1 expression also entails *cis*-regulatory elements, comparable to those important for bovine CYP11B and mouse CYP11B2. H295R cells, which maintain ANG II and K^+ signaling pathways, were also used to analyse the human CYP11B2. Reporter constructs with serial deletions in this gene were used to localize the functionally important elements, which was further characterized by mutation, electrophoretic mobility shift assays and DNase I footprinting analysis. Two elements that were both required and adequate for basal reporter gene expression or for activity stimulated by either cAMP or calcium signaling pathways were identified at positions -78/-72 and -136/-121. The -78/-72 element is highly homologous to a consensus CRE and

corresponds to elements, which are known for their importance in the expression of murine CYP11B2, bovine CYP11B and human CYP11B1 genes. The -136/-121 element of human CYP11B2 shows 80% homology with the Ad5 element in bovine CYP11B. Mutations or deletions with this element decreased cAMP, ANG II and K^+ stimulated expression of the human reporter [60, 61].

2.4.4. Regulation of CYP11B2 by Angiotension II and potassium

Angiotensin II and extracellular potassium concentrations are the primary inducers of mineralocorticoid synthesis and secretion in the zG of the adrenal cortex. Angiotensin II, resulting from the action of the kidney protease, *rennin*, on liver-derived angiotensinogen, stimulates the zG cells by binding to specific G-protein-coupled receptors (AT1 receptors), which is affixed to phospholipase C. Phospholipase C further promotes the intracellular formation of inositol 1,4,5-triphosphate (IP_3), which causes a rise in the intracellular concentrations of free calcium ($[Ca^{2+}]_i$), and 1,2-diacylglycerol (DAG), leading to the activation of protein kinase C (PKC). The elevated $[Ca^{2+}]_i$ stimulates numerous Ca^{2+}/calmodulin-dependent protein kinases (CaM kinases) to phosphorylate and trigger activating transcription factors (ATF)-1, ATF-2 and cAMP-response-element binding protein (CREB) to initiate the transcription of the steroidogenic enzymes and subsequently increases the production of aldosterone (Figure 2.14) [23, 62].

The synthesis of aldosterone is extremely responsive to minute changes in extracellular $[K^+]$. An increase in $[K^+]$ triggers the depolarization in the cell membrane of the zG, which causes the opening of voltage-dependent L- and T-type Ca^{2+} channels, leading to a swift increase in the $[Ca^{2+}]$i. CaM and CaM kinases subsequently promote the phosphorylation of transcription factors to stimulate CYP11B2 gene transcription, which is therefore regulated by Ang II and K^+ through common Ca^{2+}-dependent signaling pathways and common transcription factors (Figure 2.15) [23, 44].

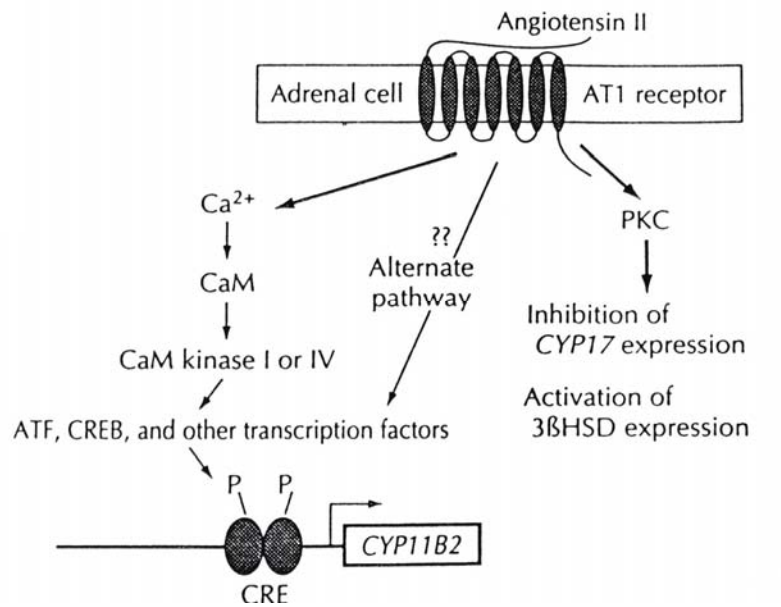

Figure 2.14. Actions of angiotensin II on the expression of steroidogenic enzymes. Angiotensin II is hypothesized to activate multiple signaling pathways that affect the expression of steroidogenic enzymes in different ways. ANG II increases intracellular levels of Ca^{2+}, activating CaM and CaM kinases as seen with potassium. ANG II, however, may have alternate pathways that can also increase CYP11B2 expression [62].

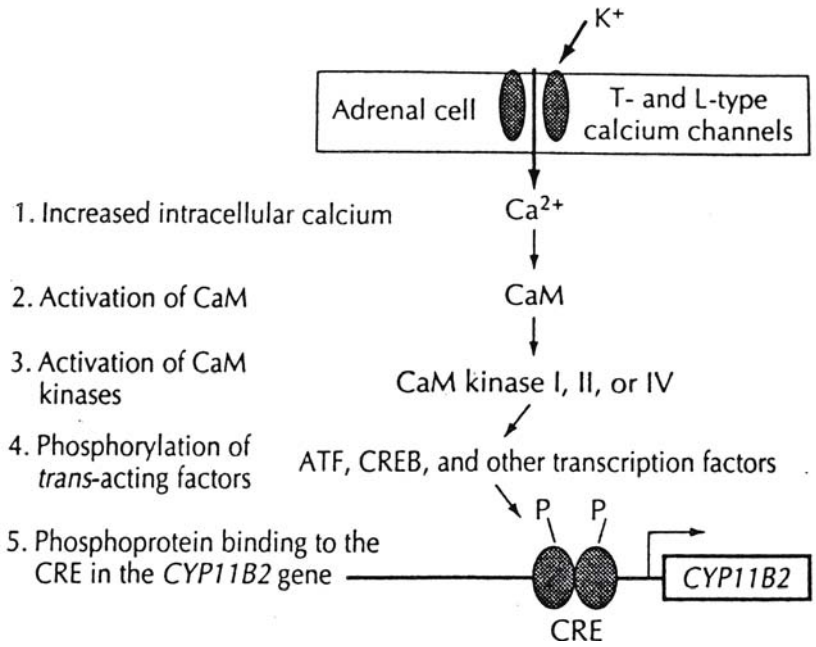

Figure 2.15. Actions of potassium on the expression of CYP11B2. Potassium increases the level of intracellular calcium, which activates CaM and the CaM kinases. CaM kinases I, II, or IV may phosphorylate several of the transcription factors that bind to the CYP11B2 CRE sequence and promote transcription [62].

Three main *cis*-elements that are important for the regulation of the differential expression of the human CYP11B2 gene in the adrenal zG have been identified as a CRE at -71/-64, a *cis*-element namely Ad5 at -129/-114 and, therein, another element called NBRE-1, which is a Nerve Growth Factor-Induced clone B (NGFIB) response element and is located at -766/-759. The CRE is common to both human CYP11B isozymes and is regulated by both PKA- and CaM-dependent protein kinase-dependent mechanisms. NBRE-1 and Ad5 of the human CYP11B2 promoter region are not found in the 5'-flanking region of human CYP11B1, indicating that these elements might be specific to the regulation of CYP11B2 transcription. The NBRE-1 and Ad5 sites can bind to members from the NGFIB family. Human CYP11B2 CRE binds activating transcription factors, ATF-1 and ATF-2, and CREB. Phosphorylation of ATF-1 and/or CREB by CaM-kinases increases the ability of these factors to enhance gene transcription (Figure 2.16.) [63].

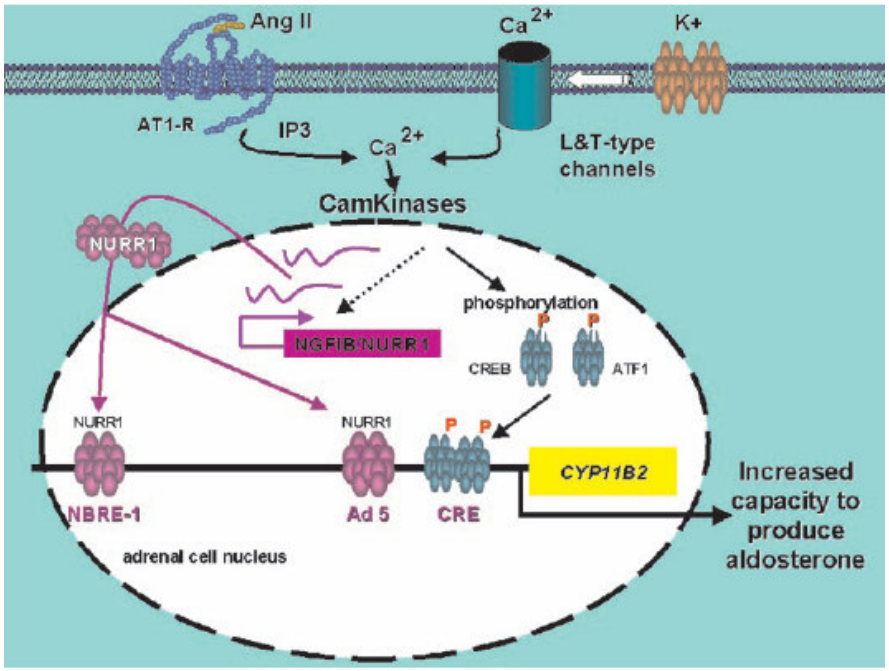

Figure 2.16. Schematic model of ANG II and K^+ regulation of human CYP11B2. ANG II, acting through the type I ANG II receptor (AT 1), and K^+ increase intracellular calcium, which, in turn, activates CaMK I and CaMK IV. CaMK I and/or CaMK IV phosphorylates ATF-1 and CREB, which increases binding to the human CYP11B2 CRE. Expression of NGFIB and NURR1 mRNA and protein are induced by ANG II, in part through the action of CaMK I and/or CaMK IV. NGFIB and/or NURR1 bind to the Ad5 and NBRE-1 *cis*-elements. Bound ATF-1/CREB and NGFIB/NURR1 activate human CYP11B2 gene expression. This increase in CYP11B2 transcription directly determines the capacity of the adrenal glomerulosa to produce aldosterone [63].

As in the case of glucocorticoid synthesis, ACTH stimulates the increase in the amount of circulating androgens. ACTH binds to its receptors on the cell surface of the adrenal cortex where it activates an adenylate cyclase *via* a G_s-coupled protein. This generates an increase in cAMP with a subsequent activation of PKA, which further phosphorylates cholesterol ester hydroxylase, allosterically activating it. This results in an increase in free cholesterol, which is then converted to pregnenolone. Pregnenolone subsequently enters the steroid biosynthesis pathways and undergoes various hydroxylations to yield the androgens.

2.5 SUMMARY

Adrenocortical steroids, classified as glucocorticoids, mineralocorticoids and androgens, are essential endocrine factors that control the maintenance of energy mobilization, stress response, sodium/potassium homeostasis and sexual differentiation. The steroidogenic pathway is catalyzed by several enzymes, which are expressed in a tissue- and species-specific manner, converting cholesterol to various steroid hormones. The first and rate-limiting step is facilitated by StAR, which translocates cholesterol from the outer to the inner mitochondrial membrane, where CYP11A1 catalyzes the metabolism of this substrate. The microsomal P450 enzymes, CYP17 and CYP21, are responsible for synthesizing the intermediates, 11-DOC and 11-deoxycortisol, for mineralocorticoid- and glucocorticoid synthesis, respectively. The mitochondrial CYP11B1 catalyzes the formation of corticosterone and cortisol from 11-DOC and 11-deoxycortisol, respectively, while CYP11B2 further metabolizes corticosterone to aldosterone.

In the normal human adrenal cortex the final steps in glucorticoid and mineralocorticoid production are catalyzed by the CYP11B isozymes, CYP11B1 and CYP11B2, respectively. The closely related human CYP11B isozymes catalyze key reactions in the biosynthesis of steroid hormones. CYP11B1 is expressed at high levels in the zF/R of the adrenal cortex where 11-deoxycortisol is hydroxylated at the 11β-position to synthesize cortisol, the major human glucocorticoid. The principal mineralocorticoid, aldosterone, is produced by CYP11B2, which is expressed at very low levels in the zG. The limitation of CYP17 expression in the zF/R and CYP11B2 to the zG leads to functional zonation of cortisol and aldosterone biosynthesis to these respective zones. Cortisol is formed by the 11β-hydroxylation of 11-deoxycortisol and plays a crucial role in the energy mobilization, stress response and the immune response of the human body and is generally secreted 100 to 1000-

fold in excess over aldosterone. This major mineralocorticoid plays an important part in the regulation of the salt and water maintenance of the body, thereby regulating blood pressure. The final steps in the synthesis of aldosterone are the 11β-hydroxylation of 11-DOC to corticosterone, which is further 18-hydroxylated and 18-oxidated to yield 18-hydroxycorticosterone and finally aldosterone, respectively. Mutations in the structural genes of these isozymes lead to various human diseases, which have major physiological effects. Mutations in the CYP11B1 gene cause 11β-hydroxylase deficiencies, leading to CAH, which is characterized by androgen excess and hypertension. Mutations in CYP11B2 cause a defect in the aldosterone biosynthesis that can lead to hyponatremia, hyperkalemia, and hypovalemic shock in infants and failure to thrive in childhood. Unequal crossing-over between the CYP11B genes can produce a duplicated chimeric gene with the transcriptional regulatory region of CYP11B1, with adequate coding sequences from CYP11B2 so that the encoded enzyme has CYP11B2 activity and is expressed under the regulation of ACTH. This recombinant CYP11B1/CYP11B2 gene leads to glucocorticoid suppressible hyperaldosteronism, which is a form of genetic hypertension, inherited in an autosomal dominant manner.

ACTH and angiotensin II, which have vital effects on the tissue-specific expression of steroidogenic enzymes, primarily regulate adrenal steroidogenic production of glucocorticoids and mineralocorticoids.

CHAPTER THREE

BABOON CYP11B1: THE LOCALIZATION AND CATALYTIC ACTIVITY IN BABOON ADRENAL TISSUE

3.1. INTRODUCTION

The biosynthesis of glucocorticoids and mineralocorticoids is catalyzed by a single CYP11B enzyme in some species while two or more CYP11B isozymes have been identified in other species. In cattle, pigs, sheep and frogs only one CYP11B catalyzes the biosynthesis of glucocorticoids and mineralocorticoids. Immunohistochemical investigations in cattle revealed that CYP11B is expressed in the zF and to a lesser extent in the zG of the adrenal cortex [43]. Sheep CYP11B is uniformly expressed throughout the three cortical zones of the adrenal gland [64]. In pigs, the 11β- and 18-hydroxylation of 11-DOC takes place in the zF/R, while the conversion of 11-DOC to aldosterone takes place in the zG [44].

In humans and rats *in situ* hybridization and immunohistochemical studies into the localization of the enzyme showed that CYP11B1 and CYP11B2, which exhibit zone specific activities, are uniquely expressed in the zonae of the adrenal cortex. As with mouse and rat, the hamster CYP11B2 gene is expressed in the zG, while CYP11B1 is expressed in the zF/R [44, 65]. In contrast to the other species, the rat also possesses two additional CYP11B genes, namely CYP11B3 and CYP11B4. CYP11B3, which is highly homologous to CYP11B1, hydroxylates 11-DOC to 18-hydroxy-corticosterone and corticosterone, but not to aldosterone. CYP11B4 lacks a sequence corresponding to exon three and a part of exon four, which is present in the other isoforms, and is therefore considered to be a pseudogene [66, 67]. Three genes, CYP11B1, CYP11B2 and CYP11B3, encoding CYP11B isozymes, have also been cloned from the guinea pig. Since guinea pig CYP11B3 is not expressed it is believed to be a pseudogene [68].

In situ hybridization investigations of Cape baboon CYP11B1 localized mRNA transcripts of this enzyme primarily to the zF/R. Signal was also detected in the zG and scattered within the medulla. The signal obtained in the zG could be attributed to sequence similarity between baboon CYP11B1 and CYP11B2. Immunohistochemical studies revealed that Cape baboon

CYP11B1 was expressed only in the zF/R and the medulla; this gene was not found to be expressed in the zG [2, 69]. The presence of CYP11B1 mRNA transcripts has also been reported in the human and rat adrenal medulla, which is closely interconnected with the cortical cells. These hybridization signals were detected in clusters of cortical cells situated in the medulla [66, 70, 71, 72]. Immunohistochemical studies to localize the CYP11B1 in the rat adrenal cortex also showed the staining of cortical tissue scattered intramedullary [66].

Immunohistological studies revealed the presence of CYP11B in histologically distinct regions of the adrenal, the cortical zF/R and the medulla [2]. Since two baboon CYP11B isoforms were identified, the localization of CYP11B was further investigated in adrenal medullary- and cortical tissue homogenates using Western blot analysis to establish if both isoforms were present in the adrenal cortex and medulla. The presence of the redox proteins, AdR and AdX, which is essential for catalytic activity of CYP11B1, was also investigated in these tissue homogenates. As a control the presence of the mitochondrial CYP11A1 and microsomal CYP21 in these homogenates were also examined. The catalytic activity of baboon CYP11B1 in these adrenal homogenates was determined by following the conversion of 11-DOC and corticosterone.

3.2. MATERIALS AND METHODS

3.2.1. Animals

Adrenal tissue was obtained from randomly selected normal adult Cape baboons housed at the animal units of the University of Cape Town Medical School and the University of Stellenbosch Medical School. All anesthetic and surgical procedures were permitted by the Animal Research and Ethics committee of the two Universities and complied with the "Principles of Laboratory Care" and the "NIH Guide for the Care and Use of Laboratory Animals" 1996.

3.2.2. Reagents

11-DOC, corticosterone, aldosterone and isocitrate dehydrogenase were obtained from Sigma Chemical Co. (St Louis, MO, USA). Isocitrate and NADPH were acquired from Merck, Darmstadt, Germany and Boehringer Mannheim GmbH, Germany, respectively. A

SuperSignal1 West Pico Chemiluminescent Kit was purchased from Pierce Chemical Company, Rockford, USA. Thin layer chromatography (TLC) plates were from Merck, Darmstadt, Germany. Tritiated steroids (^{3}H-DOC, ^{3}H-Corticosterone) were obtained from Amersham Life Science (Amersham Laboratories, Buckinghamshire, England). All other chemicals were purchased from local supply houses and were of the highest purity.

3.2.3. Preparation of baboon adrenal cortical- and medullary tissue homogenates

Baboon adrenal cortex and medulla were microscopically dissected under a Nikon T104 microscope and a crude homogenate of each adrenal preparation was obtained by homogenizing the respective tissue (5 g) in five volumes of 0.25 M sucrose solution (1 mM EDTA, pH 7.4) at 4 °C. The protein concentrations of the homogenates were subsequently determined using the Pierce BCA method. The cytochrome P450 content was determined by preparing a 1:4 dilution of the respective homogenates in 0.1 M sodium phosphate buffer (10% ethylene glycol). Each suspension was saturated with carbon monoxide for 30 seconds and a baseline was subsequently recorded between 400 nm and 500 nm. Sodium dithionite was added to the sample cuvette and the contents of the cuvette mixed by gentle inversion. A difference spectrum was recorded between 400 and 500 nm for each homogenate. The concentrations of cytochrome P450 in each preparation were calculated using a millimolar extinction coefficient of 91 $mM^{-1}.cm^{-1}$ [73]. The homogenates were stored at -20 °C until further use.

3.2.4. SDS-PAGE and Western blot analyses of baboon adrenal cortical- and medullary tissue homogenates

Baboon adrenal cortical- and medullary tissue homogenates, sheep testes microsomes and purified sheep CYP11B1, CYP11A1 and AdR were subjected to SDS-PAGE (12.5%; 20 µg protein per lane) and transferred onto a nitrocellulose membrane. Western Blot analysis was carried out using rabbit anti-sheep CYP11B1-, AdR-, AdX-, CYP11A1- and CYP21 IgG (1:1000). Immunoreacting proteins were detected using SuperSignal® West Pico Chemiluminescent Substrate (Pierce Chemical Company, Rockford, USA), according to the manufacturer's instructions. This method of detection allowed detection of picogram amounts of antigen.

3.2.5. Determination of CYP11B1 activity in baboon adrenal tissue homogenates

3.2.5.1. TLC analysis of 11-DOC and corticosterone metabolites in crude adrenal tissue homogenates

A pilot study to ascertain CYP11B1 activity in baboon adrenal tissue homogenates was performed. Two parallel conversion assays for 11-DOC to corticosterone and corticosterone to 18-hydroxy-corticosterone, were carried out in triplicate in adrenal cortical- and medullary tissue homogenates as previously described [69]. The steroid metabolites were subsequently analyzed by TLC.

11-DOC (1 µM) and tritiated DOC (100 000 cpm/5 µl) were pipetted onto filter paper, placed into microcentrifuge tubes and dried under vacuum. Tris-HCl buffer (50 mM, pH 7.4, containing 50 mM NaCl and 1% BSA), 2.2 µM isocitrate, 0.398 U isocitrate dehydrogenase and 22 µM $MgCl_2$ were added to each tube, to a final volume of 500 µl and the reaction mixtures were preincubated for 10 minutes in a shaking waterbath at 37°C. The two respective adrenal tissue homogenates (0.5 µM P450) were added to the reaction mixtures and incubated for an additional 5 minutes. Aliquots (50 µl) were removed from each reaction mixture, as zero time points, and immediately transferred to 5 ml ice-cold dichloromethane, containing 450 µl water. The reaction was initiated by the addition of NADPH to a final concentration of 22 µM of the total volume. Aliquots (50 µl) were removed and immediately mixed with 5 ml dichloromethane and 450 µl water, at specific intervals of 10, 20, 30, 40 minutes. The steroid metabolites were subsequently extracted by vortexing each sample for 30 seconds and separating the organic and aqueous phases by centrifugation, after which the aqueous phase was aspirated off. Anhydrous sodium sulphate was added to the organic phase and the mixture was centrifuged on a bench top centrifuge at room temperature for 5 minutes. After centrifugation, the steroid-containing dichloromethane was removed, dried at room temperature under N_2 and subsequently analyzed by TLC.

The dried steroid metabolites were redissolved in 100 µl dichloromethane by vortexing for 2 minutes. 11-DOC and corticosterone (2 mg/ml ethanol) standard solutions were prepared and, together with the samples, spotted onto a TLC plate. The TLC plate was transferred to a chromatographic tank, containing $CHCl_3$/MeOH (98:2), and developed for 1.5 hours. Each

metabolite was identified using the corresponding steroid standards. The separated steroids were cut out from the TLC plate and transferred to a scintillation vial containing 8 ml Beckman Ready Flo Scintillation fluid. The samples were stored in the dark for 12 hours before analyses in a Beckman LS 3801 scintillation counter.

Corticosterone conversion by the crude adrenal tissue homogenates was investigated as described above using corticosterone, 18-hydroxycorticosterone and aldosterone as steroid standards during TLC analyses of the reaction products.

3.2.5.2. HPLC analysis of 11-DOC and corticosterone metabolites in crude adrenal tissue homogenates

Conversion assays of 11-DOC (10 μM) and corticosterone (10 μM) were carried out in adrenal cortical- and medullary tissue homogenates and steroid metabolites were extracted as described in 3.2.5.1. The steroid metabolites, redissolved in 100 μl methanol, were subsequently analyzed using high pressure liquid chromatography (HPLC) on a Waters (Milford, MA) high performance liquid chromatograph coupled to a WISP^{TM} automatic injector (Waters) and a radioactive flow detector (Radiomatic, Tampa, FL). Steroid standards and metabolites were separated on a Novapak® C_{18} column at a flow rate of 1 ml/min. The mobile phase consisted of solvent A (water) and solvent B (100% methanol). Steroids were eluted using a linear gradient from 100% A to 100% B in 40 minutes.

3.2.5.3. APcI-MS analysis of a steroid metabolite formed during corticosterone metabolism in adrenal medullary tissue homogenate

HPLC analysis of the corticosterone conversion assay in the adrenal medullary tissue homogenates revealed a steroid metabolite eluting at the same retention time as the steroid standard, aldosterone. In order to unambiguously identify this steroid metabolite, a conversion assay with unlabeled corticosterone (10 μM) was performed as described in 3.2.5.1 and an aliquot was removed from the reaction mixture after 50 minutes. The steroid metabolites were extracted as described in 3.2.5.1 and subjected to HPLC analysis under the same conditions described in 3.2.5.2. The steroid metabolite, eluting at retention time 28.5 minutes, was collected, dried at room temperature under N_2 and subjected to atmospheric pressure chemical

ionization-mass spectrometry (APcI-MS). The samples were redissolved in 100 µl methanol, containing 0.5% (v/v) formic acid. Samples and an aldosterone standard, 10 µl, were injected through a Rheodyne injection port and delivered to the system using methanol, containing 0.5% (v/v) formic acid as the carrier solvent at 50 µl/min. An APcI positive ionization mode was used, with source and probe heater temperatures of 120°C and 200°C, respectively. The cone voltage was set at 55V.

3.3. RESULTS

The concentration of the P450 in the crude preparations was determined spectrophotometrically by the method of Sato and Omura, as 13.3 nmol P450/mg protein and 16.7 nmol P450/mg protein for the medullary- and cortical tissue homogenates, respectively [8]. Figure 3.1.A and B shows the carbon monoxide induced difference spectra, which was used to determine the P450 content for the medullary- and cortical tissue homogenates respectively, indicating the presence of active P450 enzymes (absorbance maximum at 450 nm). The slight shoulder observed at approximately 425 nm in Figure 3.1.A can be attributed to the presence of cytochrome b5.

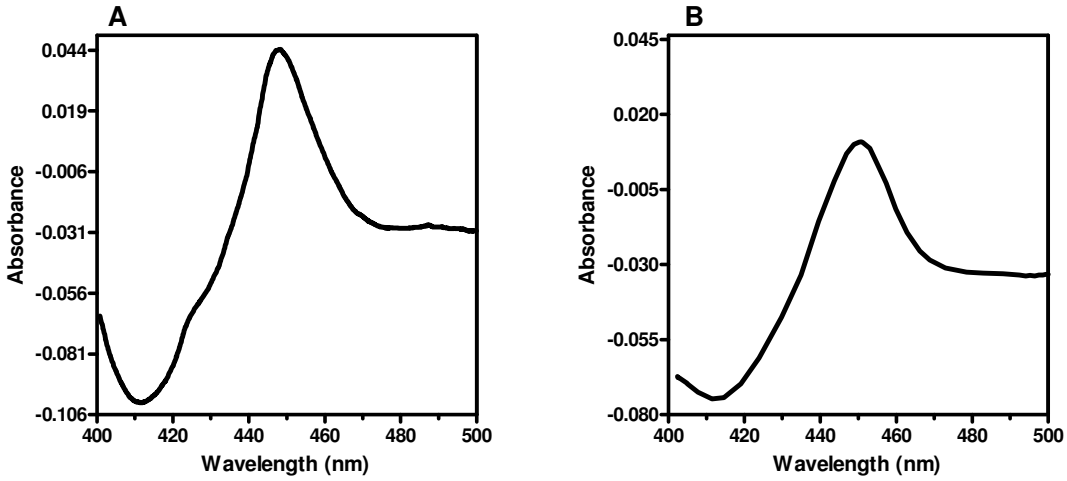

Figure 3.1. Sodium dithionite-reduced carbon monoxide-induced difference spectrum of P450 in (A) Medullary- and (B) Cortical tissue homogenates.

3.3.1. SDS-PAGE and Western Blot Analyses

Purified sheep CYP11B1, CYP11A1, AdR, cortical- and medullary tissue homogenates, sheep microsomes, together with molecular mass markers, were subjected to SDS-PAGE. Purified sheep CYP11B1 was used as a reference protein as purified baboon CYP11B1 was not available and expression of baboon CYP11B1 in COS-1 cells did not yield sufficient protein for detection using Western blot analyses. The molecular mass markers were used to determine the apparent molecular masses of the purified proteins and those in the adrenal tissue homogenates and sheep microsomes. The purified proteins were used as references to determine the presence and size of the respective proteins in the baboon adrenal homogenates. The sheep testes microsomes were used as a control.

The localization of CYP11B1, AdR, AdX, CYP11A1, and CYP21 was investigated in baboon adrenal cortical- and medullary tissue homogenates and sheep testes microsomes using Western blot analysis. Since baboon CYP11B1 antibodies were not available, CYP11B1 in the cortical- and medullary tissue homogenates was identified using a rabbit anti-sheep CYP11B1 antibody. CYP11B1 was demonstrated as a single band in the cortical tissue homogenate and as two distinct bands in the medullary tissue homogenate (Figure 3.2). The single band in the cortical tissue homogenate corresponded to an apparent Mr of approximately 54 kDa. A band indicating a protein of similar mass was identified in the medullary tissue homogenate as well as a second band, corresponding to an apparent Mr of approximately 51 kDa.

The presence of AdR (54 kDa) in both the cortical- and medullary tissue homogenates, could not be established with certainty as the precipitation bands were not well defined on the Western blot. AdX (14 kDa), however, was detected clearly only in the cortical tissue homogenate. CYP11A1 and CYP21 were used as controls to monitor cross contamination between the cortical tissue and medullary tissue homogenates. Baboon CYP11A1 and CYP21 were detected in the cortical tissue homogenate only with apparent molecular weights of 52 kDa and 47 kDa, respectively (Figure 3.3).

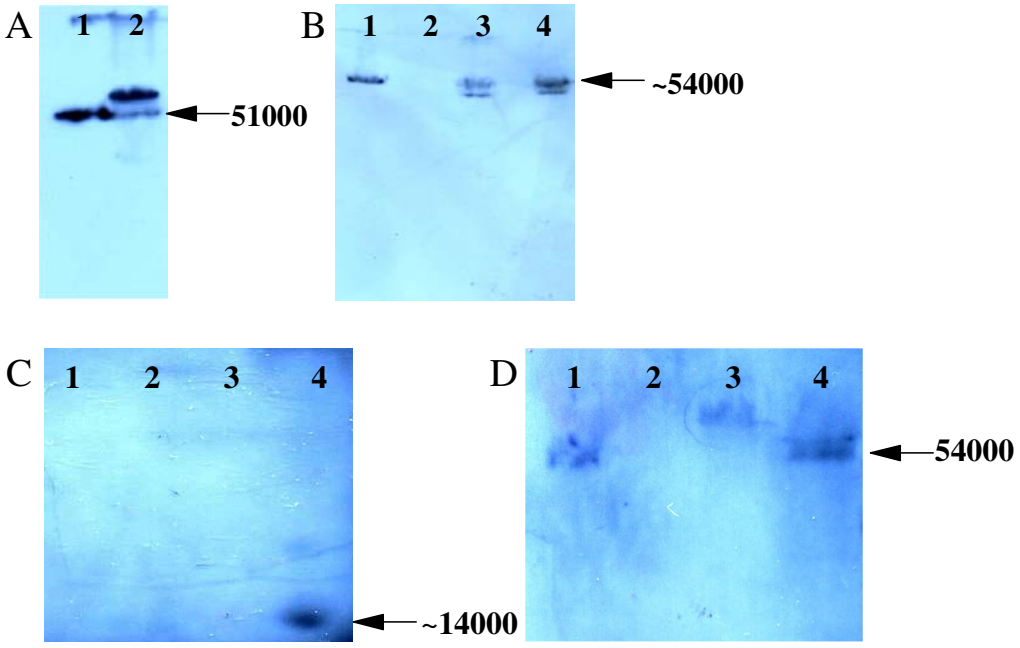

Figure 3.2. Immunoblots of baboon adrenal cortical tissue-, medullary tissue homogenates and testes microsomes with rabbit anti-sheep IgG. Purified sheep CYP11B1 (5 µg protein/lane), purified sheep AdR (5 µg protein/lane), tissue homogenates (20 µg protein/lane) and testes microsomes (20 µg protein/lane) were separated on 12.5% SDS-PAGE. Proteins were detected using: rabbit anti-sheep CYP11B1 IgG (A, B), rabbit anti-sheep AdX IgG (C), rabbit anti-sheep AdR IgG (D), respectively. **A:** Lane 1, purified sheep CYP11B1 (52 kDa); and lane 2, medullary tissue homogenate (51 kDa and ~54 kDa); **B:** Lane 1, cortical tissue homogenate; lane 2, sheep testes microsomes; lanes 3 and 4, medullary tissue homogenate; **C:** Lane 1, medullary tissue homogenate; lane 2, testes microsomes; lanes 3, medullary tissue homogenate, and lane 4, cortical tissue homogenate; **D:** Lane 1, medullary tissue homogenate; lane 2, testes microsomes; lanes 3, cortical tissue homogenate, and lane 4, purified sheep AdR.

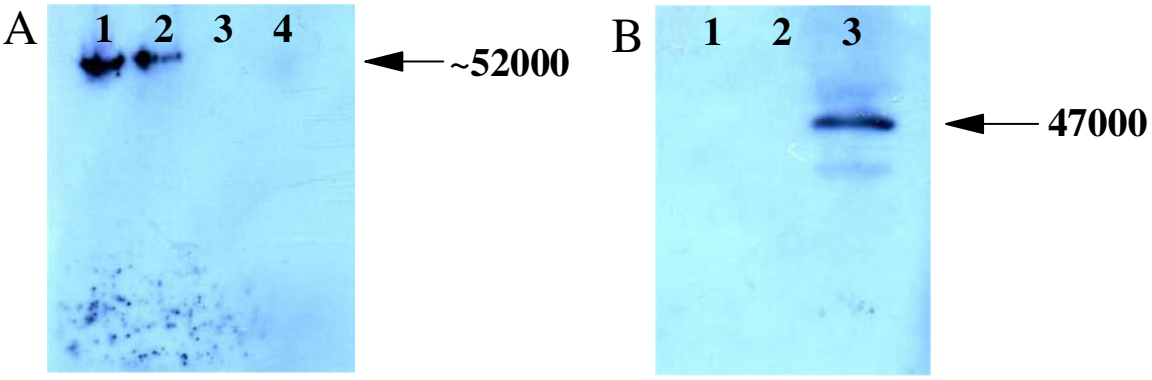

Figure 3.3. Immunoblots of baboon adrenal cortical tissue-, medullary tissue homogenates and testes microsomes with rabbit anti-sheep IgG. Purified sheep CYP11A1 (5 µg protein/lane), tissue homogenates (20 µg protein/lane) and testes microsomes (20 µg protein/lane) were separated on 12.5% SDS-PAGE. Proteins were detected using: rabbit anti-sheep CYP11A1 IgG (A) and rabbit anti-sheep CYP21 IgG (B), respectively. **A:** Lane 1, purified sheep CYP11A1 (52 kDa); lane 2, cortical tissue homogenate; lane 3, medullary tissue homogenate; and lane 4, testes microsomes; **B:** Lane 1, sheep testes microsomes; lane 2, medullary tissue homogenate; lane 3, cortical tissue homogenate.

The localization of CYP11B1 in the cortical- and medullary tissue homogenates prompted further investigations of CYP11B1 activity towards 11-DOC and corticosterone in the cortical- and medullary tissue homogenates.

3.3.2. Analyses of CYP11B1 activity in baboon adrenal tissue homogenates

3.3.2.1. TLC analyses of 11-DOC and corticosterone metabolites in adrenal tissue homogenates

TLC analyses of the steroid metabolites obtained in the metabolic conversion assays showed that, in the cortex, CYP11B1 exhibited 11β-hydroxylase activity towards 11-DOC only. The metabolism of 11-DOC in the cortical tissue homogenate yielded a 23% conversion to corticosterone, which was not further metabolized to 18-hydroxycorticosterone and aldosterone (Figure 3.4.A). As this was a pilot study, no statistical analysis was performed on the data which is the average of three experiments.

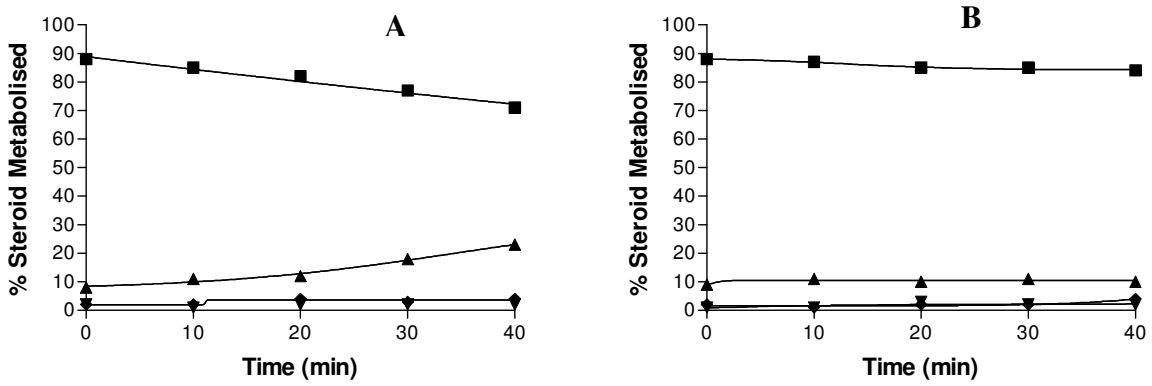

Figure 3.4. 11-DOC metabolism in (A) baboon adrenal cortical tissue homogenate and **(B)** medullary tissue homogenate. 11-DOC (■), corticosterone (▲), 18OH-corticosterone (▼), aldosterone (♦).

In the medullary tissue homogenate, the metabolism of 11-DOC yielded negligible corticosterone, with no detectable downstream conversion (Figure 3.4.B). However, when corticosterone was added to the reaction assay as substrate, approximately 25% corticosterone was converted to 18-hydroxycorticosterone, with the subsequent formation of aldosterone (Figure 3.5.B). No intermediates or aldosterone were detected during corticosterone metabolism in the cortical tissue homogenate (Figure 3.5.A).

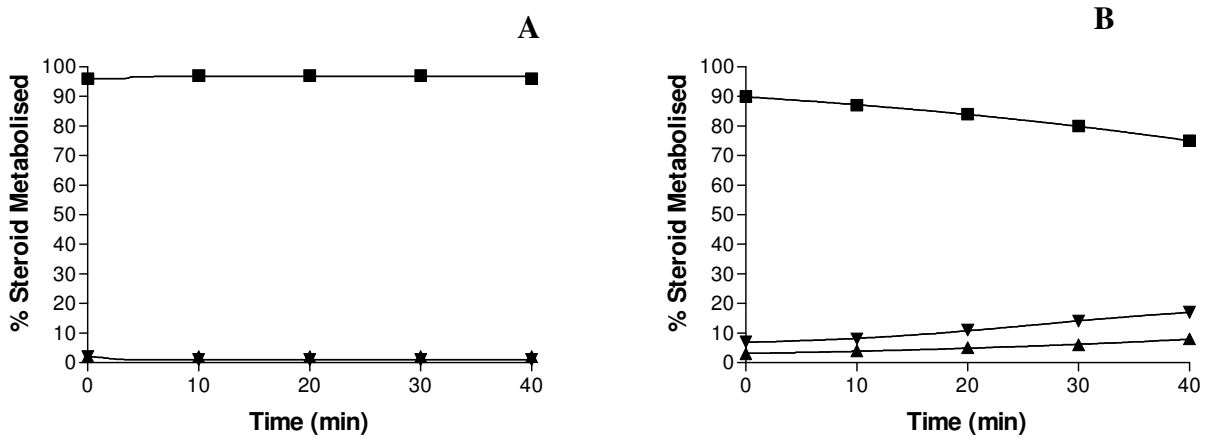

Figure 3.5. Corticosterone metabolism in (A) baboon adrenal cortical tissue homogenate and (B) medullary tissue homogenate. Corticosterone (■), 18OH-corticosterone (▲), aldosterone (▼).

Analysis of 11-DOC and corticosterone metabolism in baboon adrenal cortical- and medullary tissue homogenates after 50 minutes showed that the conversion of 11-DOC and corticosterone differed markedly (Figure 3.6). In the cortical tissue homogenates 11-DOC was converted to 34% corticosterone, while its conversion in the medullary tissue homogenates was 18%. Corticosterone conversion in the cortical tissue homogenates was less than 2%. However, the conversion in the medullary tissue homogenates was 28%.

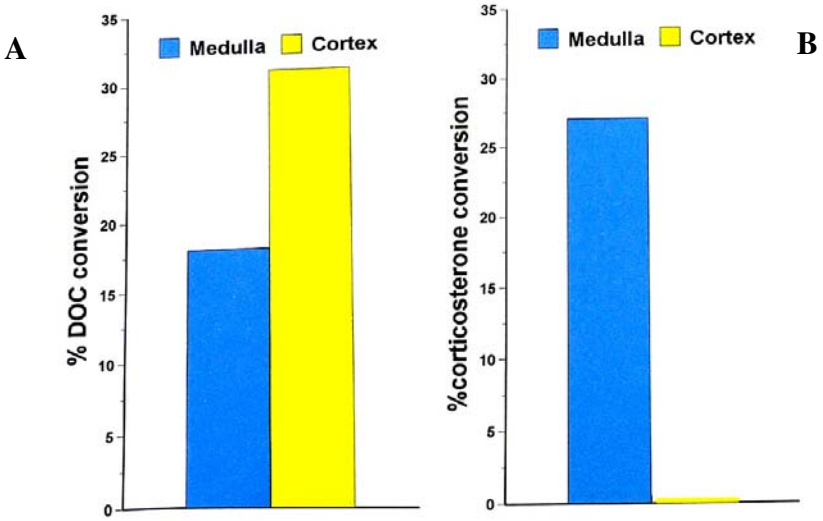

Figure 3.6. 11-DOC and corticosterone metabolism in baboon adrenal cortical- and medullary tissue homogenates. A: Corticosterone (1µM) conversion in the medullary- and cortical tissue homogenates. **B:** 11-DOC (1µM) conversion in the medullary- and cortical tissue homogenates.

Steroid metabolites produced in the conversion assays of 11-DOC and corticosterone were subsequently subjected to more stringent analyses using HPLC as well as APcI-MS analyses.

3.3.2.2. HPLC analyses of 11-DOC and corticosterone metabolites in adrenal tissue homogenates

HPLC analyses of 11-DOC metabolism after an incubation period of 40 minutes confirmed that the steroid was metabolized to only corticosterone in the cortical tissue homogenate. The chromatograms in Figure 3.7.A, B show 11-DOC (peak 1) and corticosterone (peak 2) eluting at 34.5 and 32.4 minutes, respectively. No 18-hydroxy-corticosterone or aldosterone was detected. Furthermore, no aldosterone was detected when corticosterone metabolism was assayed in the cortical tissue homogenates (Figure 3.8.A, B).

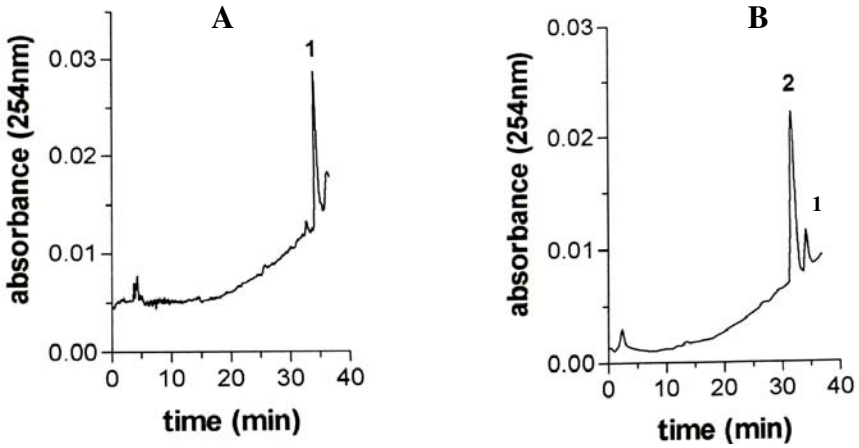

Figure 3.7. HPLC analyses of 11-DOC (10 μM) metabolites assayed in the baboon cortical tissue homogenates after 40 min. A: Metabolites assayed at time zero: **1,** 11-DOC, retention time 34.5 minutes. **B:** Metabolites assayed after 40 minutes: **1**, 11-DOC, retention time 34.5 minutes and **2**, corticosterone, retention time 32.4 minutes.

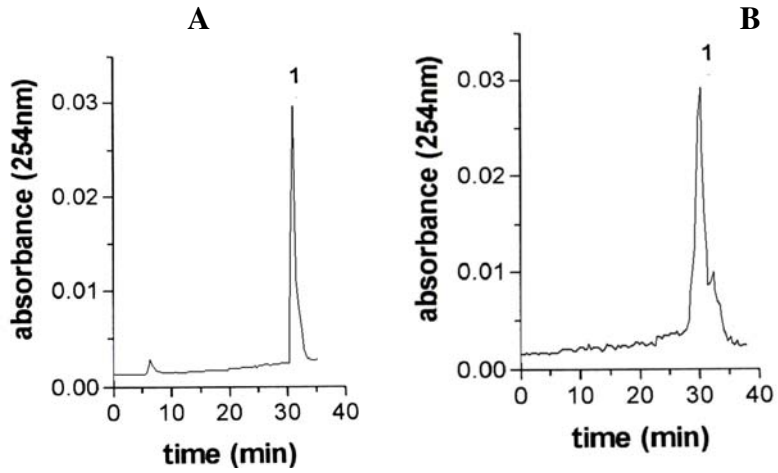

Figure 3.8. HPLC analyses of corticosterone (10 μM) metabolites assayed in the baboon cortical tissue homogenates after 40 min. A: Metabolites assayed at time zero: **1,** corticosterone, retention time 32.4 minutes. **B:** Metabolites assayed after 40 minutes: **1**, corticosterone, retention time 32.4 minutes.

Analyses of the conversion of 11-DOC in the medullary tissue homogenate showed that less corticosterone was produced, with no 18-hydroxy-corticosterone or aldosterone being detected (Figure 3.9.A, B). However, when corticosterone metabolism was investigated in the medullary tissue homogenates, 18-hydroxy-corticosterone and aldosterone metabolites were detected with retention times, 30.5 and 28.5 minutes, respectively (Fig. 3.10.A, B). The retention times of these metabolites corresponded with that of the steroid standards.

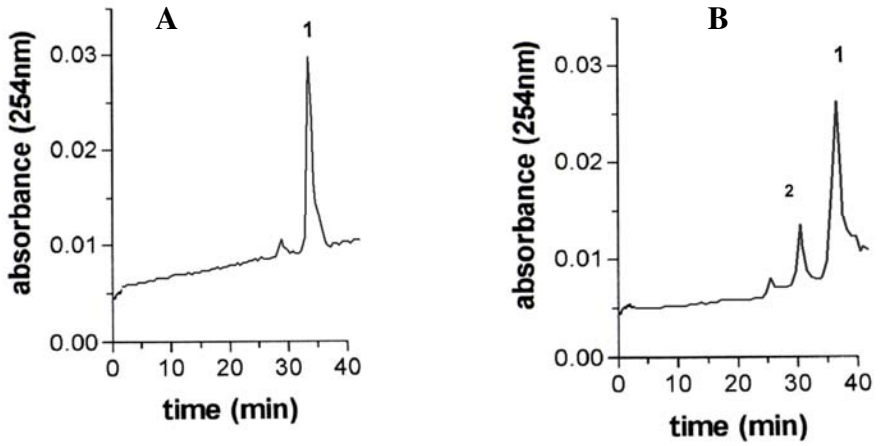

Figure 3.9. HPLC analyses of 11-DOC (10 μM) metabolites assayed in the baboon medullary tissue homogenates after 40 min. **A:** Metabolites assayed at time zero: **1,** 11-DOC, retention time 34.5 minutes. **B:** Metabolites assayed after 40 minutes: **1**, 11-DOC, retention time 34.5 minutes and **2**, corticosterone, retention time 32.4 minutes.

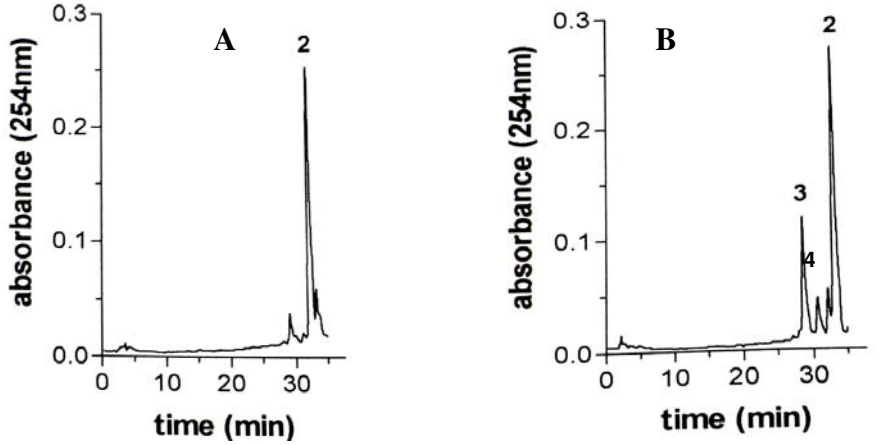

Figure 3.10. HPLC analyses of corticosterone (10 μM) metabolites assayed in the baboon medullary tissue homogenates after 40 min. **A:** Metabolites assayed at time zero: **2,** corticosterone, retention time 32.4 minutes. **B:** Metabolites assayed after 40 minutes: **2**, corticosterone, retention time 32.4 minutes; **3**, aldosterone, retention time 28.5 minutes and; **4**, 18-hydroxycorticosterone, retention time 30.5 minutes.

The presence of aldosterone, produced in the medullary tissue homogenates, during the metabolism of corticosterone was subsequently confirmed by APcI-MS. Figures 3.11.A and B

show the ionization patterns of the aldosterone standard and corticosterone metabolite identified in the conversion assay (see Figure 3.10.B, peak 3). These spectra are similar and show major peaks at m/z 361 and 343 for the aldosterone standard (Figure 3.11.A) and the corticosterone metabolite (Figure 3.11.B). Since the molecular weight of aldosterone is 360, the peak at m/z 361 corresponds with $[M+H]^+$ ion peak of aldosterone. The peak at m/z 343 could be attributed to the loss of water, $[MH-H_2O]^+$ ion of the steroid. Minor peaks at m/z 375 and 325 are seen in both samples and could be due to the $[MH+ CH_2]^+$ and $[MH-2H_2O]^+$ ions of aldosterone, respectively.

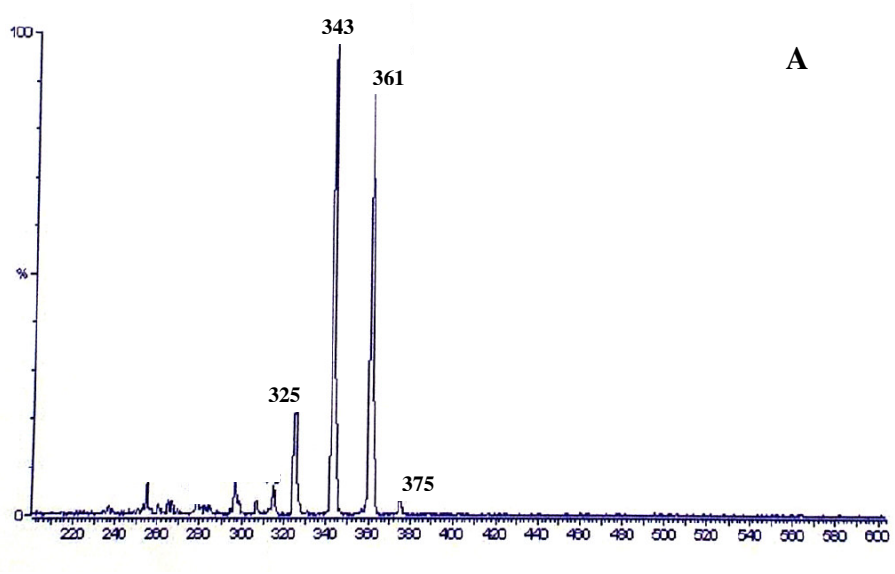

Figure 3.11.A. APcI-MS analyses of the aldosterone standard.

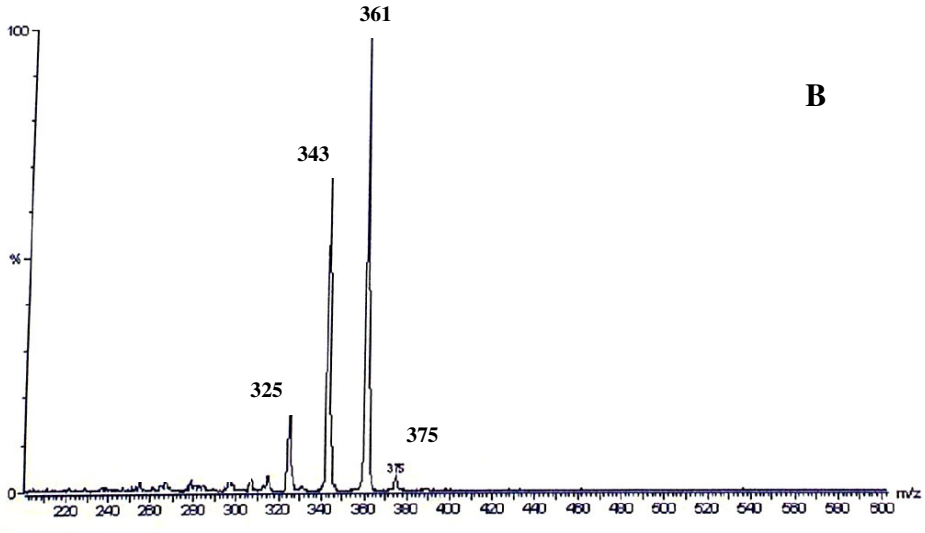

Figure 3.11.B. APcI-MS analyses of aldosterone formation in the baboon adrenal medullary tissue homogenates.

3.4. DISCUSSION

The presence of more than one CYP11B in certain species, including man, is well established [44, 65]. In these species CYP11B1 is responsible for the 11β-hydroxylase activity in the zF/R of the adrenal cortex to yield the glucocorticoids, corticosterone and cortisol. In addition a second CYP11B gene, CYP11B2, is expressed in the zG and this isoform of the enzyme is responsible for the production of the mineralocorticoid, aldosterone. In contrast certain species, like the cow, only has one CYP11B which catalyses both cortisol, corticosterone and aldosterone biosynthesis.

Western blot investigations into the localization of CYP11B1 in baboon adrenal cortical- and medullary tissue homogenates indicated CYP11B1 as a single band (54 kDa) in the cortical tissue homogenate and as two distinct bands (54 and 51 kDa) in the medullary tissue homogenate. The possibility that CYP11B2 may be present in the cortex at protein levels below the detection limit of the sheep CYP11B1 antibody must also be considered. Future studies will concentrate on the over expression of the recombinant baboon CYP11B1 and CYP11B2 for protein purification and subsequent antibody production. Using these baboon CYP11B specific antibodies the presence of CYP11B2 in the baboon adrenal cortex can be unambiguously established.

Two bands were obtained when the medullary tissue homogenate was subjected to Western blot analyses. The first band, indicated in the cortical tissue homogenate (54 kDa), corresponded to the molecular mass of the CYP11B1. The second band corresponded to an apparent molecular mass of ~51 kDa. Human CYP11B2 has an apparent molecular mass of 48.5 kDa. These results, however, do not suggest that CYP11B2 is absent in the medulla. As shown in Figure 3.6 only 18% 11-DOC was converted to corticosterone, the only product of CYP11B1 catalyses in the medullary tissue homogenates, whereas 34% of the 11-DOC was converted to corticosterone in the cortical tissue homogenates. As corticosterone was the only product resulting from 11-DOC conversion in both tissue types, this catalytic activity was attributed to CYP11B1. Furthermore, corticosterone was metabolized to 18-hydroxy-corticosterone and aldosterone in the medullary tissue homogenates only. It is believed that CYP11B2 catalyzed the consecutive 11β-hydroxylation, 18-hydroxylation and 18-oxidation of 11-DOC to aldosterone without the release of the intermediates [18]. However, it has been reported that CYP11B2 can use corticosterone as a substrate for aldosterone synthesis,

although not as efficiently as 11-DOC [18, 74]. We therefore believe that the CYP11B isoforms that exhibited the 18-hydroxylase and 18-oxidase activities towards corticosterone may possibly be attributed to CYP11B2 activity. Contamination of the medullary tissue homogenate with cortical tissue homogenate was unlikely since the zG, where CYP11B2 is uniquely expressed, is located near the capsule of the adrenal.

The presence of AdR was tentatively indicated in both the cortical- and medullary tissue homogenates. This enzyme exhibited a single band at an apparent molecular mass of 54 kDa, but it was not possible to unambiguously assign these bands to AdR as the precipitation was not well aligned with the purified sheep AdR precipitation band. These discrepancies might be due to the fact that the sheep AdR IgG used was not specific for the baboon enzyme. AdX was only detected in the cortical tissue homogenate as a single band corresponding to a molecular mass of approximately 14 kDa.

Although the baboon adrenal cortex and medulla were dissected under a microscope by a histologist from the Physiology Department, University of Stellenbosch, it was still deemed necessary to establish, by more sensitive methods, if contamination between the two homogenates did not occur. CYP11A1 and CYP21 were used as controls, in conjunction with a more sensitive chemi-luminescent substrate for Western blot detection, to monitor cross contamination between the cortical and medullary tissue homogenates. This methodology allowed for the detection of proteins at levels ranging from 10 pg/ml to 50 pg/ml. Cape baboon CYP11A1 was detected as a single band, corresponding to an apparent molecular mass of 52 kDa, in the cortical tissue homogenate only. This molecular mass correlates well with the molecular mass of purified sheep CYP11A1 [75]. Human CYP11A1 has an apparent molecular mass of 56 kDa. Baboon CYP21 was indicated as three bands, with a prominent band corresponding to an apparent molecular mass of 47 kDa, in the cortical tissue homogenate only. Humans and mice express two CYP21 genes of which one is a pseudogene [18]. It is therefore possible that the Cape baboon expresses more than one CYP21 isoform. Human CYP21 has a molecular mass of 56 kDa. Although the results presented show that CYP11A1 and CYP21 were not detected in the medullary homogenate, it is possible that these enzymes may be expressed at much lower levels and were therefore not detected by methods employed in the study. More sensitive methods, such as immunohistochemistry or RNA-analyses, could be employed in future studies to determine unambiguously if CYP11A1 and CYP21 are indeed expressed in the baboon medulla.

These results are in agreement with the findings of Swart *et al.*, who, with *in situ* hybridization and immunohistochemistry, showed the presence of CYP11B in both the cortex and medulla of the Cape Baboon adrenal gland [2, 69]. Although these two techniques revealed the distribution of CYP11B in the baboon adrenal gland, it cannot distinguish between the different CYP11B isoforms. Therefore, the expression of the CYP11B isoforms in the adrenal tissue homogenates was determined by Western blot analyses. The presence of 2 CYP11B proteins in the medullary tissue homogenates, exhibiting different molecular masses were indicated using rabbit anti-sheep CYP11B1 antibodies.

CYP11B1 catalytic activity towards 11-DOC and corticosterone was determined in the cortical- and medullary tissue homogenates. The enzyme hydroxylated 11-DOC at the C11 position to yield corticosterone in both tissue homogenates. However, the 11β-hydroxylase activity in the cortical tissue homogenate was higher than the 11β-hydroxylase activity in the medullary tissue homogenate. Furthermore, CYP11B1 exhibited no 18-hydroxylase and 18-oxidase activity in the cortical tissue homogenate when corticosterone was used as substrate.

In the medullary tissue homogenates, CYP11B exhibited both 18-hydroxylase and 18-oxidase activity towards corticosterone, yielding 18-hydroxycorticosterone and aldosterone when the metabolism of corticosterone was investigated. A detection method, using APcI-MS, was developed for the identification process of steroid metabolites to confirm the formation of aldosterone in the adrenal medullary tissue homogenates. The fragmentation patterns for the aldosterone standard and samples were identical, indicating that aldosterone was the terminal product of corticosterone metabolism in the baboon adrenal medullary tissue preparation. This method would be useful when investigating the multiple steps in the production of aldosterone from 11-DOC or corticosterone in future studies.

The results obtained from the catalytic activity studies of Cape baboon CYP11B1 in tissue homogenates indicated that more than one isoform of this enzyme, with different catalytic activities toward 11-DOC and corticosterone, may exist. CYP11B1 in the adrenal cortical tissue homogenates seems to have a higher 11β-hydroxylase activity towards 11-DOC than that assayed in the adrenal medullary tissue homogenates; there is a marked difference in the amount of corticosterone produced in the respective adrenal tissue homogenates. CYP11B1 shows no 18-hydroxylase activity towards corticosterone in the cortical tissue homogenates.

However, in the medullary tissue homogenates a CYP11B isoform, which apparently exhibits 18-hydroxylase and 18-oxidase activities towards corticosterone, but no 11β-hydroxylase activity towards 11-DOC, was indicated.

The results presented in this chapter supply evidence that corticoid synthesis, which is considered to be confined to the adrenal cortex, may occur in the baboon adrenal medulla. It has been reported that the medulla contains areas of cortical cells, referred to as cortical cuffs [76]. These cortical cells are surrounded by medullary veins and are believed to comprise both zG and zF cells. 3β-HSD, which is found in the zG and zF of the adrenal cortex, has been shown to be expressed in these cortical cuffs in the rhesus macaque monkey [76]. The results presented in this thesis are the first to indicate CYP11B enzyme activity in the medulla. The fact that aldosterone was not detected in the Cape baboon adrenal cortex may be due to low levels of CYP11B2. The function of aldosterone in the medulla is still unclear and may be of physiological importance.

The detection of AdR in the medullary tissue homogenates by Western blot analysis, suggests that a redox protein system, which is important for mitochondrial steroidogenesis is present in the medulla. Bulow and Bernhardt showed that the accessory protein, AdX, influences the 11β-hydroxylase activity of guinea pig CYP11B isozymes. They demonstrated that AdX has differential sensitivity towards CYP11B1 and CYP11B2, as well as the three hydroxylation steps catalyzed by CYP11B2 to the accessibility of reducing equivalents. Studies in COS-1 cells revealed that the omission of AdX leads to a decrease in the 11β-hydroxylase activity of CYP11B1, while the 11β-hydroxylase activity of CYP11B2 was unaffected. However, the 18-hydroxylase and 18-oxidase activity of CYP11B2 was markedly diminished. It was concluded that the availability of reducing equivalents may present another aspect of tissue specific regulation of aldosterone synthesis [68].

The diminished 11β-hydroxylase activity towards 11-DOC in the adrenal medullary tissue homogenate may be ascribed to the fact that no AdX was detected in the medulla. Bulow *et al.* showed that the 18-hydroxylase- and 18-oxidase activity of CYP11B2 is strongly dependent on the presence of high levels of reducing equivalents. A CYP11B isoform, which exhibits aldosterone synthase activities towards corticosterone, is present in the adrenal medullary tissue homogenate and it is possible that a protein, other than AdX, may act as a

redox partner in shuttling electrons from AdR to CYP11B isozymes in the medulla. This may contribute to the tissue specific regulation of aldosterone synthesis in the Cape baboon adrenal.

The production of aldosterone from 11-DOC in the adrenal medulla may be dependent on a high corticosterone concentration. It is possible that the corticosterone levels produced from 11-DOC in the medullary tissue homogenates were too low and could therefore not yield sufficient amounts of 18-hydroxycorticosterone and aldosterone.

The detection of the CYP11B isozymes in the medulla has been reported to be localized to islets of cortical cells in the medulla [2, 69]. It is as yet unclear why CYP11B is expressed in the Cape baboon adrenal medulla and what possible influence this could have on electrolyte and water homeostasis in the animal.

The findings of the different catalytic properties of Cape Baboon CYP11B in adrenal tissue homogenates prompted a further investigation into the genes encoding this enzyme. As mentioned in Chapter one three baboon CYP11B genes were cloned in our laboratory. To determine if the steroidogenic activity of any of the cloned genes coincided with the CYP11B activities found in the adrenal cortex and medulla, the catalytic activities of the two expressed baboon CYP11B genes were subsequently studied in non-steroidogenic COS-1 cells. This work will be discussed in the following chapter.

CHAPTER FOUR

THE EXPRESSION OF CAPE BABOON CYP11B1 IN NON-STEROIDOGENIC COS-1 CELLS

4.1. INTRODUCTION

As mentioned in chapter one three CYP11B genes, namely CYP11B1a[1], CYP11B1wt and CYP11B1S were previously cloned from Cape baboon adrenals in our laboratory [69]. Sequence analyses showed that CYP11B1a and CYP11B1wt differed by three amino acid substitutions in exon three *viz*, Val177Leu, Glu182Asp and Ile188Val. CYP11B1S has a nucleotide variation that leads to an amino acid substitution, Ala168Gly, in exon one. These cloned baboon cDNAs showed a 96.5% sequence homology with human CYP11B1 and a 94.6% homology with human CYP11B2 [69]. The alignment of cDNAs and amino acid residues of baboon CYP11B1a, CYP11B1wt and CYP11B1S with human CYP11B1 and CYP11B2 are shown in Appendix A and B, respectively.

Human CYP11B1 and CYP11B2 share a sequence homology of 95% in the coding regions and 90% in the introns. Although these enzymes are very similar in their primary sequence, their catalytic activities differ. *In vitro* studies showed that CYP11B1 is a pure 11β-hydroxylase and exhibits no 18-hydroxylase or 18-oxidase activities. This enzyme is also unable to 11β-hydroxylate 18-hydroxy-DOC. In contrast, CYP11B2 has 18-hydroxylase and 18-oxidase activities, which is necessary for aldosterone synthesis. This enzyme also has the ability to 18-hydroxylate and 18-oxidize cortisol. Both enzymes have the capacity to 11β-hydroxylate 11-DOC and 11-deoxycortisol. However, CYP11B2 demonstrates a much weaker 11β-hydroxylase activity towards 11-deoxycortisol [45].

The mouse adrenal cortex expresses two CYP11B isozymes, CYP11B1 and CYP11B2. The two genes encoding these isozymes share 84% identity in their coding regions and contain sequences in the heme binding domain, the aromatic region and the region, including the ozol

[1] The genes were assigned CYP11B1wt, CYP11B1a and CYP11B1S once the sequence analyses and catalytic activities of the expressed enzymes had been established in our laboratory. As one of the genes exhibited activities towards 11-DOC and 11-deoxycortisol, which were comparable to human CYP11B1, it was designated CYP11B1wt. The second gene exhibited enzymatic activities similar, but not identical to CYP11B1wt and was designated CYP11B1a. CYP11B1S was inactive due to a premature stop codon.

peptide, which is basically identical to that of the human CYP11B genes. CYP11B1 has a high 11β-hydroxylase activity towards 11-DOC, whereas CYP11B2 is essential for the 11β-hydroxylation of 11-DOC to corticosterone and the subsequent 18-hydroxylation and 18-oxidation to produce aldosterone. It is believed that the hydroxylated intermediates bind tightly to the active site of CYP11B2 and do not dissociate from the enzyme during aldosterone biosynthesis. Aldosterone exhibits a significantly higher dissociation constant than the intermediates, facilitating its release from the enzyme [18, 43].

Two CYP11B isozymes, CYP11B1 and CYP11B2, which share 90% homology in their nucleotide sequence, have been identified in the hamster. CYP11B1 possesses a high 11β-hydroxylase activity, 18-hydroxylase activity and in contrast to other species, this enzyme also exhibits high 19-hydroxylase activity, whereby 11-DOC is converted to corticosterone, 18-hydroxy-DOC and 19-hydroxy-DOC. It was also established that hamster adrenal CYP11B1 has the highest 19-hydroxylase activity of all species. The hamster CYP11B2 catalyzes the 11β-hydroxylase-, 18-hydroxylase- and 18-oxidase activities of 11-DOC to ultimately produce aldosterone [18, 44].

The rat genome expresses four CYP11B genes, namely CYP11B1, CYP11B2, CYP11B3 and CYP11B4. The nucleotide sequence homology between the coding regions of CYP11B1 and CYP11B2, CYP11B1 and CYP11B3, and CYP11B2 and CYP11B3, is 88%, 96% and 86%, respectively. CYP11B1, CYP11B2 and CYP11B3 have similar molecular structures consisting of nine exons; the location of the introns in these genes is identical. CYP11B1, CYP11B2 and CYP11B3 can catalyze the 11β- and 18-hydroxylation of 11-DOC, yielding corticosterone and 18-hydroxycorticosterone. In addition to these two activities CYP11B2 also possesses the 18-oxidase activity to produce aldosterone. CYP11B4 is considered to be a pseudogene [18, 43, 67].

Three CYP11B genes, CYP11B1, CYP11B2 and CYP11B3 have been identified in the guinea pig. CYP11B1 catalyzes the 11β-hydroxylation of 11-DOC to form corticosterone. This enzyme also exhibits very low levels of 18- and 19-hydroxylase activities, yielding trace amounts of 18-hydroxy-DOC and 19-hydroxy-DOC. CYP11B2 has 11β-, 18-hydroxylase and 18-oxidase activities towards 11-DOC and can also 11β- and 18-hydroxylate 11-deoxycortisol to cortisol and 18-hydroxycortisol, respectively. This enzyme also exhibits 11β-hydroxylase

activity towards androstenedione, yielding 11β-hydroxyandrostenedione. CYP11B3 is considered to be a pseudogene. The amino acid sequence of CYP11B1 and CYP11B2 has 81% similarity. A common CYP11B ancestral gene, which possesses both 11β-hydroxylase and aldosterone synthase activities has been hypothesized [68].

As shown in the previous chapter, Cape baboon CYP11B1 was detected, using a rabbit anti-sheep CYP11B1 antibody, as a single band in the cortical tissue homogenates and as two distinct bands in the medullary tissue homogenates. Investigations into the catalytic activity of Cape baboon CYP11B1 in adrenal tissue showed that 11-DOC was metabolized to corticosterone with different efficiencies in the cortical tissue and medullary tissue homogenates. In the medullary tissue homogenates, however, corticosterone was converted to aldosterone. These results, which suggested the presence of more than one isoform of CYP11B1, together with the marked difference in 11-DOC metabolism in the tissue homogenates, prompted further investigations into the catalytic activities of the Cape baboon CYP11B1 isoforms *in vivo*.

4.2. MATERIALS AND METHODS

4.2.1. Animals

Adrenal tissue was obtained from randomly selected normal rats of both sexes housed at the Physiology Department of the University of Stellenbosch, Stellenbosch. All anaesthetic and surgical procedures were permitted by the Animal Research and Ethics committee of the University and complied with the "Principles of Laboratory Care" and the "NIH Guide for the Care and Use of Laboratory Animals" 1996.

4.2.2. Reagents

11-DOC, 11-deoxycortisol, corticosterone and cortisol were obtained from Sigma Chemical Co. (St Louis, MO, USA). Tritiated progesterone, deoxycortisol and corticosterone were purchased from Amersham Life Science (Amersham Laboratories, Buckinghamshire, England). COS-1 cells were obtained from the American Type Culture Collection, ATCC, (Manassas, VA). Dulbecco's modified eagle's medium (DMEM), Dulbecco's phosphate buffered saline (PBS), penicillin-streptomycin (pen-strep) and trypsin-EDTA were purchased

from Gibco-BRL (Gaithersburg, MD, USA). Diethylaminoethyl-dextran (DEAE-dextran), Hepes, and chloroquine were purchased from Sigma Chemical Co. (St Louis, MO, USA). Fetal calf serum (FCS) was obtained from Highveld Biologicals (Johannesburg, SA). Plasmid preparation was performed using a Nucleobond Midi Prep^{TM} kit (Machery-Nagel, Düren, Germany). A Pierce bicinchoninic acid (BCA) protein assay kit was purchased from Pierce (Rockford, IL, USA). Corticosterone production was measured using a Corticosterone HS (high sensitivity)-ELISA (enzyme immunoassay kit; Immunodiagnostic Systems Inc., USA). All other chemicals were of analytical grade purchased from local scientific supply houses.

4.2.3. Maintenance of COS-1 cells

4.2.3.1. Thawing and plating of COS-1 cells

A cryovial, containing 1 ml of frozen COS-1 cells, was removed from liquid nitrogen and thawed in a 37°C waterbath. The cells were resuspended in 1 ml warm DMEM and added to 10 ml culture medium in a 50 ml falcon tube. The cells were dispersed and plated onto a 100 mm tissue culture dish. The subsequent incubations were all carried out at 37°C and maintained at 5% CO_2 and 90% humidity. The culture medium was changed daily with 10 ml fresh medium until the cells were confluent.

For the maintenance of COS-1 cells, a one to three split of confluent cells was followed as described below. COS-1 cells, when split one to three, reach confluency within three days. One day prior to transfection, COS-1 cells are split one to five in order to allow sufficient time for efficient transfection with the recombinant cDNAs and effective growth of the transfected cells.

4.2.3.2. Splitting COS-1 cells

Confluent cells were split from a 100 mm tissue culture dish into three 100 mm dishes. The culture medium was aspirated off using a sterile Pasteur pipette, after which the cells were gently washed with 1 ml 1X warm Trypsin-EDTA medium, which was prepared from a 10X stock solution. The Trypsin-EDTA medium was removed and the cells were incubated at room temperature with 1 ml warm Trypsin-EDTA medium, for three minutes. The cells were

dispersed and collected in 30 ml culture medium, plated out into three 100 mm tissue culture dishes and incubated at 37°C, 5% CO_2 and 90% humidity.

4.2.3.3. Freezing of COS-1 cells

Confluent cells were washed with 1 ml warm Trypsin-EDTA from a 100 mm culture dish and subsequently incubated for three minutes in 1 ml warm Trypsin-EDTA. The cells were resuspended and collected in 10 ml culture medium and centrifuged at 500 x g for five minutes. The supernatant was removed and the cells were resuspended in freezing media (DMEM containing 10% DMSO), 3ml/100 mm dish. Aliquots (1 ml) were pipetted into cryovials, placed at -80°C for 48 hr and transferred to liquid nitrogen until further use.

4.2.4. Functional expression of baboon CYP11B isoforms in COS-1 cells

Recombinant Cape baboon CYP11B1 cDNAs were prepared as described by Swart *et al.* [2]. Total RNA and mRNA were prepared and isolated from surgically removed normal baboon adrenals by the guanidine hydrochloride method and by using the mRNA Capture kit (Roche/Boehringer Mannheim), respectively. RT-PCR was performed using the Titan One Tube RT-PCR system (Roche/Boehringer Mannheim) and the RT-PCR products were gel purified. A second amplification was carried out using Taq DNA polymerase (Thermoprime DNA polymerase, Advanced Biotechnologies). Baboon specific primers, which are complementary to the 5' and 3' ends of baboon CYP11B1 (Genbank: U52081-U52085), were used as forward and reverse primers in all amplification reactions. The amplified products were gel purified and three full length baboon CYP11B1 cDNAs were cloned into pTarget Vector Systems (Promega) according to the manufacturer's instructions and subsequently sequenced. Nucleotide sequence differences were confirmed by performing a second PCR amplification using a high fidelity polymerase, Pwo DNA polymerase (Roche/Boehringer Mannheim). Recombinant Cape baboon CYP11B1 cDNAs were transfected into COS-1 cells using DEAE-dextran.

4.2.4.1. Transfection of COS-1 cells

COS-1 cells were maintained at 37 °C, 90% humidity and 5% CO_2 in DMEM supplemented with 0.9 $g \cdot L^{-1}$ glucose, 0.12% $NaHCO_3$, 10% FCS and 1% pen-strep in 100 mm dishes and

confluent cells were split one to five 24 hours before transfection. The medium was removed from each dish and the cells were washed with 4 ml Hepes medium (DMEM, 20 mM Hepes, 1% pen-strep). The Hepes media was removed and 2 ml transfection medium (Hepes medium, 0.25 mg/ml DEAE-Dextran), containing the respective plasmids (5 µg/ml), was added to each plate and incubated at 37°C. The baboon wild type (pTarget^{TM}-11Bwt), CYP11B1 (pTarget^{TM}-11B1a) and CYP11B1S (pTarget^{TM}-11B1S) were co-transfected with human pCD ADX construct, 5 µg/ml, for one hour, using the DEAE-dextran method [25]. The transfection medium was subsequently removed, after which 100 µM chloroquine in DMEM was added and the cells incubated for five hours. The chloroquine medium was removed and the cells were washed with 5 ml culture medium. Fresh culture medium was added to each plate and the transfected cells were incubated for 72 hr.

For mock and positive control experiments, COS-1 cells were transfected with pTarget^{TM}-plasmid containing no insert (5 µg/ml) and baboon pTarget^{TM}-CYP17 construct (5 µg/ml), respectively, as described above. For the blank control experiments, which contained no COS-1 cells, baboon pTarget^{TM}-11B1wt, pTarget^{TM}-11B1a and pTarget^{TM}-11B1S constructs (5 µg/ml), together with human pCD ADX construct (5 µg/ml), respectively, were added to the transfection medium. For the negative control transfections, water was added to the transfection medium and incubated with COS-1 cells.

4.2.4.2. Synthesis of radioactive 11-DOC using rat adrenal microsomes

For the investigation of the catalytic activities of the baboon CYP11B isoforms tritiated-DOC was required as substrate. This form of the steroid was, however, no longer commercially available. Since rodents do not express CYP17 in the adrenal cortex, 11-DOC is the main product synthesized from progesterone. It was therefore decided to synthesize [^{3}H]-DOC from [^{3}H]-progesterone, using rat adrenal microsomes.

4.2.4.2.1. Preparations of rat adrenal microsomes

All preparations were carried out at 4°C. Adrenals were collected from freshly slaughtered rats and all fat, connective tissue and the adrenal capsules were removed. The adrenals (5g) were finely chopped using a scalpel and homogenized in 4-5 volumes sucrose-EDTA solution

(0.25 M sucrose, 1 mM EDTA, pH 7.4) using a Waring-blender followed by a Potter-Elvejhem glass homogenizer. The homogenate was centrifuged at 850 x g for 8 minutes to remove cell debris. The supernatant was centrifuged at 21 500 x g for a further 10 minutes. The resulting supernatant was centrifuged at 70 000 x g for 60 minutes. The microsomal pellet was homogenized in 0.15 M KCl and the homogenate was centrifuged at 70 000 x g for 30 minutes. The pellet was resuspended in 100 mM potassium phosphate buffer (20% glycerol, 100 µM EDTA, 100 mM DTT, pH 7.2) and used immediately to prepare tritiated-DOC.

4.2.4.2.2. Conversion of tritiated-progesterone to tritiated-DOC by rat adrenal microsomes

Radio-labeled progesterone (1 536 000 cpm/5 µl) and unlabeled progesterone (10 µM) were pipetted onto filter paper, placed in a 2 ml microcentrifuge tube and dried at room temperature under N_2. The reaction was carried out in a 50 mM Tris buffer solution (1% BSA, 50 mM NaCl, pH 7.4), 0.44 µmol $MgCl_2$ and 398 milli-units isocitrate dehydrogenase, in a total volume of 500 µl. The reaction mixture was preincubated for 10 minutes in a 37°C shaking water bath. The microsomal suspension was added and the reaction mixture was agitated for 5 minutes at 37°C. A 50µl aliquot (zero time point) was removed from the mixture, added to ice-cold 5 ml dichloromethane, containing 450 µl water, and mixed immediately by vortexing for 30 seconds. The reaction was initiated by the addition of 420 nmol isocitrate and 0.44 µmol NADPH. The reaction mixture was incubated for 30 minutes, after which 50 µl aliquots were withdrawn and placed into glass tubes containing 5 ml dichloromethane and 450 µl water. The steroids were extracted with the dichloromethane by vortexing, followed by the separation of the organic and aqueous phases by centrifugation. The aqueous phase was aspirated off and anhydrous sodium sulphate was added to each tube. The sodium sulphate was removed by centrifugation and the steroid containing dichloromethane was dried under N_2. Steroid metabolites were subsequently separated using TLC.

4.2.4.2.3. Separation and extraction of tritiated-progesterone and tritiated-DOC

Dichloromethane (100 µl) was added to each tube containing the dried steroid extracts and the resultant solution was vortexed for 2 minutes to completely redissolve the dried steroid metabolites. A standard solution of progesterone and 11-DOC, 2 mg/ml ethanol, was prepared

and, together with the samples, spotted onto preparative glass-backed TLC plates (Kieselgel 60 F_{254}). Each TLC plate was transferred to a chromatographic tank, containing chloroform:ehtylacetate (80:20), and developed for 1.5 hours. The steroid metabolites were identified under UV-light using the corresponding steroid standards. Silica, containing the radioactive 11-DOC, was collected from the plates, eluted with methanol and dried under N_2. The sample was dissolved in 500 µl ethanol, transferred to Beckman Ready Flo Scintillation fluid (1 µl/8 ml) and the radio activity determined using a Beckman LS 3801 scintillation counter. The radioactive steroid (10 µl) was reapplied to an aluminium TCL plate and developed as above to ascertain the purity of the synthesized tritiated-DOC.

4.2.4.3. Assay for 11-DOC and 11-deoxycortisol metabolism in COS-1 cells

A pilot study was performed to determine the catalytic activities of the three CYP11B clones, CYP11B1wt, CYP11B1a and CYP11B1S, expressed in COS-1 cells using 11-DOC and 11-deoxycortisol as substrates. As the CYP11B1S clone contained a termination codon at position 168, it was expected that the expressed enzyme would be inactive. The clone was, however, included in the pilot study for control purposes. The baboon pTarget™-CYP17 construct was used for the positive control transfection, while pTarget™, containing no insert, was used in the mock experiment. Additional control experiments, in which a transfection was carried out using water and another in a culture dish containing no cells, were also performed. All experiments were performed in triplicate.

Steroid hydroxylation reactions were initiated 72 hours after transfection by incubating the cells with culture medium containing [^{3}H]-DOC (100 000 cpm/ml) and non-radioactive 11-DOC (1 µM) and [^{3}H]-deoxycortisol (100 000 cpm/ml) and non-radioactive deoxycortisol (1 µM), respectively. Aliquots, 0.5 ml, were collected from each dish immediately after substrate addition to represent time zero. Samples (0.5 ml) were subsequently collected at specific time intervals thereafter and steroid metabolites were extracted in 5 ml dichloromethane, containing 450 µl water, by vortexing followed by separation of the organic and aqueous phases by centrifugation. The aqueous phase was aspirated off. Anhydrous sodium sulphate was added to the organic phase and after 5 minutes the resultant mixture centrifuged. After centrifugation, the organic phase was dried under N_2 at room temperature and subsequently analyzed by TLC. The extracted steroids were redissolved in 100 µl dichloromethane and

applied to an aluminium TLC plate (silica gel F_{254}) together with steroid standards dissolved in the same solvent. The TLC plate was allowed to develop for 1.5 hours in a CH_2Cl_2/MeOH (98:2) mixture after which each respective steroid standard and sample were identified under UV-light, cut from the TLC plate and placed in 8 ml Beckman Ready Flo scintillation fluid overnight. The radioactive steroid metabolites were quantified using a Beckman scintillation counter.

The positive control experiment, using pTarget™-CYP17 construct (5 µg/ml), was performed as explained above with ^{3}H-progesterone (100 000 cpm/ml) and non-radioactive progesterone (1 µM) as substrates. In the mock transfection, in which pTarget™-plasmid containing no insert (5 µg/ml) was used, ^{3}H-progesterone (100 000 cpm/ml) and non-radioactive progesterone (1 µM) were used as substrates. In the transfection carried out with water, [^{3}H]-DOC (100 000 cpm/ml) and non-radioactive 11-DOC (1 µM) and [^{3}H]-deoxycortisol (100 000 cpm/ml) and non-radioactive 11-deoxycortisol (1 µM), respectively, were used as substrates. In addition, non-radioactive and tritiated steroid substrates, 11-DOC and 11-deoxycortisol, were added to two culture dishes containing no cells. Samples were extracted at time zero and after 16 hours.

4.2.4.4. Enzyme activity assay of CYP11B1a and CYP11B1wt in COS-1 cells

The catalytic activity of baboon CYP11B1a and CYP11B1wt was subsequently investigated to determine the Km- and V-values of these two enzymes for the substrates 11-DOC and 11-deoxycortisol.

Transfection of COS-1 cells with plasmids containing baboon wild type and CYP11B1a cDNAs and pTarget™-CYP17 constructs were performed as described in section 4.2.3. Since tritiated steroid substrates were no longer available, the assay conditions were modified. Steroid metabolites were analyzed using a corticosterone enzyme linked immunoassay (ELISA) kit for the analyses of 11-DOC conversion, while a liquid chromatography-mass spectrometry (LC-MS) method was developed for the analysis of 11-deoxycortisol conversion. These methods allowed the use of steroid substrates, in a concentration range from 0.125 µM to 8 µM. All experiments were performed in triplicate.

11-DOC metabolites were analyzed using a corticosterone high sensitivity ELISA kit according to the manufacturer's instructions. Aliquots of media (50 µl) were collected from each dish at the beginning of the experiment as the time zero sample. Additional samples (50 µl) were collected at specific time intervals thereafter. The steroids were extracted with 2 ml dichloromethane by vortexing for one minute. Aliquots of 500 µl were pipetted from the dichloromethane layer into glass tubes and dried under N_2 at room temperature. The dried samples were redissolved in 100 µl calibrator diluent, after which, together with standard dilutions, samples were heat treated at 80 °C for 30 minutes. The samples and standards were allowed to cool to ambient temperature and 100 µl of each were pipetted onto a microtitre plate. Enzyme conjugate (aqueous solution containing corticosterone labeled with horseradish peroxidase), 100 µl, was added to each sample and the resultant mixtures were incubated at room temperature for 4 hours. The contents of the microtitre plate wells were removed and the wells were rinsed three times with 100 µl washing buffer. Tetramethylbenzidine (TMB) substrate (200 µl) was added to each well and the microtitre plate was incubated at room temperature for 30 minutes. The reaction was arrested by the addition of an 0.5 M hydrochloric acid solution (100 µl) to each well. The absorbance of each well at 450 nm was subsequently determined using a Titertek Multiskan® PLUS, model MK II, microtitre plate reader. A standard curve was generated by calculating the percentage binding of the corticosterone standard samples and plotting this value against the concentration of the corticosterone standards. The concentrations for the 11-DOC metabolites were subsequently determined by calculating the percentage binding of corticosterone in the extracted samples and determining the corticosterone concentration from the calibration curve.

For analysis of 11-deoxycortisol conversion, 0.5 ml aliquots were extracted with 5 ml dichloromethane, containing 450 µl water. The two phases were separated by centrifugation and the steroid-containing dichloromethane extractions were dried as described above. The dried samples and steroid standards, 11-deoxycortisol and cortisol, ranging from 0.04 µM to 10 µM, were redissolved in 100 µl 68% acetonitrile and 0.1% formic in water for LC-MS analysis. LC-MS analysis was performed on a Waters API Q-TOF Ultima instrument operating with an electrospray ionization source. The analytes and standards were separated on a Phenomenex Luna C18 (2 mm) 3um 0.2x150mm column. The mobile phase, delivered at a flow rate of 0.23 ml/min, consisted of 68% acetonitrile and 0.1% formic acid in water. The samples, 40 µl, were injected into the solvent stream and introduced through a conventional

electrospray probe with the capillary voltage set at 3.5 kV, cone voltage at 35 V and the source temperature at 100°C. The multiple charged ions were observed by scanning the mass analyzer from m/z 200–500 at a scanning speed of 100 amu/s (atomic mass units per second). The detection was made in the positive mode. A standard curve was generated and the metabolite concentrations were calculated by comparing their ratios of peak areas to those of the standards.

4.2.4.5. Determination of 18-hydroxylase and 18-oxidase activity of baboon CYP11B expressed in COS-1 cells

To establish if the baboon CYP11B clones exhibited 18-hydroxylase and 18-oxidase activities, transfections with plasmids containing baboon wild type and CYP11B1a cDNAs constructs were performed in our laboratory as described above in 4.2.3. Baboon pTarget™-CYP17 constructs were used as negative control. Non-radioactive substrates, 11-DOC (2 μM), 11-deoxycortisol (2 μM) and corticosterone (2 μM), respectively, were used as substrates and samples were extracted after 8 hours of incubation. The extracted steroid metabolites were subsequently analyzed by LC-MS. The steroid standards, 11-DOC, corticosterone, 18-hydroxycorticosterone, aldosterone, 11-deoxycortisol and cortisol ranging from 0.02 μM to 2 μM, were used to generate a calibration curve.

LC-MS analysis was performed on a Waters API Quattro Micro instrument. For analysis of 11-DOC and corticosterone metabolites, the mobile phase consisted of water and methanol and was delivered to the system at a flow rate of 0.35 ml/min. For analysis of 11-deoxycortisol metabolites, a mobile phase containing formic acid and acetonitrile was delivered to the system at a flow rate of 0.4 ml/min. The operating conditions for the MS were determined as: capillary voltage, 3.5 kV; cone voltage, 30 V; source temperature, 100°C; desolvation temperature, 450°C; desolvation gas, 450 L/h and the cone gas, 50 L/hr. A standard curve was generated and the metabolite concentrations were calculated as mentioned above.

4.2.4.6. Determination of the protein content of COS-1 cells

On completion of each experiment, the cells were harvested and the total protein content was determined. COS-1 cells were washed, collected in 3 ml PBS and homogenized using a small glass homogenizer. The protein concentrations were determined using the Pierce BCA method. The total protein content of the mock transfection assays was determined and deducted from the experimental assays. The total protein content was used as a measure of the reproducibility of the assay conditions and to compare transfection efficiency between experiments.

4.3. RESULTS

The metabolism of 11-DOC and 11-deoxycortisol was assayed in COS-1 cells transfected with pTarget^{TM}-CYP11B1wt, pTarget^{TM} -CYP11B1a and pTarget^{TM} -CYP11B1S to determine the activities of the cloned enzymes. In order to ascertain the respective CYP11B1 isoform's 11β-hydroxylase activities towards 11-DOC, tritiated-DOC was prepared since it was not commercially available. Approximately 93% tritiated-DOC was synthesized from tritiated-progesterone in rat adrenals. TLC analysis of the tritiated-DOC showed that the steroid solution contained no other by-products.

4.3.1. Metabolism of 11-DOC and deoxycortisol in COS-1 cells

The metabolism of 11-DOC in COS-1 cells transfected with CYP11B1wt, CYP11B1a and CYP11B1S, respectively, is shown in the progression curves in Figure 4.1. As this was a pilot study, no statistical analysis was performed on the data; the experiments were, however, performed in triplicate.

At 16 hours CYP11B1a converted approximately 73% of the 11-DOC to corticosterone (Figure 4.1.A), while CYP11B1wt converted only 34% of the substrate to corticosterone (Figure 4.1.B). CYP11B1S showed no steroid hydroxylase activity due to a termination codon in exon one (Figure 4.1.C). The formation of 18-hydroxy-corticosterone and aldosterone by CYP11B1a and CYP11B1wt was negligible.

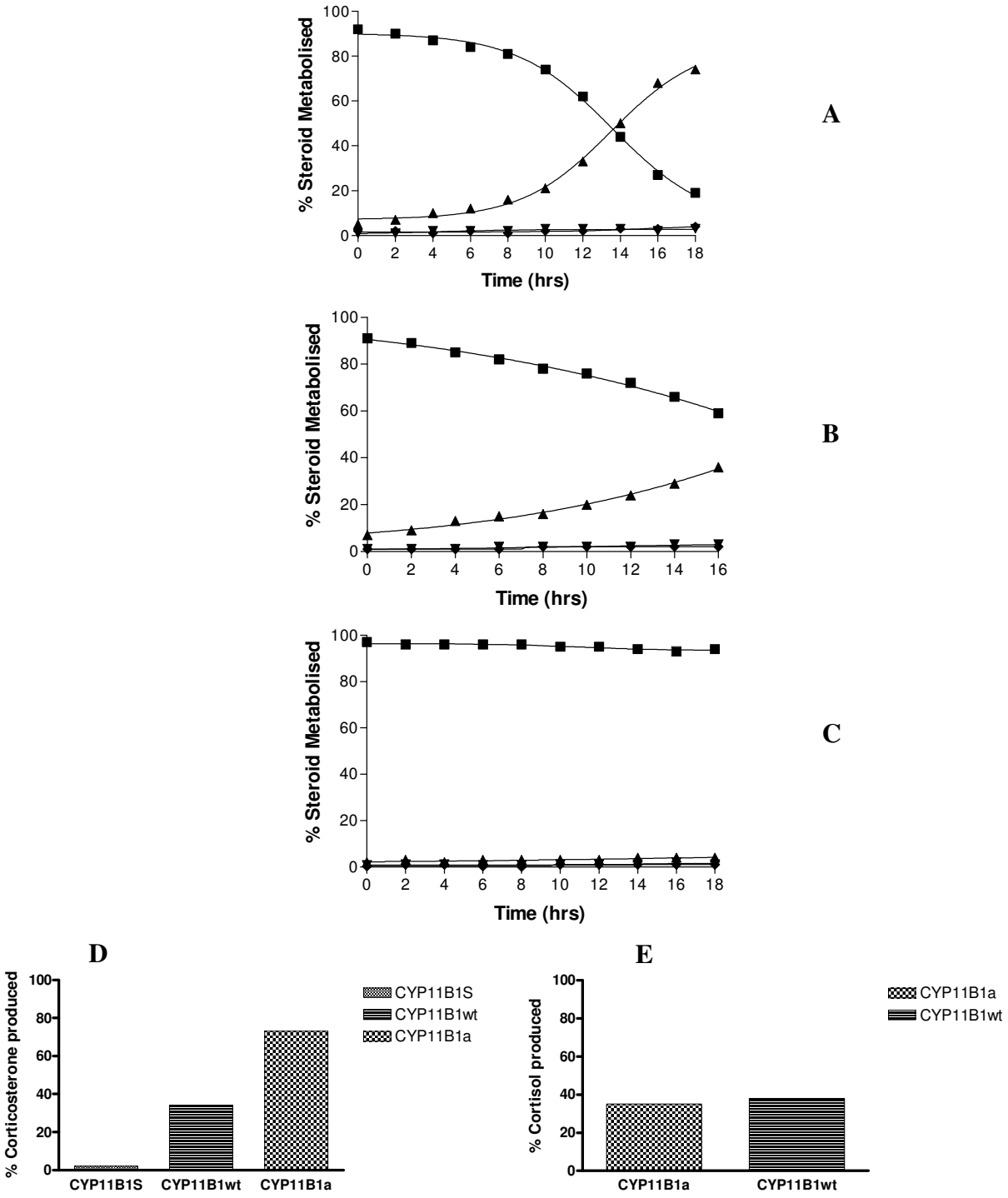

Figure 4.1. A time course of (A) 11-DOC (1 μM) metabolism by baboon CYP11B1a, **(B)** 11-DOC (1 μM) metabolism by CYP11B1wt and **(C)** 11-DOC (1 μM) metabolism by CYP11B1S in COS-1 cells. **(D)** Production of corticosterone by CYP11B1a and CYP11B1wt in COS-1 cells. **(E)** Production of cortisol by CYP11B1a and CYP11B1wt in COS-1 cells. 11-DOC (■), corticosterone (▲), 18OH-corticosterone (▼), aldosterone (♦).

The 11β-hydroxylase activities of CYP11B1wt and CYP11B1a towards 11-DOC and 11-deoxycortisol are shown in Figures 4.1.D and 4.1.E, respectively. The conversion of 11-DOC

by CYP11B1wt and CYP11B1a produced 34% and 73% corticosterone, respectively. The conversion of 11-deoxycortisol by CYP11B1wt and CYP11B1a yielded 38% and 35% cortisol, respectively.

In the positive control transfection experiments, the conversion of progesterone to 17α-hydroxprogesterone by baboon pTarget™-CYP17 constructs was followed in COS-1 cells. After 16 hours of incubation baboon CYP17 converted 65% of the progesterone to 17α-hydroxprogesterone. In the mock transfection experiments, no 17α-hydroxprogesterone could be detected after 16 hours. In the transfection experiments carried out with water and no COS-1 cells no intermediates were produced when 11-DOC and 11-deoxycortisol was assayed. Results are not shown.

4.3.2. Analysis of the enzyme activity assays of CYP11B1wt and CYP11B1a in COS-1 cells

The production of corticosterone from 11-DOC was determined by using a corticosterone ELISA kit. The percentage binding of the corticosterone standard samples was calculated and a standard curve of the % binding of the standard samples against the concentration of corticosterone standards was generated (Figure 4.2).

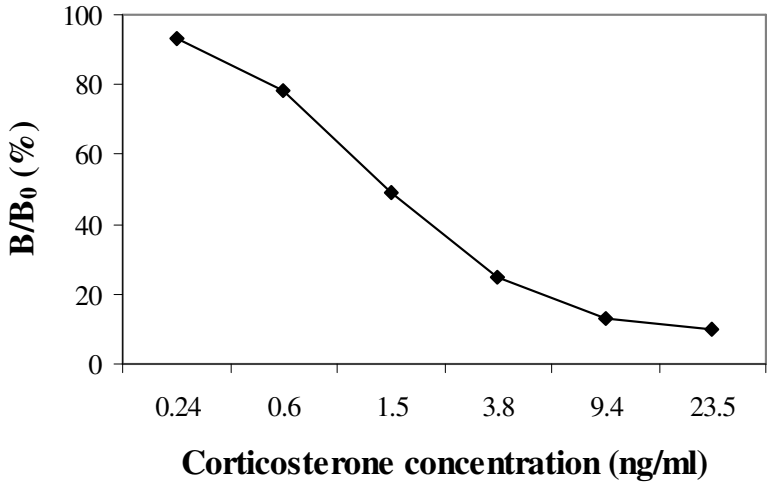

Figure 4.2. Graph of a standard curve of the % binding of corticosterone standard samples to a microtitre plate, pre-coated with a polyclonal antibody specific for corticosterone, against corticosterone concentration.

The percentage binding of corticosterone in the extracted samples was calculated and the corticosterone concentration determined from the calibration curve. After assaying the extracted samples, the calculated corticosterone concentration value was multiplied by the dilution factor.

The initial reaction rates of the formation of corticosterone were determined by linear regression for substrate concentrations, ranging from 0.125 μM to 8 μM. At least 6 time points were used for each rate determination. The R-squared value for all initial rate regression analyses was always higher than 0.95.

The apparent *K*m- and *V*-values for 11-DOC metabolism by the recombinant baboon CYP11B1 isoforms, expressed in COS-1 cells, were determined using the Lineweaver-Burke, Eadie-Hoffstee, Hanes-Woolf and Direct Linear plots. Statistical analyses were performed using Graphpad Prism 4. One-way ANOVA test was applied to all groups (four methods used to determine the *K*m- and V-values for the respective isoforms) and $P < 0.05$ was considered significant. No significant difference was found in the Km and V values as determined by the four different methods for both baboon CYP11B isoforms. However, when the kinetic data for CYP11B11a was statistically compared to CYP11B1wt, using the t-test, the values were significantly different ($P<0.05$). The apparent *K*m- and *V*-values for 11-DOC metabolism by the wild type and CYP11B1a are summarized in Table 4.1.

Table 4.1. The apparent *K*m- and *V*-values for 11-DOC metabolism by CYP11B1wt and CYP11B1a, expressed in COS-1 cells, as determined by Direct Linear, Eadie-Hoffstee and Hanes-Woolf plots.

	Direct Linear Plot		**Eadie-Hoffstee Plot**		**Hanes-Woolf**	
	Km[1]	**V[2]**	**Km[1]**	**V[2]**	**Km[1]**	**V[2]**
CYP11B1a	0.40 ± 0.16	9.92	0.30 ± 0.13	8.91	0.44 ± 0.19	9.62
CYP11B1wt	0.79 ± 0.08	6.59	0.81 ± 0.06	6.85	0.74 ± 0.05	6.62

[1]: *K*m values are expressed in μM as the mean±S.E.M. of three independent experiments.
[2]: *V*-value is expressed in nmol/hr/mg protein as the mean±S.E.M. of three independent experiments.

The apparent *K*m- and *V*-values for CYP11B1a with 11-DOC as substrate, as determined by the Lineweaver-Burke plot, were 0.48 ± 0.1592 μM and 10.35 ± 0.8529 nmol/hr/mg protein respectively (Figure 4.3.A), while CYP11B1wt exhibited values of 0.74 ± 0.06207 μM and 6.62 ± 0.1584 nmol/hr/mg protein, respectively (Figure 4.3.B). Statistical analysis showed a significant difference (P = 0.035) in the apparent *K*m-values between CYP11B1a and CYP11B1wt for 11-DOC utilization.

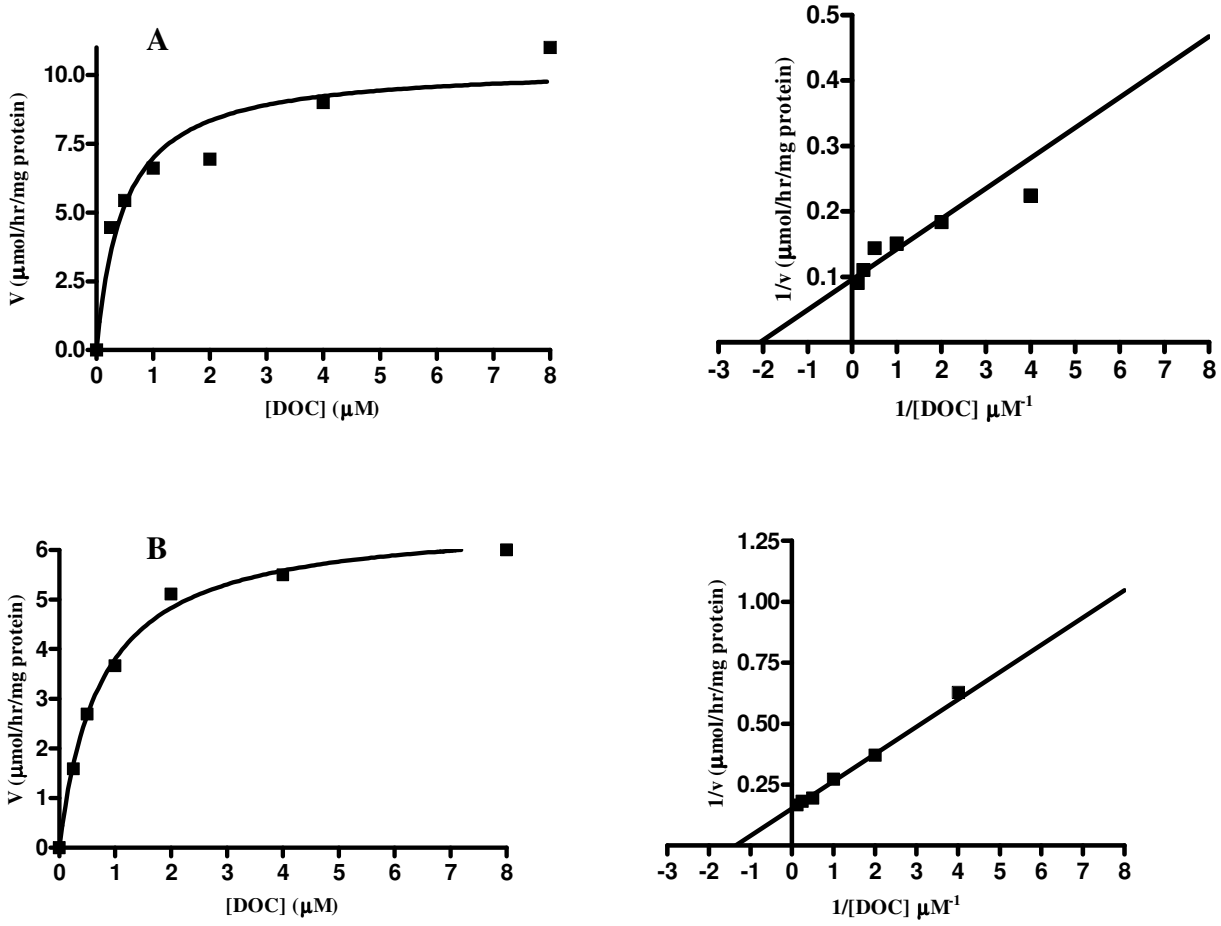

Figure 4.3. Kinetic analysis of 11-DOC metabolism by Cape Baboon CYP11B1 isoforms expressed in COS-1 cells. (A) The Michaelis-Menten curve showing the effect of 11-DOC concentration on the velocity of the 11β-hydroxylase reactions and the Lineweaver-Burk plot for the 11β-hydroxylation of 11-DOC to corticosterone by CYP11B1a. Results are representative of three independent experiments. (**B)** The Michaelis-Menten curve showing the effect of 11-DOC concentration on the velocity of the 11β-hydroxylase reactions and the Lineweaver-Burk plot for the 11β-hydroxylation of 11-DOC to corticosterone by CYP11B1wt. Results are representative of three independent experiments.

11-Deoxycortisol metabolites were identified and quantified using LC-MS. Figure 4.4 shows a mass spectrum of a cortisol standard with ions corresponding to the molecular ion, *m/z* 363.21; the loss of water ($[M-H_2O]^+$), *m/z* 345.21 and the sodium adducts ($[MH^+ + Na]^+$) and ($[MH^+ + 2Na]^+$), *m/z* 387.18 and *m/z* 387.18, respectively.

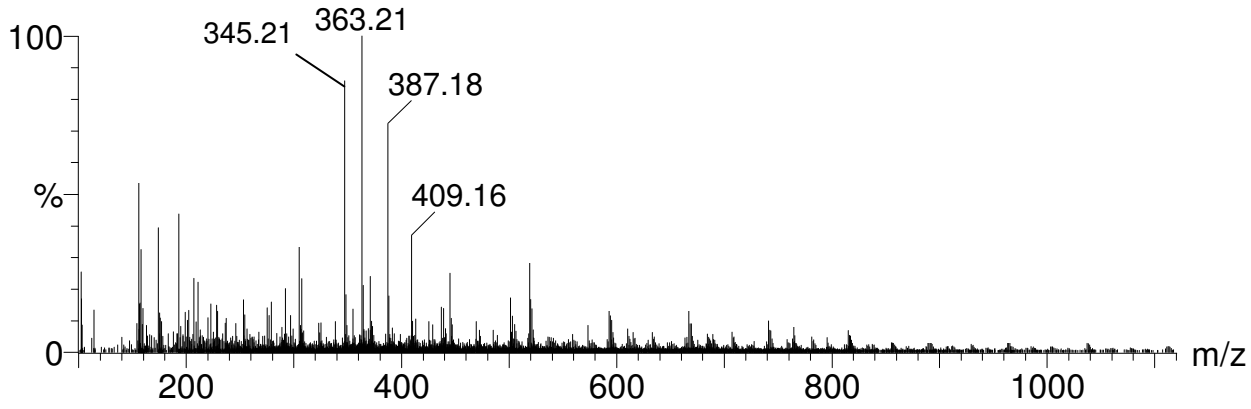

Figure 4.4. A mass spectrum of a cortisol standard, separated on a Phenomenex Luna C18(2 mm) 3um 0.2x150mm column using 68% acetonitrile and 0.1% formic in water as mobile phase. MS conditions: capillary voltage, 3.5 kV; cone voltage, 35 V; temperature source, 100°C. Ions were generated in the ion positive mode, because of a stronger signal obtained than in the negative mode.

Standard curves for 11-deoxycortisol and cortisol were constructed ranging from 0.04 µM to 10 µM of steroid standards. An example of steroid standards (0.625 µM), separated on a C18 column, is shown in Figure 4.5. 11-Deoxycortisol, with a molecular weight of 347.3, elutes at 3.11 minutes (Figure 4.5.A) while cortisol, with a molecular weight of 363.3, elutes at 2.75 minutes (Figure 4.5.B).

The ratios of the peak areas of 11-deoxycortisol and cortisol, respectively, were plotted against the steroid standard concentrations. The calibration curves were linear over concentrations 0.04 µM to 5µM (excluding the 10 µM steroid standard) with regression correlation coefficients above 0.99 (Figure 4.6). The 10 µM steroid standard was excluded because the linear range of the method limits its accuracy up to 5 µM.

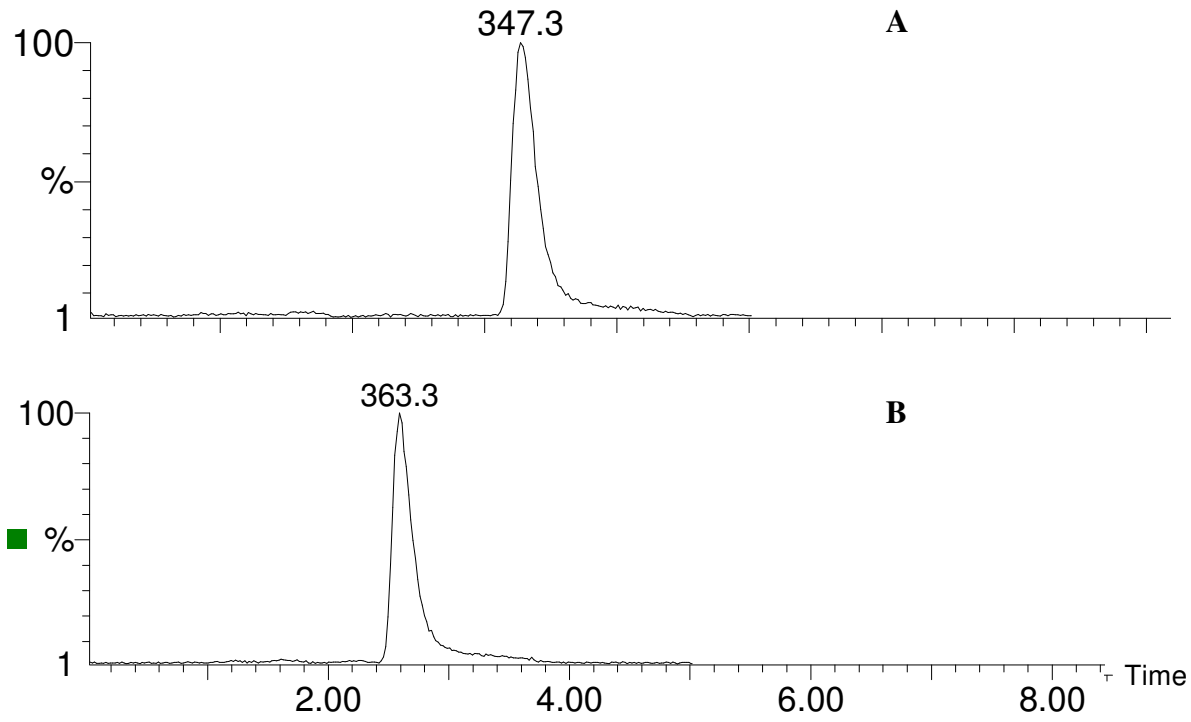

Figure 4.5. Chromatograms of 11-deoxycortisol standard and cortisol standards separated on a Phenomenex Luna C18(2 mm) 3um 0.2x150mm column using 68% acetonitrile and 0.1% formic acid in water as mobile phase. (A) 11-Deoxycortisol, Mr 347.3, eluting at 3.11 minutes and (B) cortisol, Mr 363.3, eluting at 2.75 minutes.

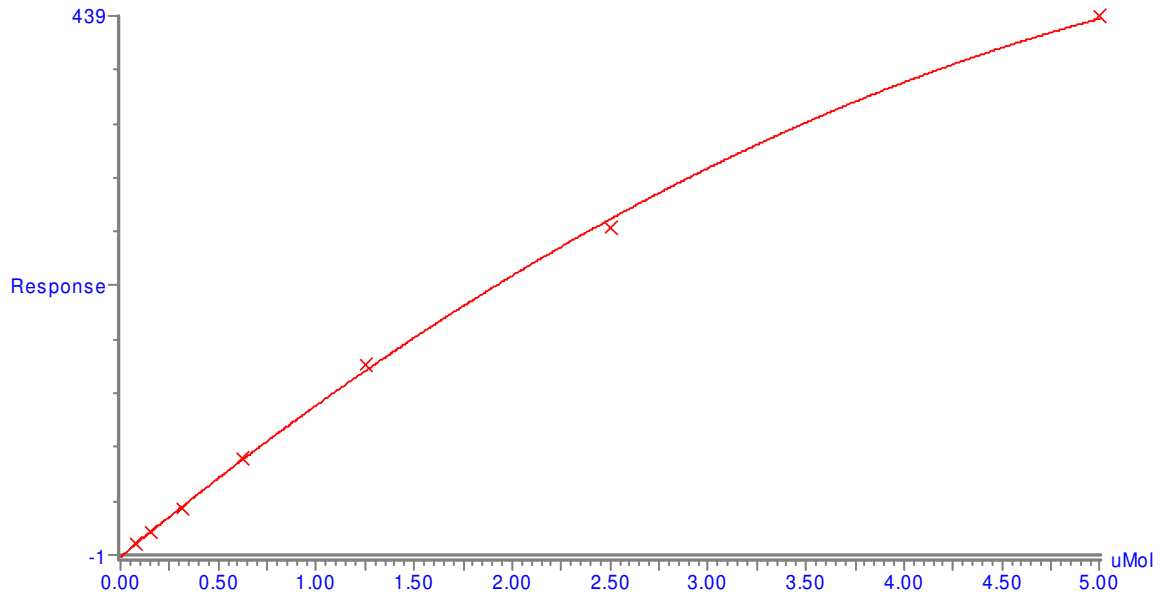

Figure 4.6. Calibration curve of cortisol standards ranging from 0.04 µM to 5µM. This curve was used to quantify cortisol in the steroid samples.

The steroid metabolite concentrations were calculated by comparing their ratios of peak areas to those of the standards. An example of the peak areas of a sample, containing 11-deoxycortisol, and an 11-deoxycortisol standard is shown in Figure 4.7.

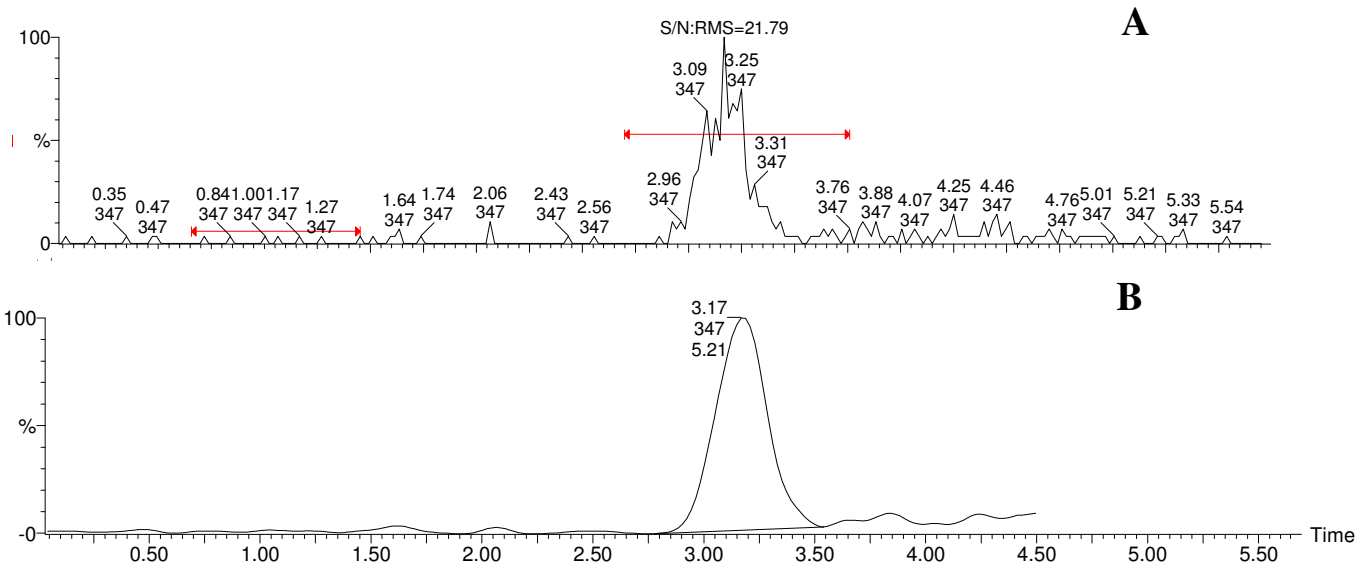

Figure 4.7. Example of the peak areas of a sample, containing (A) 11-deoxycortisol, Mr 347.3, eluting at 3.25 minutes and (B) 11-deoxycortisol standard, Mr 347.3, eluting at 3.17 minutes.

The apparent *K*m- and *V*-values for 11-deoxycortisol metabolism by the recombinant baboon CYP11B1 isoforms, expressed in COS-1 cells, were determined using the Lineweaver-Burke, Eadie-Hoffstee, Hanes-Woolf and Direct Linear plots. The apparent *K*m- and *V*-values for 11-deoxycortisol metabolism by CYP11B1wt and CYP11B1a are summarized in Table 4.2. One way ANOVA test showed no significance between the *K*m- and *V*-values determined by the four methods for both isoforms.

The Michaelis-Menten and Lineweaver-Burke plots for the metabolism of 11-deoxycortisol by both CYP11B1a and CYP11B1wt are shown in Figure 4.8. The apparent *K*m- and *V*-values for 11-deoxycortisol metabolism by CYP11B1a are 0.8009 ± 0.1621 µM and 7.40 ± 0.5275 nmol/hr/mg protein (Figure 4.8.A), whilst CYP11B1wt demonstrated values of 1.07 ± 0.06657 µM and 7.075 ± 0.1703 nmol/hr/mg protein, respectively (Figure 4.8.B). The initial reaction rates for 11-deoxycortisol at substrate concentrations ranging from 0.125 µM to 4 µM were determined by linear regression. At least 6 time points were used for each rate determination and a R-squared value for all initial rate regression analyses was always higher

than 0.95. Statistical analysis showed no significant difference (P = 0.055) in the apparent *K*m-values between CYP11B1a and CYP11B1wt for 11-deoxycortisol utilization.

Table 4.2. The apparent *K*m- and *V*-values for 11-deoxycortisol metabolism by CYP11B1wt and CYP11B1a, expressed in COS-1 cells, as determined by Direct Linear, Eadie-Hoffstee and Hanes-Woolf plots.

	Direct Linear Plot		**Eadie-Hoffstee Plot**		**Hanes-Woolf**	
	Km[1]	**V[2]**	**Km[1]**	**V[2]**	**Km[1]**	**V[2]**
CYP11B1a	1.12 ± 0.21	8.98	1.05 ± 0.08	8.26	0.77 ± 0.24	7.19
CYP11B1wt	0.97 ± 0.06	6.89	0.98 ± 0.26	6.83	1.03 ± 0.22	6.99

[1]: *K*m values are expressed in μM as the mean±S.E.M. of three independent experiments.
[2]: *V*-value is expressed in nmol/hr/mg protein as the mean±S.E.M. of three independent experiments.

The positive control transfection experiments showed that progesterone was metabolized to 60% 17α-hydroxprogesterone by baboon pTarget™-CYP17 constructs, expressed in COS-1 cells. In the mock transfection experiments, no 17α-hydroxprogesterone was produced. The transfection experiments carried out with water and no COS-1 cells also showed that 11-DOC and 11-deoxycortisol, respectively, was not converted to its intermediates. Results are not shown.

For the mock experiments in COS-1 cells, transfected with pTarget™-CYP17 constructs, using 11-DOC and 11-deoxycortisol as substrates, respectively, did not metabolize any of the steroid substrates. However, when progesterone was used as substrate, 17α-hydroxyprogesterone was produced. The control experiments using no plasmid and no cells did not convert 11-DOC or 11-deoxycortisol to their respective metabolites. Results are not shown.

4.3.3. Determination of 18-hydroxylase and 18-oxidase activity of baboon CYP11B expressed in COS-1 cells

To establish if the cloned baboon CYP11B genes displayed 18-hydroxylase and 18-oxidase activity towards 11-DOC, 11-deoxycortisol or corticosterone, the conversion of these three

substrates (2 μM) to products was assayed in COS-1 cells, transfected with the respective plasmids.

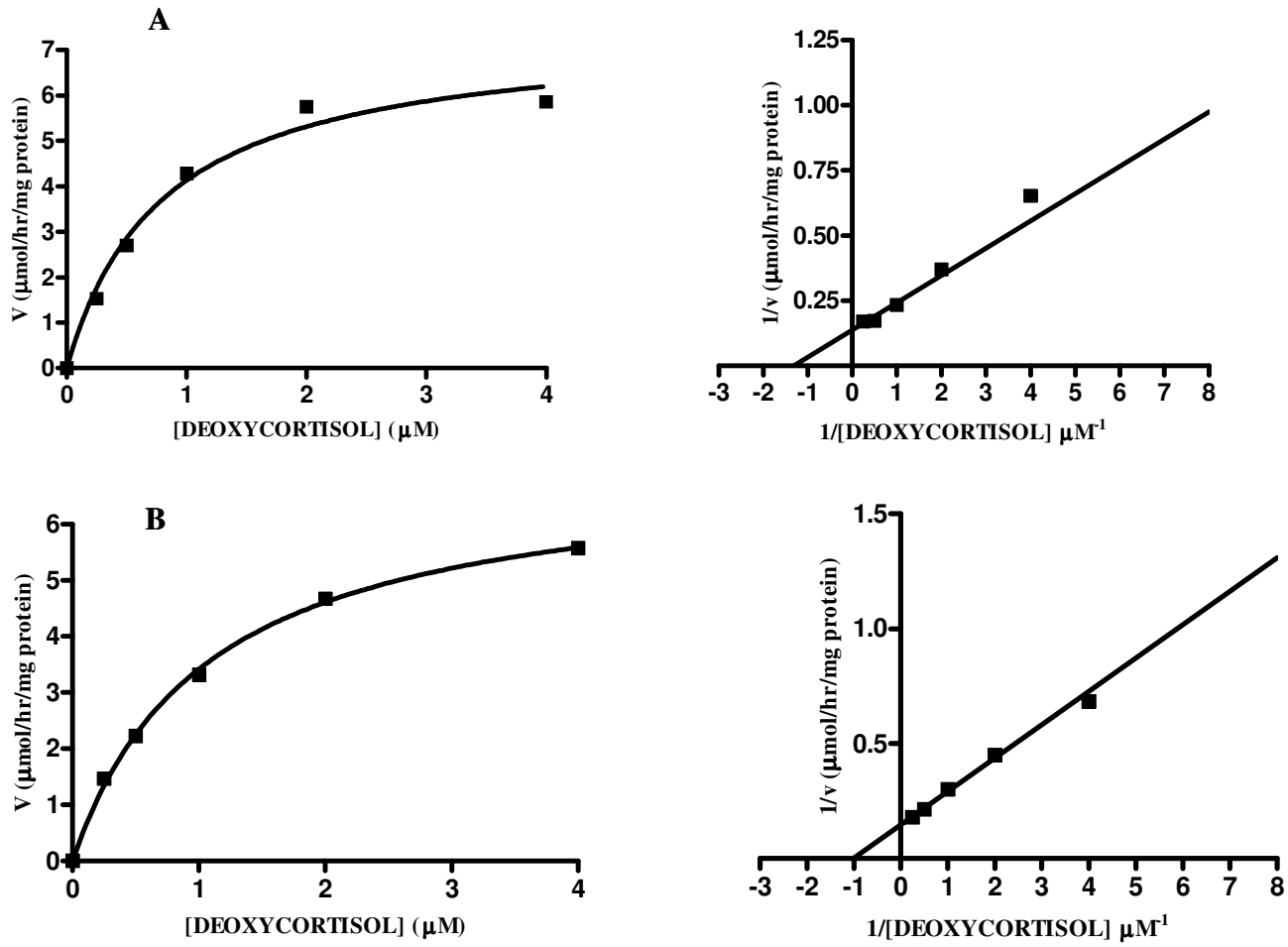

Figure 4.8. Kinetic analysis of 11-deoxycortisol metabolism by Cape Baboon CYP11B1 isoforms, expressed in COS-1 cells. (A) The Michaelis-Menten curve showing the effect of 11-deoxycortisol concentration on the velocity of the 11β-hydroxylase reactions and the Lineweaver-Burk plot for the 11β-hydroxylation of 11-deoxycortisol to cortisol CYP11B1a. (**B**) The Michaelis-Menten curve showing the effect of 11-deoxycortisol concentration on the velocity of the 11β-hydroxylase reactions and the Lineweaver-Burk plot for the 11β-hydroxylation of deoxycortisol to cortisol by CYP11B1wt. Results are representative of three independent experiments.

11-DOC metabolites were identified using LC-MS. Figure 4.9 shows the steroid standards, 11-DOC, corticosterone, 18-hydroxy-corticosterone and aldosterone, which were used to identify the metabolites.

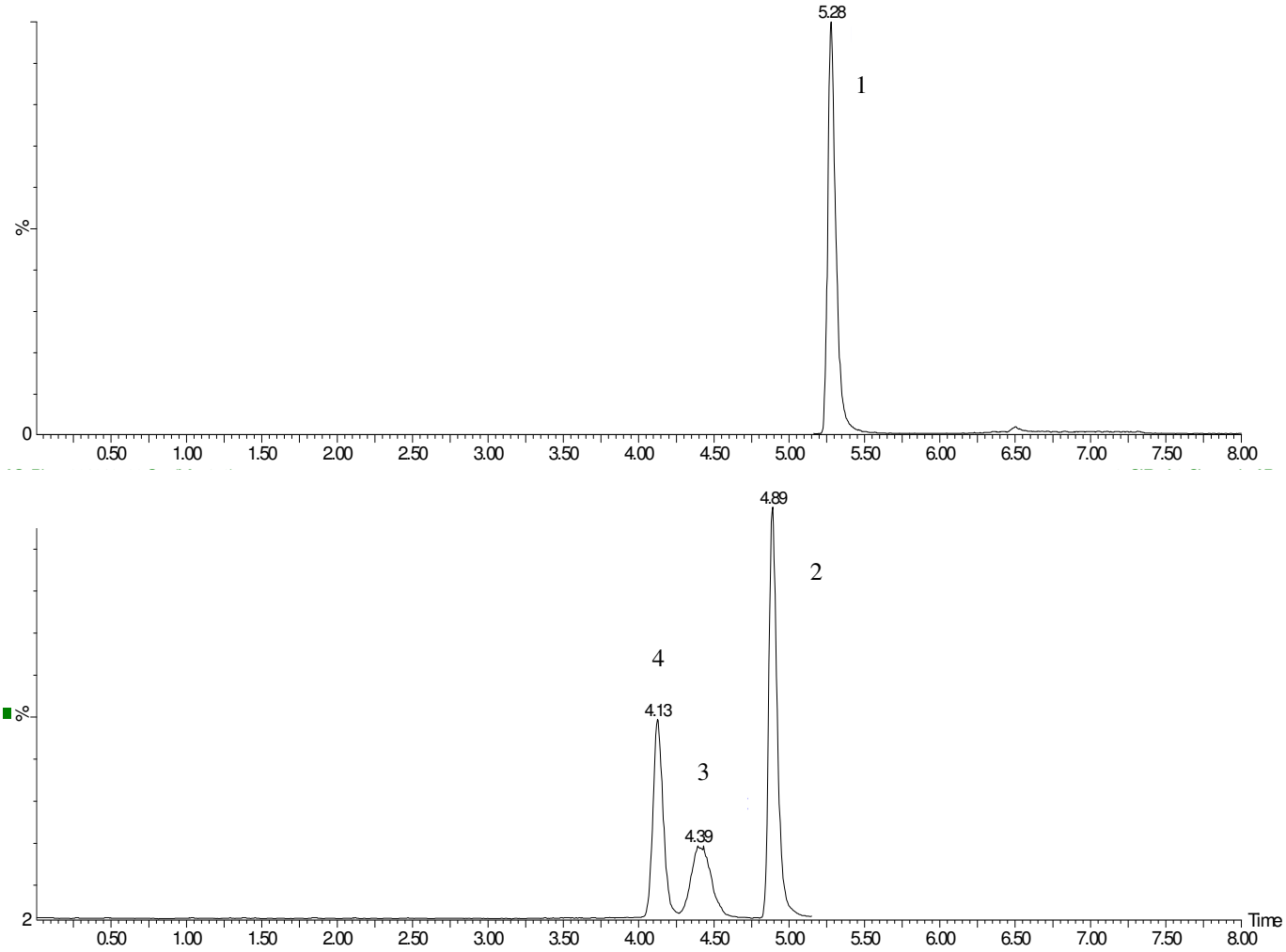

Figure 4.9. Chromatograms of steroid standards separated on a Phenomenex Luna C18(2 mm) 3um 0.2x150mm column using water and methanol as mobile phase. (1) 11-DOC, Mr 331.2, eluting at 5.28 minutes; (2) corticosterone, Mr 363.3, eluting at 4.89 minutes; (3) 18-hydroxy-corticosterone, Mr 363, eluting at 4.39 minutes and (4) aldosterone, Mr 361, eluting at 4.13 minutes.

CYP11B1a and CYP11B1wt metabolized 11-DOC to corticosterone only; no 18-hydroxy-corticosterone and aldosterone were formed (Figure 4.10). No 18-hydroxy-corticosterone and aldosterone were detected when corticosterone was assayed in COS-1 cells; results are not shown.

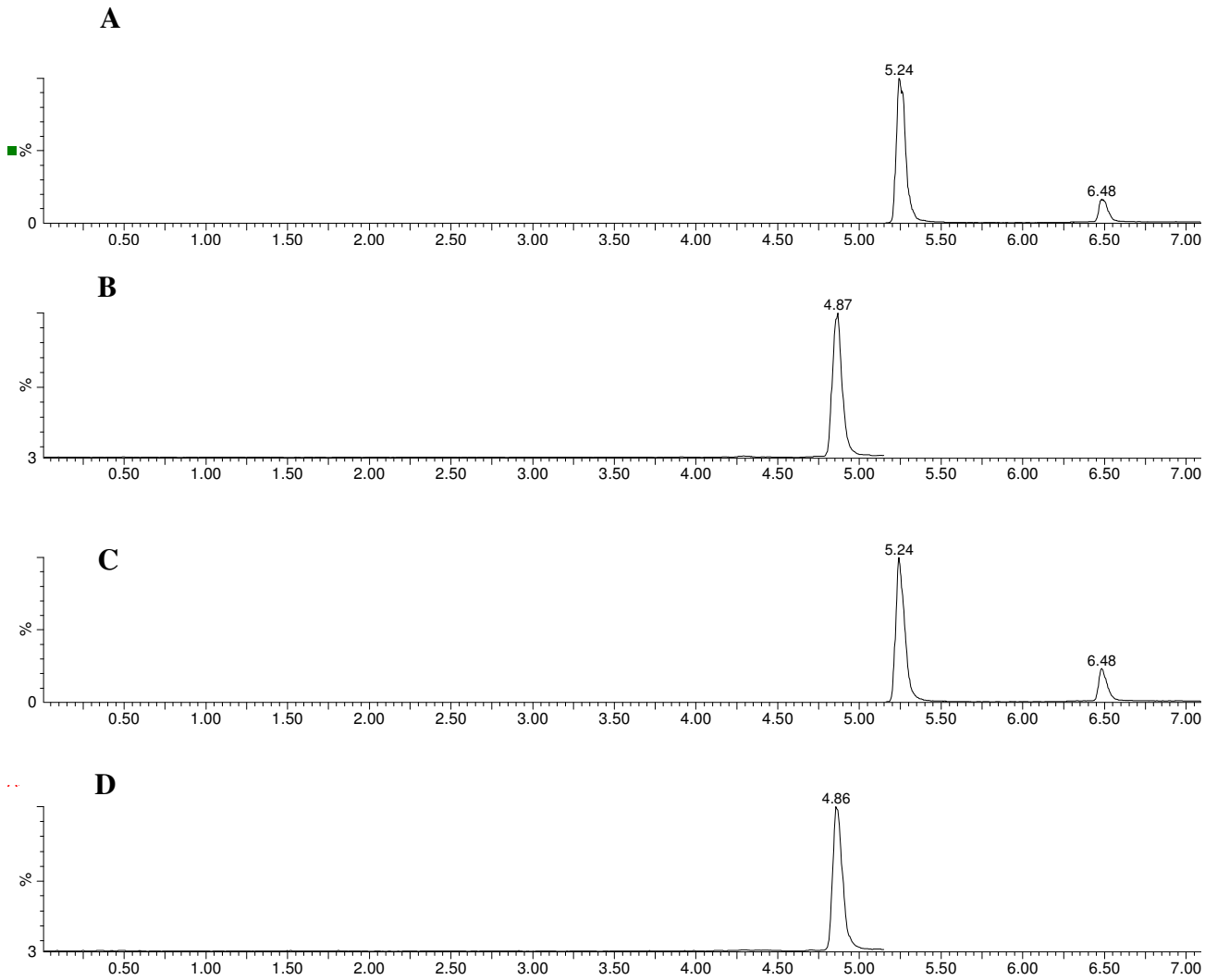

Figure 4.10. Chromatograms of steroid metabolites for 11-DOC metabolism. (A, B) 11-DOC metabolism by CYP11B1a after 8 hours. 11-DOC, Mr 331.2, eluting at 5.24 minutes and corticosterone, Mr 363.3, eluting at 4.87 minutes. (C, D) 11-DOC metabolism by CYP11B1wt after 8 hours. 11-DOC, Mr 331.2, eluting at 5.24 minutes and corticosterone, Mr 363.3, eluting at 4.86 minutes.

Figure 4.11 shows the 11-deoxycortisol and cortisol standards, which were used to identify the steroid metabolites when 11-deoxycortisol conversion was assayed in COS-1 cells. 11-Deoxycortisol was metabolized to cortisol only by the two Cape baboon CYP11B1 cDNAs (Figure 4.12). It appears as if the utilization of 11-deoxycortisol by CYP11B1a and CYP11B1wt, presented in Figure 4.12, differs from that shown in Figure 4.1.E. It seems as if CYP11B1wt converts 11-deoxycortisol to cortisol at a slower rate than CYP11B1a at 8 hours, while at 16 hours (Figure 4.1.E) a comparable 11β-hydroxylase activity for both isoforms towards 11-deoxycortisol is seen. These results suggest that it takes longer for CYP11B1wt to metabolize 11-deoxycortisol than CYP11B1a. Although not statistically significant, the *V*-

values found in Table 4.2 confirms that CYP11B1a has a higher conversion rate for 11-deoxycortisol than CYP11B1wt.

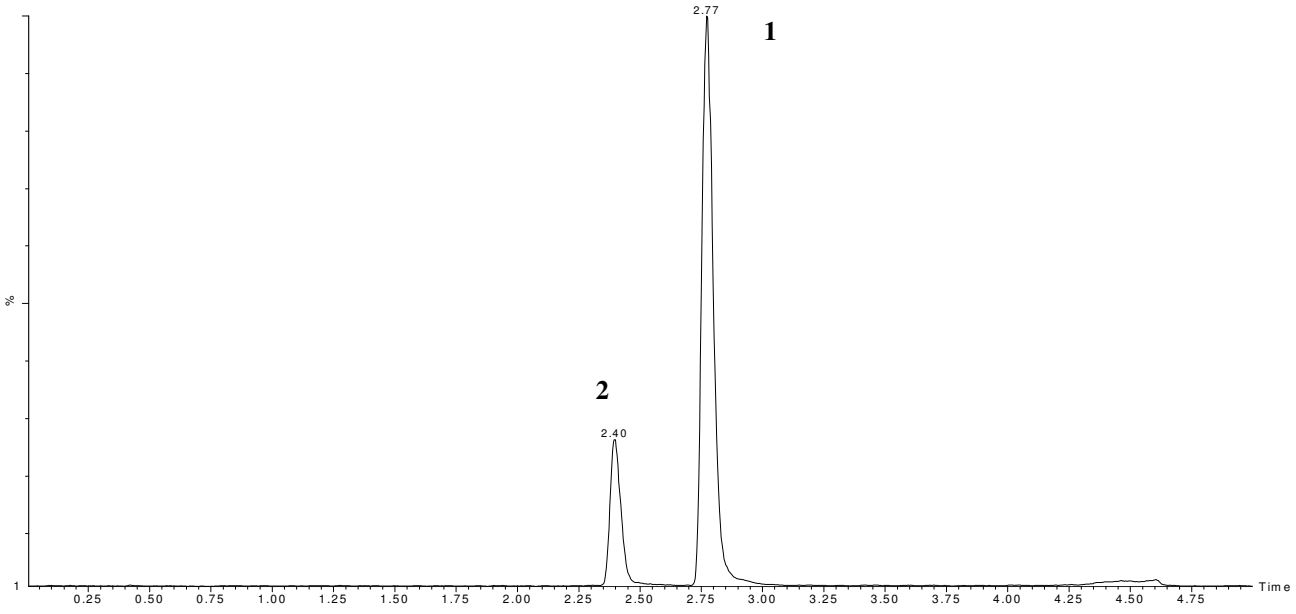

Figure 4.11. Chromatograms of steroid standards separated on a Phenomenex Luna C18 (2 mm) 3um 0.2x150mm column using formic acid and acetonitrile as mobile phase. (1) 11-Deoxycortisol, Mr 347.5, eluting at 2.77 minutes and (2) cortisol, Mr 363.3, eluting at 2.40 minutes.

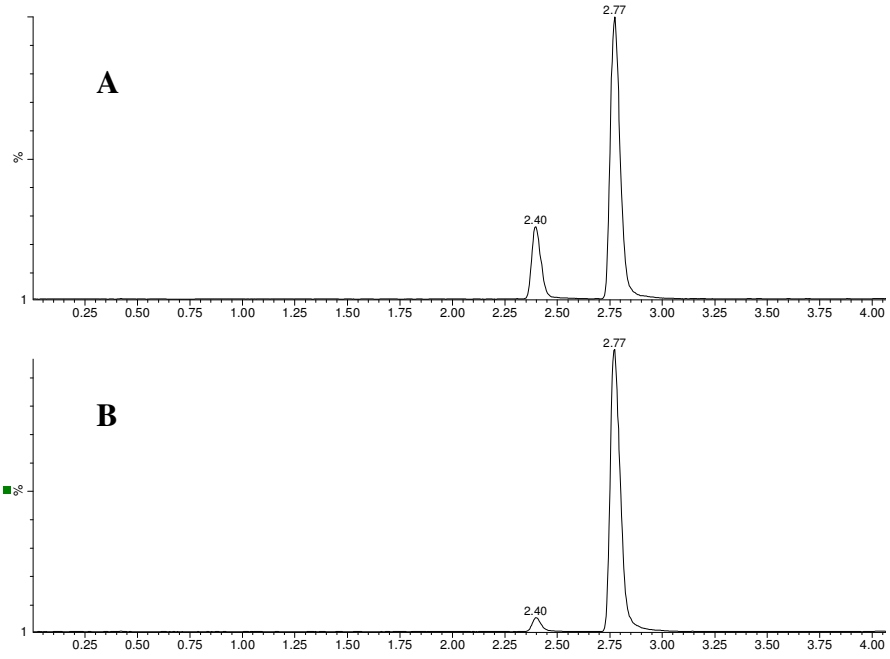

Figure 4.12. Chromatograms of steroid metabolites for 11-deoxycortisol metabolism. (A) 11-Deoxycortisol metabolism by CYP11B1a after 8 hours. 11-Deoxycortisol, Mr 347.5, eluting at 2.77 minutes and cortisol, Mr 363.3, eluting at 2.40 minutes. (B) 11-Deoxycortisol metabolism by CYP11B1wt after 8 hours. 11-Deoxycortisol, Mr 347.5, eluting at 2.77 minutes and cortisol, Mr 363.3, eluting at 2.40 minutes.

4.3. DISCUSSION

Three genes encoding CYP11B1 were cloned from Cape baboon adrenals and used in expression studies in COS-1 cells. Two of the CYP11B1 isoforms, namely CYP11B1a and CYP11B1wt, were shown to be functional enzymes and catalyzed the metabolism of 11-DOC to corticosterone only, with negligible amounts of 18-hydroxycorticosterone and aldosterone being formed. The third gene, CYP11B1S, exhibited no steroid hydroxylase activity. The results indicated that these genes encode CYP11B1 and have little or no detectable aldosterone synthase activity.

Results obtained from the enzymatic activity study, using 11-DOC and 11-deoxycortisol as substrates, showed that both CYP11B isoforms 11β-hydroxylate the respective substrates with different efficiencies and selectivities. CYP11B1wt and CYP11B1a both catalyzed the formation of corticosterone from 11-DOC, however, at different rates. Both isoforms exhibited comparable 11β-hydroxylase activities towards 11-deoxycortisol. It is possible that these differences observed with regards to the catalytic activities of the baboon CYP11B1 isoforms may be due to the three amino acid substitutions resulting from the nucleotide changes in exon three.

Kinetic data for both baboon cDNAs were determined using Direct Linear, Eadie-Hoffstee, Hanes-Woolf and Lineweaver-Burke plots to assess the accuracy of the kinetic experiments carried out with the two heterologously expressed baboon CYP11B enzymes. Theoretically, the Lineweaver-Burke, Eadie-Hoffstee, Hanes-Woolf plots and the Direct Linear plot are all relatively similar to each other as they are based on an algebraic conversion of the Michaelis-Menten equation to give a straight line equation. Of these, the Direct Linear plot is regarded as the most accurate since it holds several advantages over the other well-known plots. As the Direct Linear plot is entirely composed of straight lines, which intersect at the same point, the estimated true values for the kinetic parameters are reflected. Velocity is plotted against substrate concentrations; since a vertical line drops from the intersection to the substrate axis and a horizontal line to the velocity axis, the *K*m- and *V*-values can be determined directly from the graph. Data represented by the Lineweaver-Burke plot is often scattered, particularly in the area that represents lower substrate concentrations. This plot exaggerates the error at these low concentrations where measurements are often less precise as velocities are slower. The Eadie-Hofstee plot also shows a bit of scatter, which results in *K*m- and *V*-values that are

skewed away from the true values. The error is not as severe as with the Lineweaver-Burke plot and is generally regarded as being a better technique. The Hanes-Woolf plot also shows some scatter, but is less severe that in the Lineweaver-Burke or Eadie-Hofstee plots [77, 78]. Since there was no significant difference in the data obtained from these four methods and the values showed a similar trend in the substrate affinities for CYP11B1a and CYP11B1wt, the Lineweaver-Burke kinetic data was used for the *K*m- and *V*-values as it is also generally accepted that the Lineweaver-Burke plot is used to represent kinetic data. Kinetic analysis for the baboon cDNAs revealed that CYP11B1a has a higher affinity for 11-DOC than CYP11B1wt, with Lineweaver-Burke apparent *K*m-values of 0.48 μM and 0.74 μM, respectively. Statistical analysis showed that the apparent *K*m-values for 11-DOC utilization by CYP11B1a and CYP11B1wt differed significantly ($P = 0.035$). CYP11B1a exhibited a *K*m-value of 0.80 μM for 11-deoxycortisol utilization, showing that this isoform has a higher affinity for 11-DOC than for 11-deoxycortisol. CYP11B1wt exhibited approximately the same affinity for both substrates. An apparent *K*m-value of 1.07 μM was determined for 11-deoxycortisol utilization by CYP11B1wt. There was no significant difference in the apparent *K*m-values ($P = 0.055$) between CYP11B1a and CYP11B1wt for 11-deoxycortisol utilization.

Since CYP11B1a displayed a higher affinity for 11-DOC, which is the natural substrate for human CYP11B2, and also has only one Sma1 site as is the case with human CYP11B2, it was necessary to verify if this isoform is a true 11β-hydroxylase or has a level of equity with CYP11B2. Since CYP11B1wt has two Sma1 sites in the same position as human CYP11B1, it was assumed that this baboon isoform is a true 11β-hydroxylase. It has been shown that guinea pig CYP11B2 has a higher 11β-hydroxylase activity towards androstenedione than CYP11B1 and also exhibits 18-hydroxylase activities towards this substrate; therefore *in vivo* experiments, using androstenedione as substrate were performed in our laboratory. Using the LC-MS method, which was developed in our department for the identification and quantification of steroid metabolites, low levels of 11β-hydroxyandrostenedione were detected. CYP11B1a produced more of this intermediate than CYP11B1wt, indicating that CYP11B1a has a higher 11β-hydroxylase activity towards androstenedione than CYP11B1wt. These Cape baboon cDNAs did not exhibit any 18-hydroxylase activity towards androstenedione. These results are not shown since very little 11β-hydroxy-androstenedione was detected; these results are believed to be inconclusive and should be researched further. Corticosterone was also used as substrate to ascertain whether the Cape baboon CYP11B

cDNAs exhibit any 18-hydroxlase and 18-oxidase activity towards this substrate. Since it is believed that the recombinant Cape baboon cDNAs are isoforms of CYP11B1, we did not expect these cDNAs to metabolize corticosterone to aldosterone. The results obtained from LC-MS demonstrated that the two functional enzymes of Cape baboon CYP11B1 exhibited 11β-hydroxylase activity only.

In chapter three the possibility of another accessory protein, which may be important to deliver electrons from AdR to the CYP11B isoforms found in the Cape baboon adrenal medulla, were mentioned since no AdX was detected in the medullary tissue homogenates. Bulow and Bernhardt established that basic levels of reducing equivalents are sufficient for 11β-hydroxylase activity of CYP11B1, which may be the case with the Cape baboon CYP11B1 cDNAs, which was cotransfected with human AdX in COS-1 cells [68]. It is possible that the recombinant Cape baboon CYP11B1 isozymes did not exhibit 18-hydroxylase and 18-oxidase activity, which requires high levels of reducing equivalents, towards corticosterone produced from 11-DOC, due to the unavailability of a putative accessory protein, present in the baboon medulla.

The catalytic activity studies of Cape baboon CYP11B1 in adrenal tissue homogenates demonstrated that more than one isoform of this enzyme might exist. A CYP11B1 isoform was identified in the adrenal cortical tissue homogenate, which exhibited a different catalytic activity towards 11-DOC than the isoform found in the adrenal medullary tissue homogenate. The CYP11B1 isoform in the adrenal cortical tissue homogenates seemed to have a higher 11β-hydroxylase activity towards 11-DOC than the enzyme located in the adrenal medullary tissue homogenates; a marked difference in the amounts of corticosterone produced in the respective adrenal tissue homogenates were observed. The diminished 11β-hydroxylase activity towards 11-DOC in the adrenal medullary tissue homogenate could be ascribed to the fact that no AdX was detected in the medulla. Since Bulow *et al.* showed that the 18-hydroxylase- and 18-oxidase activity of CYP11B2 is strongly dependent on the presence of high levels of reducing equivalents [68], and the fact that a CYP11B isoform, which exhibits these activities towards corticosterone, is present in the adrenal medullary tissue homogenate, it is possible that a protein other than AdX may act as a redox partner in shuttling electrons from AdR to CYP11B isozymes in the medulla.

It would seem that CYP11B1a, which has a higher affinity for 11-DOC than CYP11B1wt, is representative of the isoform found in the baboon adrenal cortex. CYP11B1wt might be representative of the isoform, which is located in the adrenal medulla and has a lower 11β-hydroxylase activity towards 11-DOC.

Sequence analysis of the Cape baboon CYP11B1a and CYP11B1wt showed that nucleotide changes in exon three resulted in the amino acid changes, Val177Leu, Glu182Asp and Ile188Val, respectively. Previous studies with Dahl rat CYP11B2 and human CYP11B1 and CYP11B2 showed that a Glu to Asp mutation in exon three might substantially affect the enzyme activity. The Dahl rat CYP11B2, with a Glu136Asp mutation in exon three, encoded an enzyme with a greater apparent maximum velocity and a lower apparent *K*m, resulting in an increased rate of 11-DOC conversion to aldosterone [79]. The Glu147Asp mutation in the human CYP11B enzymes led to a decrease in the affinity of CYP11B1 for 11-DOC as shown by an increase in the apparent *K*m of the enzyme from 2.5 μM in the human wild type to 7.5 μM in the mutant. The mutation did not affect the 11-deoxycortisol conversions to cortisol by human CYP11B1. The Asp147Glu mutation in human CYP11B2 enhanced the conversion of 11-DOC to corticosterone, but did not change the conversion of 11-deoxycortisol to cortisol. The *K*m-values for the wild type and mutant CYP11B2 are 5 μM and 1.4 μM, respectively. It was concluded that the function of residue 147 in the human CYP11B enzymes is substrate dependent and that the 17α-hydroxyl group of 11-deoxycortisol interacts with the enzymes in a way that obviates the role of the amino acids; the residue also contributes to the functional specificity of the enzymes. In the baboon, residue 147 is located at the interface between the D- and E-helices and it may interact in some way with the substrate and heme-binding domain regions where it possibly maintains the correct orientation of the substrate within the active site [79, 80].

The contrasting catalytic activities of baboon wild type and CYP11B1a towards 11-DOC and 11-deoxycortisol, respectively, may possibly be due to the differences in their amino acid sequences. It is possible that the conservative change, Glu182Asp in exon three, of these two enzymes can affect the steroid metabolism significantly and that the residue at 182 can contribute to the functional specificity of the two enzymes.

Amino acid sequence alignment of Cape baboon CYP11B1a and CYP11B1wt showed that these isoforms are more closely related to human CYP11B1 than CYP11B2. Cape baboon CYP11B1a, CYP11B1wt and CYP11B1S contain six amino acid residues, Ser112, Ser288, Pro301, Asp302, Val320 and Asn335, which are important for 11β-hydroxylase activity of human CYP11B1 and only two amino acid residues, Asp147 and Val386, which are important for aldosterone synthase activity of human CYP11B1. Leu301 in CYP11B2 is important for 18-oxidase activity. Cape baboon CYP11B1 isoforms have Pro in this position. The expressed Cape baboon CYP11B cDNAs exhibited only 11β-hydroxylase activity towards 11-DOC and 11-deoxycortisol. A comparison of amino acid sequences between the cloned CYP11B baboon genes and human CYP11B1 show a 96% homology. These results indicate that the baboon CYP11B investigated in this study are isoforms of the CYP11B1 gene only.

Previous investigations into the nucleotide sequence of CYP11B genes, obtained from genomic DNA, identified both CYP11B isoforms (CYP11B1 and CYP11B2) [1]. Intron five of one of the identified baboon gene was approximately 400 bp longer than the other corresponded to the sequence of human CYP11B2 (intron five of human CYP11B2 is also 440 bp longer than intron five of CYP11B1). This led to the assumption that CYP11B2 is present in the Cape baboon. Additionally, the CYP11B1 and CYP11B2 promoters were identified in the baboon CYP11B clones, and sequence analyses showed a distinct difference between the two promoters [M. Hampf, personal communication]. The baboon CYP11B1 promoter exhibited 90% homology to the human CYP11B1 promoter [1]. These data show that the Cape baboon has both CYP11B1 and CYP11B2 isoforms and that the CYP11B investigated in this study are all isoforms of CYP11B1. Although CYP11B2 is indicated in the Cape baboon, no attempt as yet has been made to clone CYP11B2 from the Cape baboon medullary RNA.

Further investigations into the structure of CYP11B1wt and CYP11B1a were conducted in order to establish the functional implication of the three amino acid substitutions on the kinetic parameters of the two enzymes.

CHAPTER FIVE

HOMOLOGY MODELING OF CAPE BABOON CYP11B1 ISOFORMS

5.1 INTRODUCTION

Cytochrome P450 enzymes are multifaceted catalysts, which exhibit significant diversity in their substrate specificities. These ubiquitous enzymes form part of a superfamily of hemoproteins of which more than 400 individual isoforms have been identified and sequenced [81, 82, 83 and references therein]. The P450 isoforms often display strict regio- and stereospecificity towards particular compounds due to the remarkable flexibility of the structure of the heme pocket of these enzymes, which accommodate various substrates in multiple orientations. The elucidation of the structural foundation for such specificity is of immense importance in comprehending enzyme function and mechanism. Homology modeling, combined with mutagenesis studies on various P450 enzymes, have provided extensive information on which structural features control substrate specificity and have also contributed to providing important insight into the catalytic mechanisms in these enzymes. Homology modeling has also been used to acquire three-dimensional structures of P450 enzymes, for which the sequence information is available but the X-ray structures are lacking. Homology modeling has therefore, become an essential tool in understanding the structural basis of P450 enzyme function [84, 85].

To date, the crystallized structures of a number of bacterial P450 enzymes and that of a few microsomal P450 enzymes, which have been solubilized by truncation and site-directed mutagenesis, have been experimentally determined. Investigations into the crystallized structures of the bacterial P450 enzymes revealed a conserved structural fold and demonstrated the contributions of the regions surrounding the catalytic core for substrate specificity.

The first three–dimensional structures of human CYP11B1 and CYP11B2 were modeled using the crystallographic coordinates of two bacterial P450 enzymes, CYP102 and CYP108, as structural templates. Attention was given to the modeling of the active sites of the CYP11B isozymes and a comparison of the active site structures followed. Key residues in the active sites of the CYP11B isoforms were identified. The homology modeled structures were used to elucidate the structure/function relationships of these enzymes [19]. Recently, Krone *et al.* used the mammalian CYP2C5 as a template for the three-dimensional modeling of human CYP11B1

in order to study the structural and functional effects that various mutations, identified in patients suffering from CAH, have on CYP11B1. Modeling this membrane bound enzyme using a mammalian crystallized structure as template contributed towards the current knowledge with regards to the structure/function relationship of this enzyme [85].

The initial three-dimensional models of mammalian P450 enzymes, including CYP11A1, CYP19, CYP1A1, CYP2D6 and CYP2B1, were based on the structure of CYP101, the only available crystal structure at the time [86, 87]. CYP101, isolated from *Pseudomonas putida*, catalyzes the stereospecific hydroxylation of the bicyclic monoterpene camphor, yielding 5-exo-hydroxycamphor, which serves as a carbon and energy source. CYP101 is a class I enzyme and receives reducing equivalents from NADH *via* a FAD-containing putidaredoxin reductase (PdR) and a [2Fe-2S] cluster, comprising the ferredoxin, putidaredoxin (PdX) [88, 89].

In 1993, the heme binding domain of CYP102, a fatty acid monooxygenase from *Bacillus megaterium,* which exhibits a higher degree of homology with microsomal P450 enzymes than CYP101, was crystallized [90]. This enzyme forms part of the class II P450 enzymes and catalyzes the oxidation of various fatty acids using a FAD/FMN-containing reductase domain, which transfers NADPH-derived electrons to the enzyme [88, 89]. The crystallization of this unique P450 enzyme led to homology modeling of a number of P450 enzymes, which included members of the CYP1A subfamily, 2A subfamily, CYP2B1, 2B4, 2C3 and 2D6 [91].

The crystallization of other bacterial P450 enzymes, *viz.* CYP108, a α-terpineol monooxygenase from a *Pseudomonas* species, and CYP107A1, a 6-deoxyerythronolide β-hydroxylase from *Saccharopolyspora erythrea*, presented further key information about P450 enzyme structure [14, 20, 92]. Together with CYP101 and CYP102, these bacterial P450 enzyme models exhibited comparable topology in their overall three-dimensional structure and also in their secondary structure content, particularly in their heme-binding regions. These topological similarities prompted efforts to model mammalian P450 enzymes using these bacterial models as templates.

The crystal structures of the bacterial P450 enzymes, CYP101, CYP102, CYP108 and CYP107A1 revealed that these enzymes exhibit regions of high structural similarities. Evaluations of secondary structural elements of the four characterized enzymes demonstrated

the existence of 13 α-helices, consisting of the A, B, B′, and C-L helices and 5 β-sheets (β1-β5) in all four of the enzymes (Figure 5.1) [90, 93, 94]. However, CYP102 includes three additional α-helices; one positioned between helices J and K, i.e. J′, and two between helices K and L, namely K′ and K″, while two additional α-helices have been observed in CYP108. One helix is located near the amino terminus, A′, and the other one between helices K and L, namely K′. CYP101 and CYP108 also have an additional short β-structure, β6, respectively [88].

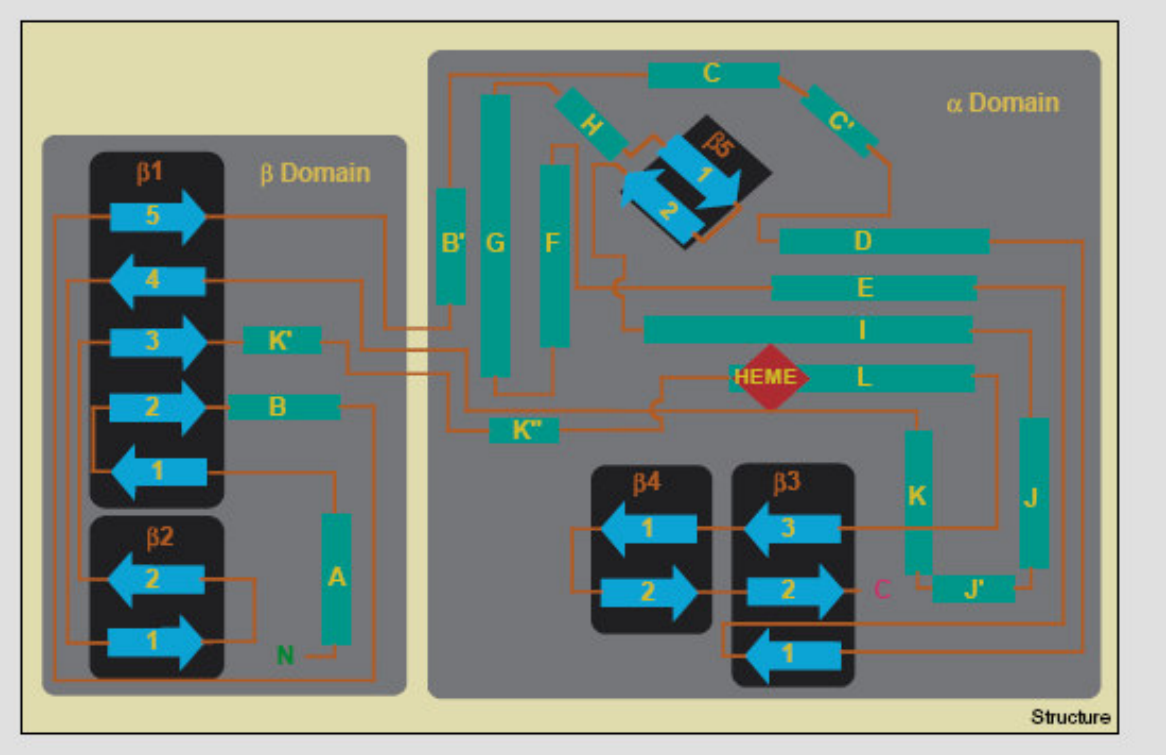

Figure 5.1. Topological representation of CYP102, illustrating the secondary structure elements of the P450 enzyme family of proteins. Green rectangles represent helices, blue arrows represent the strands of β-sheets, and orange lines represent the "random" coils connecting the helices and strands [94].

All four abovementioned enzymes contain a domain, called the meander, based on its extended wandering topology. The meander is a highly conserved region in all P450 enzymes and contains approximately 20 amino acid residues positioned between the Cys-pocket and the K′-helix on the proximal face of the enzyme. This region comprises the conserved Arg/His/Asn sequence, which forms part of the Glu352-Arg362-Arg378 triad. This triad functions as a folding motif in the meander, facilitating the stabilization of the three-dimensional structure of the meander region locking the Cys-pocket in a position that secures covalent binding of the

heme with the P450 enzymes. The Glu352 and Arg362 residues form part of the K-helix and are highly conserved in all P450 enzyme sequences and residue 378 is either Arg, His or Asn in all the P450 enzymes [95].

A well-defined core structure, which extends into the helical domain and comprises the central and carboxy-terminal portion of the I-helix, strand 1 of β-sheet 6 (β6-1), the Cys-pocket, L- and K- helices, is observed in the domains surrounding the heme (Figure 5.2). Another level of conservation involves those that form part of the internal structure of the respective bacterial P450 enzymes and includes the β1-1, β1-2, β1-3, β1-4 strands, the C-, E-, K-helices, the β2-2 and β6-2 strands and the meander region. The following structural conservations are preserved to a lesser extent and include the structures dominating the surface features of the molecules: the B-, C-, D, K′-helices, the amino-terminal segment of the I-helix, β3, β4, β1-5 and β2-1. The most divergent regions include the amino-termini, the surface helices, A-, B′-, F-, G-, which are involved in substrate recruitment and binding, the H-helix and β5 [88].

Although sequence identity within a specified P450 enzyme family shares approximately 40% homology, the secondary and tertiary structures within P450 enzymes are relatively conserved as shown by studies with X-ray crystallography, revealing primary sequence conservations among P450 enzymes. CYP102 as well as all eukaryotic P450 enzyme sequences have a common motif in the carboxy-terminus of the A-helix, X-Gly46, where X symbolizes a large hydrophobic residue, possibly anchoring the carboxy-terminus of the CYP102-A-helix, while Gly46 initiates a turn towards β1-1. The B′-helices contain a Phe77 in the β1-5 region, which serves to attach the amino-terminal flank of this strand to the core of the bacterial P450 enzymes. In the crystallized bacterial structures, the B′-C-turns are structurally similar and the bacterial enzymes display a reasonable degree of homology in this region, which is responsible for anchoring the carboxy-terminal flank of B′ in CYP102 and in eukaryotes. The well-defined amino-terminus of the C-helix of the bacterial enzymes contains the conserved Trp-X-X-X-Arg sequence, where Trp96 and Arg100 interact with the propionate side-chain of the heme group. The area between the F- and G-helices of the bacterial enzymes varies considerably in length and sequence content, which makes the prediction of borders between these helices and loops rather complex. The region between the G- and I-helices is relatively variable while the H-helix consists of a consistent sequence motif (Figure 5.3) [88].

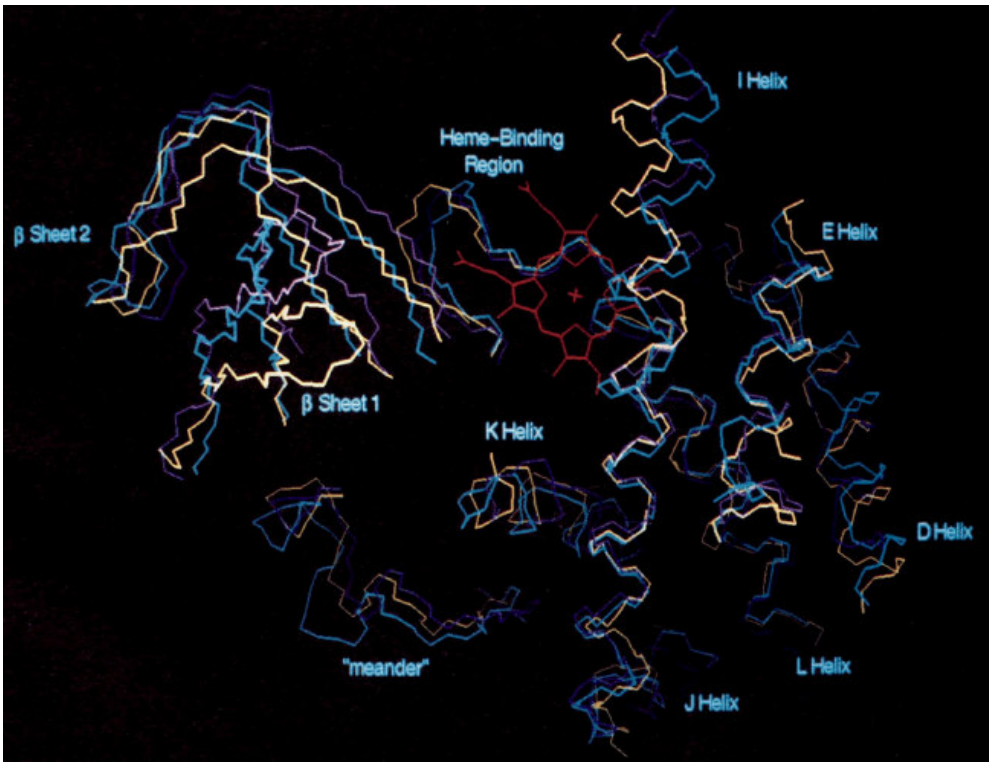

Figure 5.2. Core structures of Cytochrome P450s. Core structures of CYP101 (amber), CYP108 (purple), and the P450 domain of CYP102 (blue) are overlaid and shown along with the heme (red). The four-helix bundle on the right is composed of the I-, L-, D-, E-helixes with the heme-binding region and "meander" extending from the N-terminus of the L-helix. Conserved β -sheets on the left are composed of β-strands 1 and 2 [96].

The region between the I- and L- helices is highly conserved between P450 enzymes thus facilitating multiple alignments. CYP102 and the eukaryotic sequences have extended J- and J′-helix insertions in this region. The arrangement of the K-helices in this area is characterized by a conserved motif, Glu-X-X-Arg, which is highly conserved in all the P450 enzyme sequences examined to date. The existence of a variable β6-1 length in the bacterial P450 enzymes was also observed in the eukaryotic sequences. This variable segment is anchored at one end by the K-helix motif, Glu-X-X-Arg, and at the other end by the conserved Arg/His323 propionate ligand in the β1-4. A consistent homology is perceived in the K′-meander region, which is anchored by numerous conserved Pro residues and aromatic residues [88].

In bacterial P450 enzymes the domains most highly conserved are those engaged in heme-binding. The structures close to the heme include the B′-C-turn, the central I-helix, β6-1/β1-4, the Cys pocket and amino-terminal of the L-helix. In general, conservation of non-polar residues in this domain maintains an appropriate hydrophobic environment for the heme group.

All P450 enzyme Cys-pockets include four conserved amino acids and a high degree of sequence conservation, which extends from the Cys-pocket through most of the L-helix (Figure 5.3). The heme moiety of the P450 enzymes is covalently bound to the conserved Cys400, which is located in the hydrophobic environment in a β-"bulge" region, called the Cys-pocket. The purpose of the bulge region is to enfold the Cys residue in a hydrophobic environment. In addition to the Cys-residue, three other residues are also strictly conserved. Two of these conserved residues are Gly, one of which is in position 396 that permits the formation of a β-hairpin turn. The second Gly, at position 402, serves two purposes: (1) the residue allows for a sharp turn from the Cys-pocket into the L-helix and (2) for proximity to the heme. The third conserved amino acid residue is Phe393, which is situated fairly close to the sulfur-iron bond in the bacterial P450 enzymes. The side-chain, in combination with other side- and main-chain atom of the Cys-pocket, completes the hydrophobic shielding of the Cys-iron bond. The heme propionate side chains need polar and/or charged residues to accommodate their polarity and negative charge in the hydrophobic interior of the molecule. Four well-conserved residues, which are observed throughout the P450 enzymes, include the two residues, Trp96 and Arg100, in the amino-terminal end of the C-helix; an Arg333 residue in β1-4 and a His388 residue in the Cys-pocket [88].

The most variable domains are associated with either the amino-terminal anchoring domain or with the substrate recognition and binding domain. Gotoh predicted that the regions for substrate binding and recognition are situated close to the substrate-access channel and catalytic site and referred to these regions as substrate-recognition sites (SRSs). He defined the location of six potential SRS in the primary sequences of all P450 enzymes and established that the SRS sequences are hypervariable with regards to the remainder of the proteins. In addition to sequence hypervariability of the SRSs, he also found that there was spatial hypervariability in SRS-1, which is located in the β′-helix, SRS-2, which is situated in the carboxy-terminal region of the F-helix, and SRS-3, which is found in the amino-terminal region of the G-helix. In contrast, SRS-4, in the central I-helix, SRS-5, in the β6-1/β1-4, and SRS-6 in the β-hairpin, shows only limited spatial variability (Figure 5.3). These SRSs are flexible and move upon binding of a substrate so as to favor the catalytic reaction [88, 97].

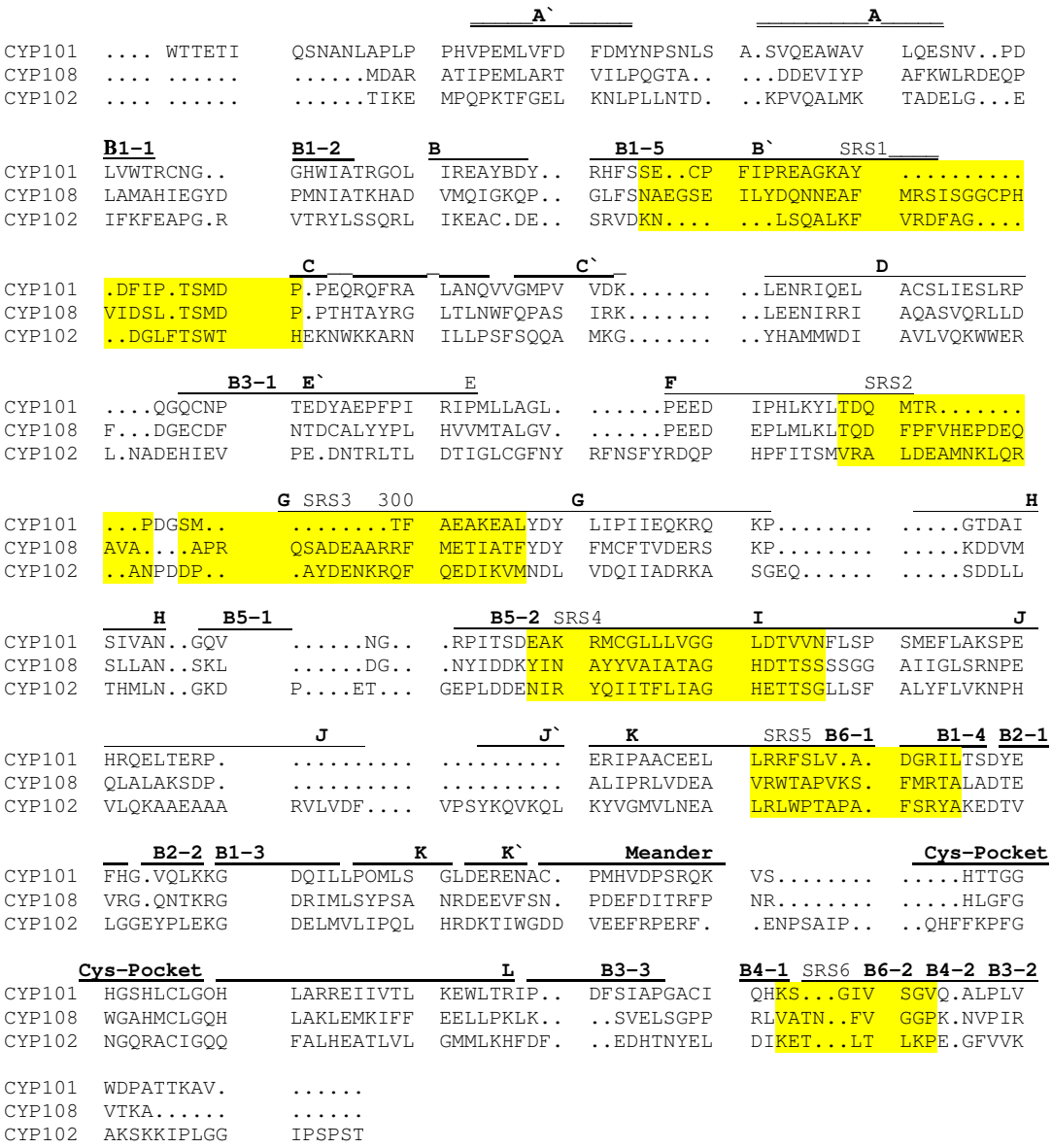

Figure 5.3. Sequence alignment of CYP101, CYP108 and CYP102 based on their structural superposition. Gaps in the alignments are indicated by dots. Names of the α-helices and β-strands are indicated above the sequences. SRSs are indicated in yellow [modified from 88].

The first crystal structure of a mammalian microsomal P450 enzyme, rabbit CYP2C5, which catalyses the hydroxylation of progesterone was solved by Williams *et al*. Although the structures of the soluble bacterial P450 enzymes reveal similar topological order, they vary considerably in detail that bestows specificity of substrate interaction. The elucidation of the topological organization of the bacterial enzymes, together with the crystallization of CYP2C5 has facilitated the accurate modeling of other mammalian P450 enzymes [98, 99].

The crystal structure of CYP2C5 was acquired by various modifications to the enzyme, which promoted crystallization and structure determination. These modifications included: the truncation of the hydrophobic N-terminal membrane anchor domain; the mutation of five amino acid residues at positions 202, 206, 207, 209, 210, which increased the solubilization of the protein by reducing the aggregation tendency of the protein; the mutation of another five residues at positions 2, 22, 23, 25, 26, which improved protein expression; and the addition of a C-terminal His tag to facilitate protein purification. Comparison of the crystal structures of the soluble bacterial P450 enzymes to the mammalian membrane-bound CYP2C5 led to further insight into the overall conservation of P450 enzyme tertiary structures, emphasizing contributions made by the regions surrounding the catalytic core for substrate specifications [98, 99]. The CYP2C5 structure was used to model human CYP19, which was previously modeled based on the crystallographic data of CYP101, CYP102 and CYP108, to study the active site, residues involved in the catalytic mechanism and to identify important structural features such as substrate recognition and redox-partner binding [100]. Rabbit CYP2C5 crystal structure displayed noticeably higher homology to the human isoforms of P450 enzymes than had been found with previous bacterial P450 enzyme structures. This led to the solving of various mammalian P450 enzyme crystal structures by X-ray crystallography, which include human CYP2C9, CYP2C8, CYP3A4, CYP2A6 and CYP2D6 isoforms. These structures were obtained with similar modifications made to the N-terminus of CYP2C5. In some cases a few mutations were introduced, which increased the solubility of the proteins [101, 102, 103, 104, 105, 106, 107].

The three-dimensional structural models of human CYP11B1 and CYP11B2 have been constructed using CYP102 and CYP108 as templates. The putative active site structures of both enzymes consist of various hydrophobic amino acids: Ala313, Phe321, Pro322, Val378, Phe381, Leu382, Tyr485 and Ile488. In addition to these, the active site of CYP11B1 includes Val316 and Val320, while CYP11B2 contains Ala320 and Leu 380 (Figure 5.4) [19].

His107 is present in both active sites, but the position of this residue differs in both proteins. Residues 301 (Leu in CYP11B1 and Pro in CYP11B2), 302 (Glu in CYP11B1 and Asp in CYP11B2) and 320 are involved in the formation of the active site. Mutations in residues 301 and 302, which are situated at the beginning of the I-helix, can cause a change in the position of the I-helix relative to the heme and the rest of the protein. Residues Thr318 and Thr319 are highly conserved and mutations at these positions, in addition to that at residue 320, can alter

the 11β-hydroxylase activities of the enzymes towards 11-DOC and 11-deoxycortisol. The structural models also showed that the active site of CYP11B1 is more spacious than that of CYP11B2. This finding correlates with the fact that the natural substrate for CYP11B1, 11-deoxycortisol, is larger than that of CYP11B2, 11-DOC, due to the presence of the additional 17α-hydroxy group of 11-deoxycortisol [10, 19, 42].

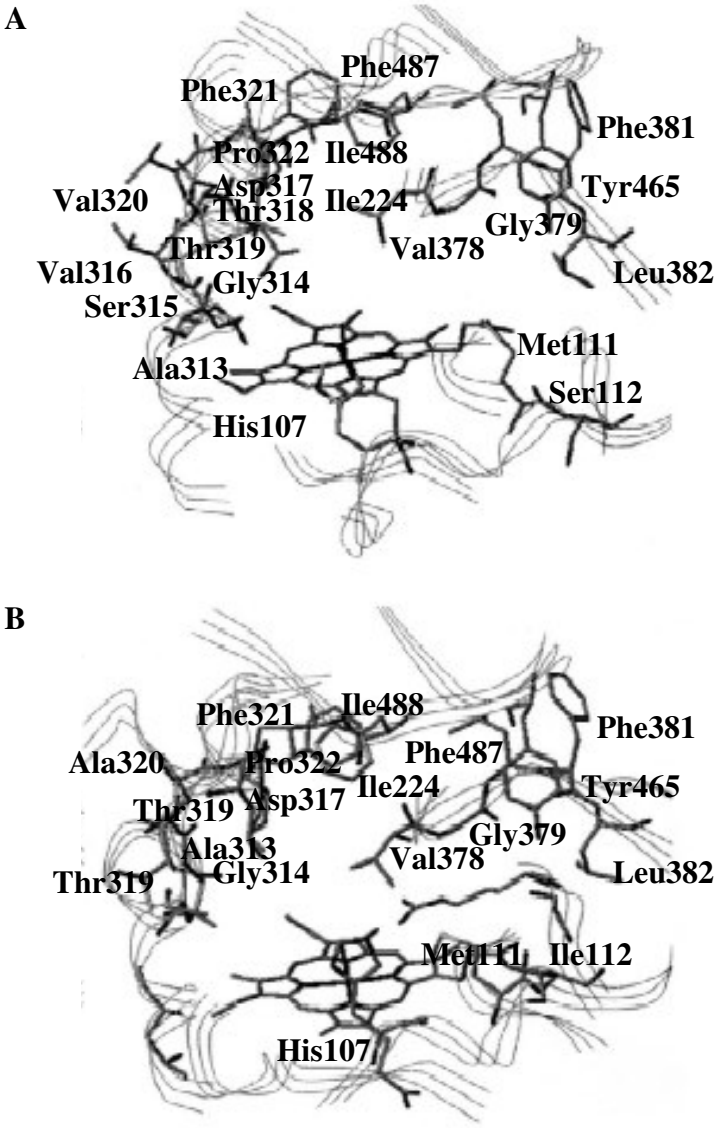

Figure 5.4. (A) Putative structure of active site of human CYP11B1 and (B) putative structure of active site of human CYP11B2 [19**].**

Homology modeling of these enzymes revealed that the overall structure is similar (Figure 5.5), but that the major difference between these two isoforms is the position of the heme in the active site. It was demonstrated that, in CYP11B2, two heme propionate groups are involved in hydrogen bond interaction with Arg448, while only one heme propionate group forms a

hydrogen bond with Arg448 in CYP11B1. The second heme propionate in CYP11B1 forms a hydrogen bond with Arg384 (Figure 5.6). The variation in the active site structures between the two isoforms is highly dependent on the orientation of the heme and the heme-binding loop in the protein molecule. In the heme-binding loop of CYP11B1 and CYP11B2 the differences in the residues are situated in the beginning (at position 439) and at the end (positions 472 and 473) of the loops. In addition, the substitution of His109 in CYP11B1 by Cys (in CYP11B2) influences side chains in close proximity to the heme and causes changes in the orientation of Arg448. In CYP11B2 Cys109 leads to a bent conformation of the Arg448 side chain, which is stabilized by a hydrogen bond between this residue and the heme propionate groups of this enzyme. In CYP11B1, His109 causes an extended conformation of Arg448, which is stabilized by another set of hydrogen bonds; one hydrogen bond is formed between Arg448 and one heme propionate group and another one forms a hydrogen bond with Arg384 [10, 19, 42].

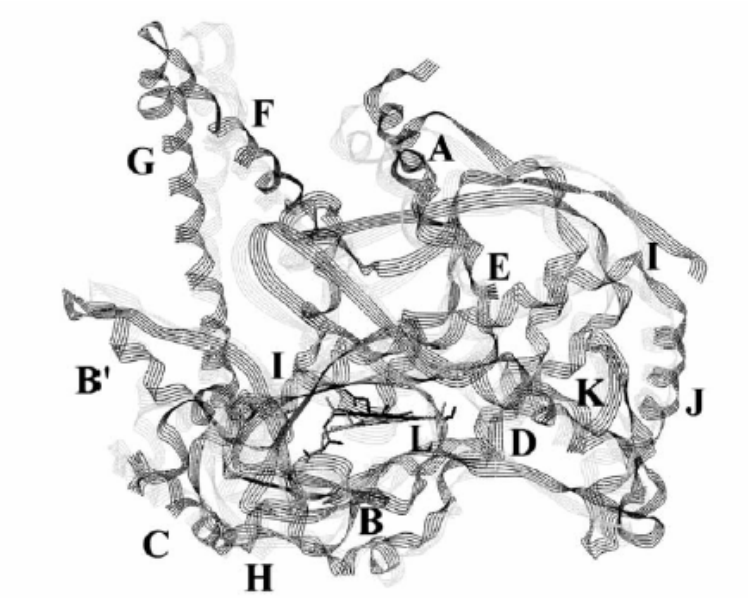

Figure 5.5. Superposition of the ribbon structures of the homology models of human CYP11B1 (black) and CYP11B2 (grey). Helices are labeled in the letter code [42].

The residues differing between human CYP11B1 and CYP11B2 in the N-terminal part of the enzymes were examined (Figure 5.7, Appendix C). Mutagenesis revealed that Ser112, Glu147, Ser288, Pro301, Asp302, Val320, Asn335 and Ala386 are important for the 11β-hydroxylase activity of CYP11B1, while Thr185, Asp147, Glu302 and Val386, together with Gly288, Leu301, Ala320 and Asp386, which is critical for 18-hydroxylase and 18-oxidase activity, are important for CYP11B2 activity. Mutagenesis studies revealed that mutations, Ile112Pro and Asp147Glu, in the N-terminal part of human CYP11B2 are responsible for a

three- and four-fold increase in the 11β-hydroxylase activities of the enzyme, respectively. A six-fold increase of the 11β-hydroxylase activity towards 11-DOC was observed when these mutations were combined. Ile112Pro showed a two-fold increase in the 18-hydroxylation activity of the enzyme. The mutation, Lys251Arg in CYP11B2 markedly increased 18-hydroxycorticosterone and aldosterone formation. Single mutations at positions 296, 301, 302, 320 and 335 in the putative I-helix of CYP11B2 exhibited a slight increased 11β-hydroxylase activity when exchanged with the corresponding ones in CYP11B1. However, the double mutant Pro301Leu/Ala320Val increased the 11β-hydroxylase activity to 60% as compared to that of the wild type CYP11B1. The additional Glu302Asp substitution further enhanced this activity to 85%. The CYP11B1 mutant, Val320Ala, either alone or in combination with Ser288Gly or Asn335Asp, exhibited CYP11B2 activities, without affecting its own 11β-hydroxylase activity [10, 19, 42].

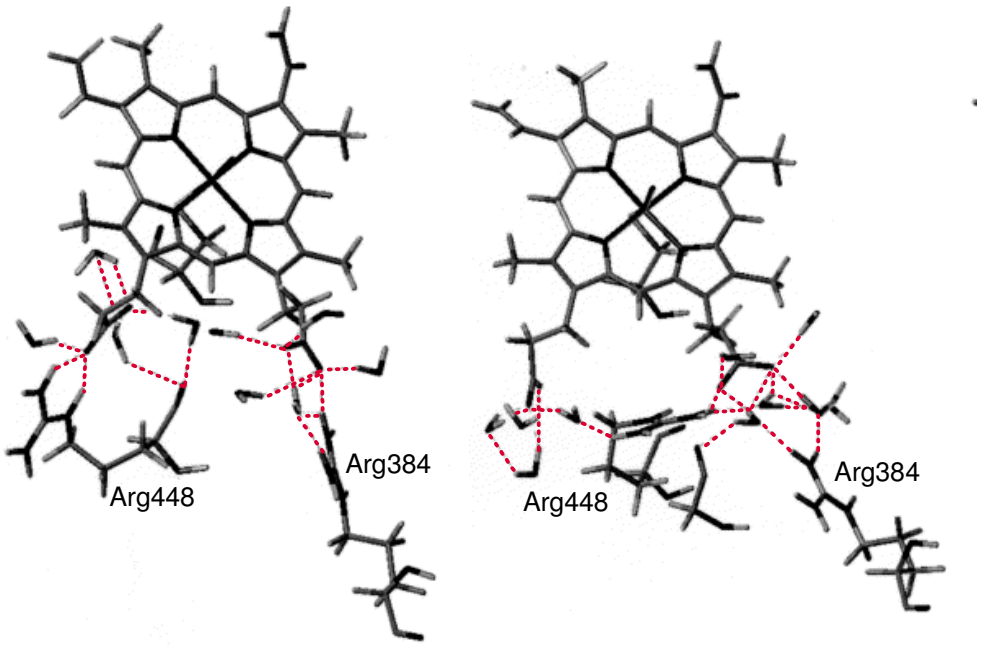

Figure 5.6. (A) The heme propionates in the model of CYP11B1 structure forms a hydrogen bond with Arg384 and Arg448 and (B) The heme propionates in the model of CYP11B2 structure forms two hydrogen bonds with Arg384 and Arg448 [19]**.**

Diverging residues in the C-terminal regions at positions 471, 472, 492, 493 and 494 of CYP11B1 and CYP11B2 were insignificant for the stereo- and regiospecificity of steroid hydroxylation. Mutagenesis studies of the diverging residues revealed that these residues are spread throughout the proteins and that some are important for proper stereoselective hydroxylation activity. The side chains of the residues located in the putative I-helix of the

CYP11B isozymes contributes considerably to substrate recognition and conversion [10, 19, 42].

Numerous aspects of enzyme function in terms of the identification of key amino acid residues, substrate docking and the mechanism of P450 enzyme catalysis have been clarified using homology modeling. Recently, Krone *et al.* studied the functional and structural effects that two novel missense mutations, Trp116Cys and Leu299Pro, and an in-frame three base pair deletion, Phe438, in the CYP11B gene have on patients suffering from CAH, which is caused by deficiency of CYP11B1. The study into the *in vitro* enzyme function, together with molecular modeling of CYP11B1, provided new insights in P450 enzyme structure-function relationship in this disease. In the molecular modeling study, mammalian CYP2C5 was used as a template for the three-dimensional model of CYP11B1 [85].

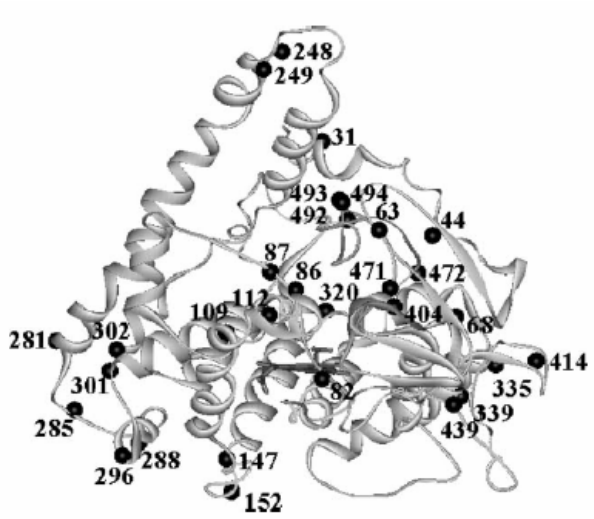

Figure 5.7. Distribution of the amino acids differing between human CYP11B1 and CYP11B2. The positions of the exchanged amino acids are labeled and shown as black balls on the ribbon structure of the homology model of CYP11B2. The heme is represented as a grey stick model. Amino acids 301, 302 and 320 can be found in the I-helix [42].

The structural model of CYP11B1 demonstrated that the Trp116 residue is situated in the B-C loop, which plays a role in substrate specificity as it possesses the SRS1. The amino acid residue Trp116 is conserved in the CYP11B1 and CYP11B2 of humans, mice and rats. A cluster of glycines is conserved in CYP11B1 and CYP11B2 at positions, 123, 128, 134, which are involved in the flexibility of the B-C loop. More specifically, the side chains of Trp116 and Leu113 interact with Phe223 and Trp247 in a key-lock-principle, attaching the lid of CYP11B1 to the body of the molecule (Figure 5.8.B), showing that a residue that is situated

relatively far from the active site has an impact on the active site. Therefore, the mutation at Trp116Cys may affect the conformational change of CYP11B1 with regards to substrate access and product release. Amino acid residue Ile112 plays an important role in the catalytic activity in the putative substrate access channel of CYP11B2. The Leu299 residue, which is highly conserved in human, mouse and rat CYP11B isozymes, is situated N-terminal from the putative I-helix of CYP11B1. This amino acid residue at position 299 is also found in human CYP21, CYP17 and CYP19A1. The Leu299 side-chain is in contact with the side-chains of the hydrophobic residues, Val290 and Ile304. The side-chain of Ile304 is also in contact with Trp137, which is situated next to Arg138. Arg138 interacts with one of the heme's propionates (Figure 5.8.C). Therefore, the mutation of Leu299Pro of CYP11B1 changes the position of the whole I-helix relative to the heme group and other parts involved in heme coordination of the CYP11B1 structure. This mutation caused a severe decrease in the 11β-hydroxylase activity of CYP11B1 *in vitro*, which might be a result of steric rearrangement of the polar and non-polar regions of the heme group relative to the enzyme. In P450 enzymes the heme is located between helices I and L. The Phe438 mutation, which involves a residue situated next to heme binding region, is flanking the non-polar part of the heme group in the three-dimensional model of CYP11B1 (Figure 5.8.A). This mutation resulted in the loss of the 11β-hydroxylase activity of the enzyme, which might have been due to steric arrangement of the heme group relative to the enzyme or disturbance of heme binding. Molecular modeling of CYP21 and CYP17 demonstrated that the I-helix plays an important role in substrate recognition and binding in P450 enzymes. By solving the crystal structures for CYP2C5, CYP2C8 and CYP2C9, it has also been shown that the I-helix is part of the substrate binding pocket. The I-helix of CYP11B1 and CYP11B2 also possess various hydrophobic amino acids, acts as the putative active site for these enzymes and is responsible for substrate specificity [85].

As in the case of CYP102, the adrenal mitochondrial P450 enzymes belong to the Class II group of P450 enzymes and also use a two-protein redox partner system. The enzymatic activity of the steroid hydroxylating system of the adrenal cortex mitochondria requires the transfer of electrons from the flavoprotein AdR *via* AdX to the CYP11 enzymes. The positively charged residues on the proximal face of the CYP11B isozymes and both the negatively charged and hydrophobic residues on the surface of AdX are important for the correct function of the ferredoxin as an efficient electron carrier [34, 108]. Results from the structural modeling of the human CYP11B isozymes showed that Asp147, located in the C′-

helix, may be involved in the electron transport interaction with AdX. According to this model Asp147 is located on the charged region of the protein surface, which is appropriate for AdX interaction [42, 109].

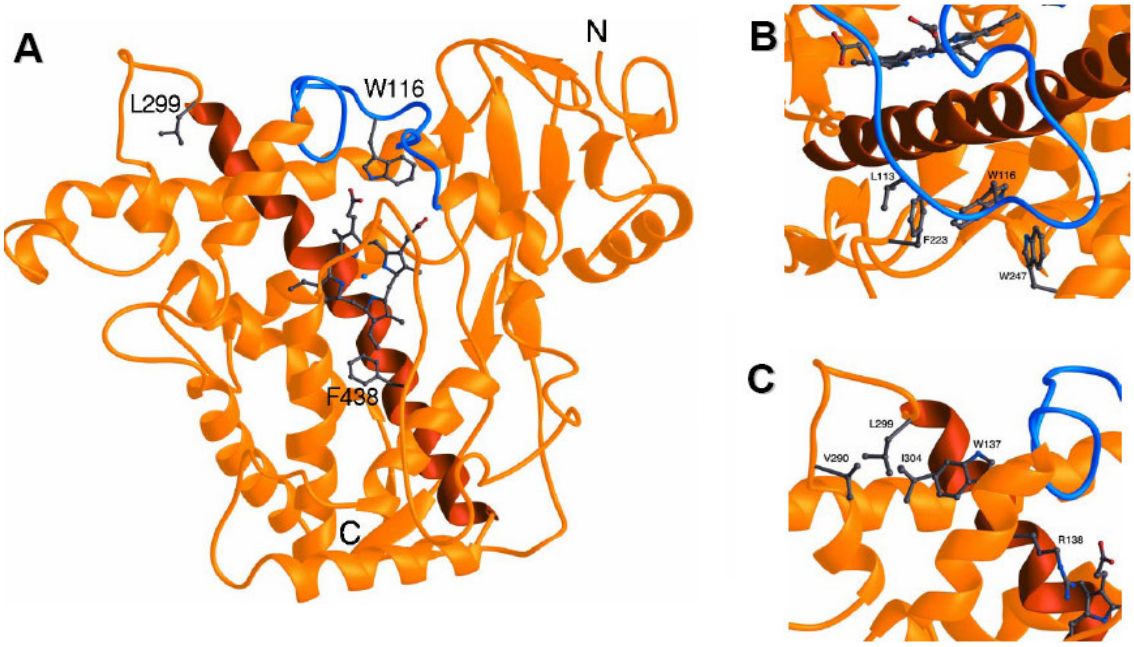

Figure 5.8. Three-dimensional molecular model of CYP11B1. (A) Total view of the three-dimensional structure of CYP11B1. Black amino acid residues: Trp116, Leu299 and Phe438. The I-helix is colored in brown, the B-C loop in light blue. **(B)** The side-chains of Trp116 and Leu113 interact with Phe223 and Trp247 in a key-lock-principle. **(C)** The interaction of the hydrophobic residues Val290, Leu299 and Ile304 side-chains is depicted. [85].

The crystal structures of two forms of bovine AdX and AdR were recently determined [110]. The crystal structures of the AdR-AdX complex revealed the general topology of the respective proteins and the molecular surroundings of the [2Fe-2S]-AdX cluster and the FAD-moiety of AdR. The crystal structure of AdR revealed that it comprises two distinctly similar domains (Figure 5.9). Both domains are equal in size and the first domain, which binds FAD (red in Figure 5.9), consists of central parallel β-sheets that are enclosed by α-helices. FAD binds in an extended conformation, with the isoalloxazine section pointing towards the NADP-domain and the adenine portion hidden in the FAD-domain. The second domain, which binds NADP (blue in Figure 5.9), is incorporated between strands β4 and β18 of the FAD-binding domain and has an additional 3-stranded anti-parallel β-sheet, which comprises the β11, β12 and β13 sheets [110].

AdR is capable of adapting to the AdX molecule, which contains a core domain consisting of a [2Fe-2S]-cluster and a small interaction domain for AdR, in the binary complex (Figure 5.10A, B, C). This adaptation is facilitated by domain orientation to various degrees, resulting in the narrowing of the distance between the anchor points, Arg240 and Lys27 in AdR to Asp70 and Asp41 in AdX. The AdR-AdX complex exhibits a highly charged surface, which arises from the interaction of the enzyme surfaces that are predominantly acidic for AdX and basic for AdR. Almost half of the AdR-Adx interface consists of polar and charged residues interacting *via* hydrogen bonds and salt bridges, facilitating the AdR-AdX-complex formation [14, 110].

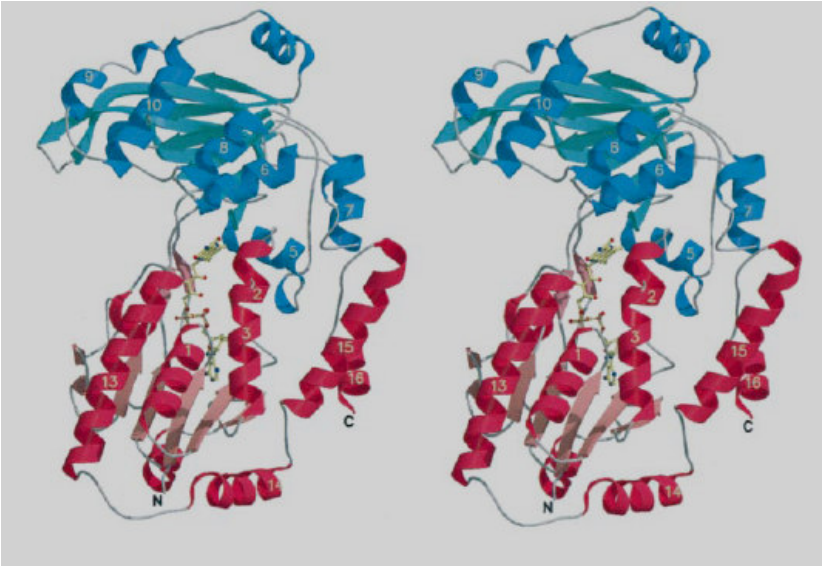

Figure 5.9. Stereo view of the AdR chain fold. The termini and some α-helices are labeled. The prosthetic group FAD (yellow) and the subdivision into FAD-domain (red) and NADP-domain (blue) are shown [110].

The crystal structures further demonstrated the primary interaction sites, which are centered around Asp39, Asp72, Asp76 and Asp79 of AdX and around Lys27, Arg211, Arg240 and Arg244 of AdR. Additional contact sites were recognized as the electron transfer region between the redox centra of AdR-AdX and the C-terminal residues of AdX. In the primary interaction region (Figure 5.10.A), polar bonds are formed between residues of the NADP-binding domain of AdR and AdX side-chains. Residues of the NADP-binding domain of AdR, Arg211, Arg240, Arg244, are involved in bond formation with the AdX-carboxyl groups, resulting in the formation of various salt bridges. In the AdX interaction domain, Asp72, Asp76 and Asp79, also take part in binding to AdR, while the acidic residues of Asp72, Asp76, Asp79, Glu73 and Glu74 of AdX face away from the interface and are believed to be involved in CYP11B binding [14, 110].

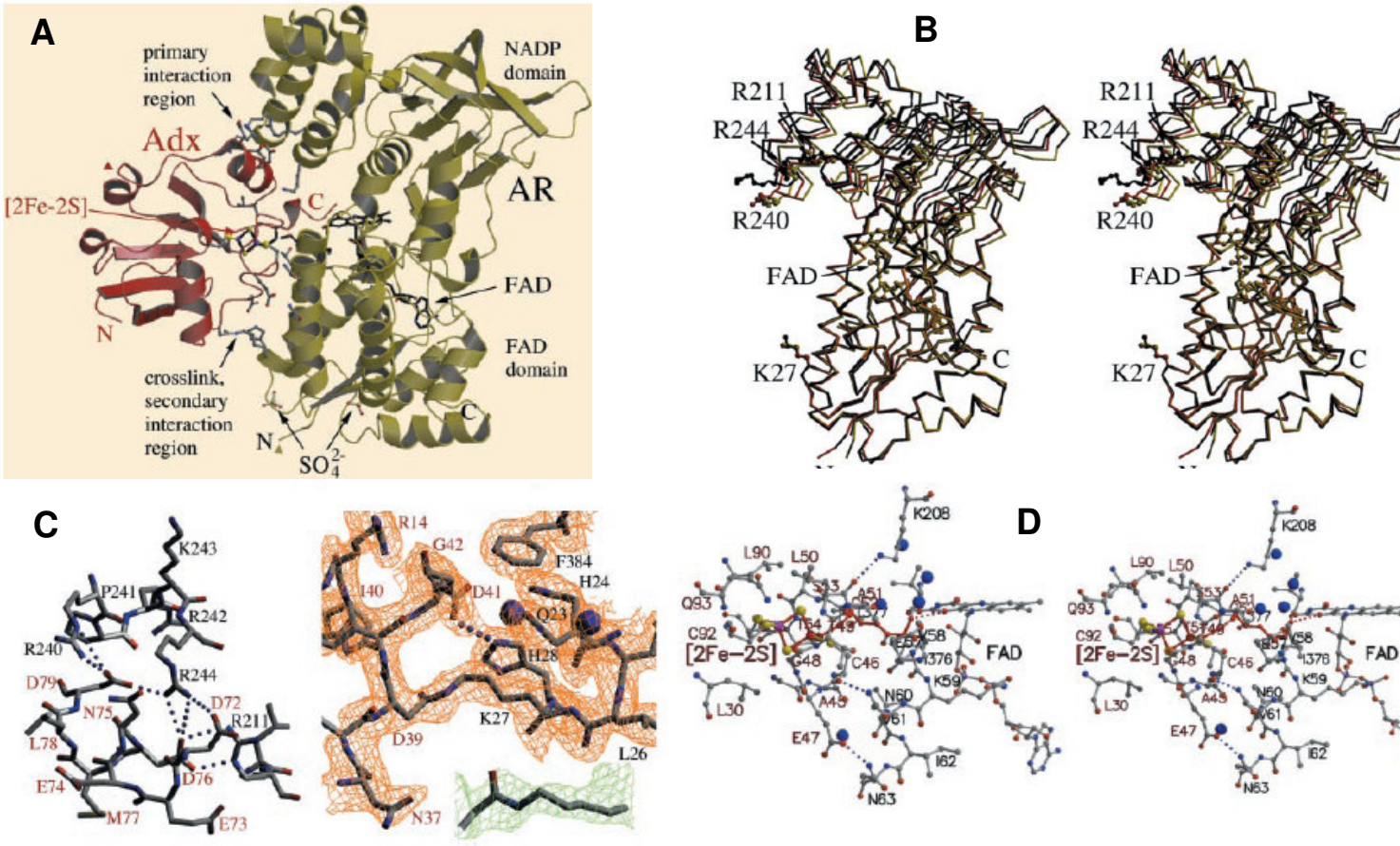

Figure 5.10. (A) Crystal structure of the AdR-AdX complex. AdR-AdX contact occurs at the primary and secondary interaction regions. For close-ups of the contact sites between side chains of some residues involved in polar AdR-AdX interactions, see C and D. **(B) Superposition of the FAD domains of AdR (bottom) of the AdR-AdX complex (molecule 1 in red and molecule 2 in gold).** In the complex, the FAD domains of AdR (top) undergo a slight domain rearrangement relative to the FAD domains that pulls the regions in contact with AdX closer together. **(C) Electrostatic interactions between AdR and AdX.** Left: salt bridges (dotted lines) connecting AdR and AdX in the primary interaction region. Residues are labeled black in AdR and red in AdX. Right: secondary interaction region in brown. A salt bridge linking His28 of AdR and Asp41 of AdX is indicated by the dotted line. **(D) Electron transfer region between the [2Fe-2S] cluster of AdX and the FAD moiety of AdR** [14, 110]**.**

Further polar interactions occur in the secondary interaction region, where the core domain of AdX binds to the FAD-binding domain of AdR, linking AdX-Asp39 with AdR-His28 *via* covalent cross-links [14]. Asp41 of AdX and Lys27 of AdR also participate in bond formation between the two enzymes. Asp39 and Asp41 are located in the core domain of AdX (Figure 5.10.A). It has been demonstrated that positively charged residues on the proximal exterior of the mitochondrial P450 enzyme and both the negatively charged amino acid and hydrophobic residues on the surface of AdX are essential for accurate functioning of the ferredoxin as an effective electron carrier [42].

The interaction of enzymes from the CYP11 family with its redox partner comprises an important aspect of enzyme activity. As previously mentioned, these mitochondrial enzymes utilize the redox partner system consisting of AdR and AdX.

In experiments using various types of chemical agents to modify the interaction sites, the important contact sites between CYP11A1 and AdX have been identified. These studies showed that lysine residues in CYP11A1 play an essential role in recognizing AdX. Treatment of the CYP11A1 hemoprotein with succinic anhydride or fluorescein isothiocyanate, which caused a drastic decrease in the binding affinity of the enzyme for Adx, identified the lysine residues at positions, 73, 109, 110, 126, 145, 148, 154, 267, 270, 338 and 343, to be involved in recognition and AdX-CYP11A1 complex formation. The role of Lys338 and Lys343 in CYP11A1 binding to AdX was confirmed in site-directed mutagenesis studies. It was also demonstrated that three areas of CYP11A1, Leu88 to Trp108, Leu368 to Trp400 and Leu401 to Trp417 and the peptide Ile7 to Lys22 of AdX are involved in the formation of covalently linked CYP11A1-AdX complex. Cross-linking studies revealed that the AdX-binding site is located near the heme-containing, catalytic domain of CYP11A1. Covalent binding of diiodofluorescein iodacetamide to C264 in CYP11A1 was shown to hinder interaction of AdX with the enzyme, which suggests a close contact site between the enzyme and the donor-docking region. Homology modeling of CYP11A1 showed that the docking of this model with the crystal structure of AdX pointed at four potential interaction sites at positions 403, 405, 267 and 264. A cross-link, which is located near the highly polar interaction areas of both enzymes, between Asp79 of AdX and Lys403 of CYP11A1 was observed. Asp79, in AdX, is situated near Asp72, Glu73 and Asp76, in a region dedicated to interact with CYP11A1. Asp76 is close to Lys338 in CYP11A1 and Glu73 is near Lys329 in CYP11A1. The [2Fe-2S]-containing loop of AdX in the cavity facing the heme group of CYP11A1 forms an additional secondary polar contact site between Asp39 or Asp41 of AdX and Lys126 of CYP11A1 across from the cross-link region. Glu73 of AdX may thereby interact with Lys343 of CYP11A1. Residues Ala109 and Ser117 of AdX protrude from this enzyme and point in the direction of a shallow groove, which is wide enough to accommodate the C-terminus, containing these residues, of AdX, on CYP11A1 [111, 112, 113].

The prediction of the three-dimensional conformation of mammalian P450 enzymes has been facilitated by homology models and has enabled investigators to deduce structure-function relationships. Until recently, homology models were based on crystal structures of the bacterial enzymes, CYP101, CYP108, CYP107A, and CYP102 [93]. One of the disadvantages in using

these models is the low sequence homology between the bacterial and eukaryotic P450 enzymes [109]. The crystallization of the microsomal CYP2C5 presented a template, with higher sequence homology, for modeling other mammalian cytochromes P450. In this study, the three-dimensional structures of two isoforms of Cape Baboon CYP11B1 were modeled using CYP102 and CYP2C5 as templates to determine the influence that specific amino acid residues at positions 177, 182 and 188 has on the catalytic activity of the enzyme.

5.2. MATERIALS AND METHODS

5.2.1. Molecular modeling of Cape baboon CYP11B1 isoforms

Two isoforms of CYP11B1, which utilize both 11-DOC and 11-deoxycortisol as substrates, were cloned from Cape baboon adrenals. Results obtained showed that both expressed isoforms hydroxylate these substrates, but with different efficiencies and selectivities. Homology model structures of these isoforms were constructed to better understand the structure-function relationships of these two isoforms.

The three-dimensional structures of the respective recombinant baboon CYP11B1 were modeled using Insight II suite of programs, Accelrys (San Diego, CA). The crystallographic structures of CYP102 and CYP2C5 were used as templates. The crystallographic coordinates of these two P450 enzymes were obtained from the Protein Data Bank and a multiple sequence positioning with the structurally aligned CYP102, CYP2C5 and two baboon P450 enzymes were performed manually. The structurally conserved regions (SCRs) of the respective proteins were ascertained based on this structural alignment. The backbone of each SCR in the model was subsequently built by fitting a portion from one of the P450 enzymes with known three-dimensional structure to the appropriate region of the framework structure.

The side-chain conformations were consequently determined based on the backbone of the secondary structure and the corresponding residues in each of the protein templates. The preferred conformations for each of the structurally variable regions (SVRs) were examined visually to identify and eliminate steric hindrances with nearby amino acids residue side chains in the surrounding protein domains. The side-chains were constructed in the same manner as the building of the SCRs. The generation of the baboon CYP11B1a model was followed by a verification step using Procheck. The model of the three-dimensional structure for the wild

type, CYP11Bwt, was created with the model of CYP11B1a as template structure by using point mutations and protein loop search for regions that were different. Both models were quenched with a layer of water and energy minimized on a DEC Vax Alpha Cluster using X-PLOR, in which the conjugate gradient method of Powell was used until the minimum energy was below 0.010 (units). To test whether these models could be used, a dynamic simulation test was used to test the robustness of the two models. No serious flaws, which could lead to the collapse of the models during simulation, were detected. A further energy minimization followed and the substrates, 11-DOC and 11-deoxycortisol, were docked manually into the active sites of the models. The substrate-protein interactions were optimized by another dynamic simulations test and further energy minimizations.

5.3 RESULTS

The sequence alignment of CYP11B1a and CYP11B1wt with CYP102 and CYP2C5 showed that the three amino acid substitutions, i.e. Val177Leu, Glu182Asp and Ile188Val, lie in the D- and E-helices of the protein (Figure 5.11). Homology modeling showed that the three substitutions are not located in the active sites of the respective enzymes.

Figures 5.12 and 5.13 shows the superimposed three-dimensional structures of the Cape baboon CYP11B1 isoforms with 11-DOC and 11-deoxycortisol as substrate, respectively.

```
CYP102          MMVDIAVQLV QKWERL.NAD EHIEVPEDMT RLTLDTIGLC GFNYRFNSFY
CYP2C5          RIQEEARCLV EELRKT.NAS .PCDPTFILG CAPCNVICSV IFHNRFD..Y
CYP11B1a        VARDFSQALR KKVVQNARES VTLDIQPSIF HYTIEASNLA LFGERLGLVG
CYP11B1wt       VARDFSQALR KKVLQNARDS VTLDVQPSIF HYTIEASNLA LFGERLGLVG
                           D Helix            E Helix
```

Figure 5.11. Structural alignment of the D- and E- helices of the Cape baboon CYP11B1 isoforms with the microbial CYP102 and microsomal CYP2C5. The amino acid residues that are different between CYP11B1a and CYP11B1wt are marked in red letters. See Appendix D for the complete structural alignment of the Cape baboon CYP11B1 isoforms with CYP102 and CYP2C5.

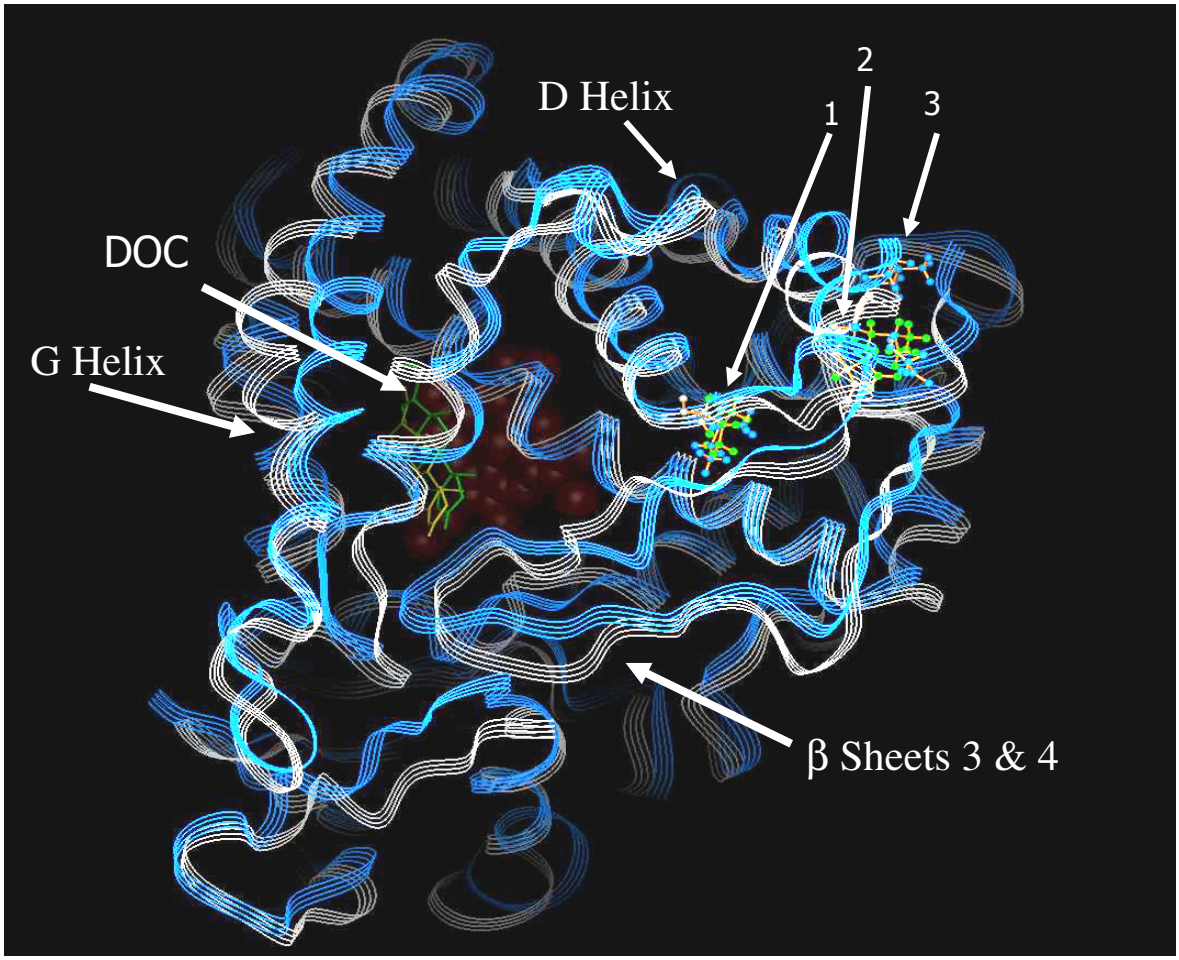

Figure 5.12. Superimposed three-dimensional structures of the Cape baboon CYP11B1 isozymes. CYP11B1a is represented in blue; CYP11B1wt is represented in white. 11-DOC is shown in green. The heme is shown in red. The amino acid substitutions are shown as (1) Val177Leu; (2): Glu182Asp and (3): Ile188Val.

Residue Leu 177 is positioned on an interface between helices D and E. The larger side-chain of this residue is in closer proximity to the residues in the I-helix than the Val residue side-chain, causing a shift of this helix. This shift can affect the topology of the substrate binding pocket. Residue Asp182 forms a salt bridge with Arg500 in β-sheet 3, which, together with β-sheet 4, forms a loop with the β-turn, lying between β4-1 and β4-2, in the active site. Phe487, which lies in the β-4 turn, is stacked on top of Phe381 in the K-helix and protrudes into the active site. The β3- and β4- strand pushes the K-helix to the β1-4 region, affecting the substrate binding pocket subtly. The Glu to Asp change may reposition the β3- and β4- sheets, causing a movement of Phe487, which could in turn affect Phe381, thus altering the active site (Figure 5.14). Residue 188 appears to have little effect on the substrate specificity of the two enzymes.

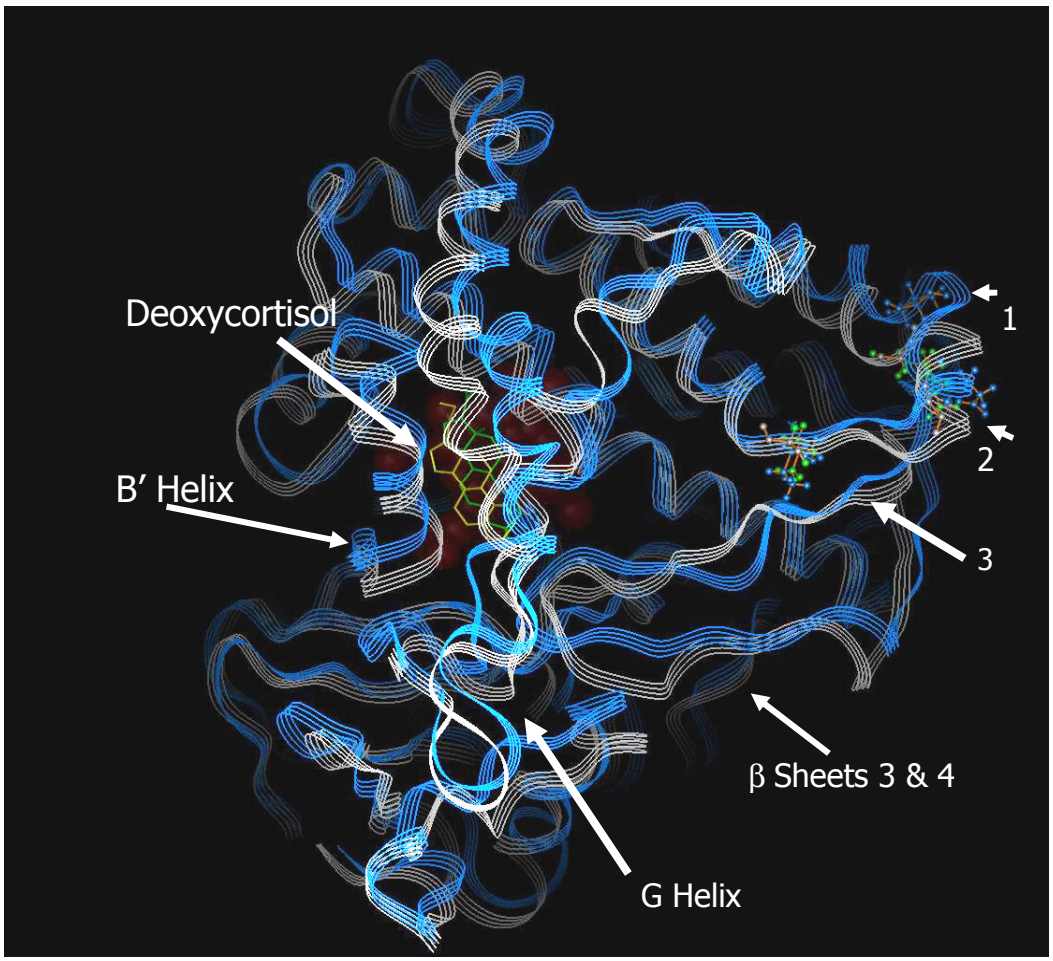

Figure 5.13. Superimposed three-dimensional structures of the Cape baboon CYP11B1 isozymes with 11-deoxycortisol as substrate. CYP11B1a is represented in blue; CYP11B1wt is represented in white. 11-Deoxycortisol is shown in yellow. The heme is shown in red. The amino acid substitutions are shown as (1) Val177Leu; (2): Glu182Asp and (3): Ile188Val.

Certain amino acid residues in human CYP11B enzymes, which have been identified as important for interaction with AdX, are located in positions 147, 152, 185 and 366. Human CYP11B1 has Glu in position 147, while human CYP11B2 has Asp in the same position. Both baboon clones encode an Asp in this position. These amino acid residues, together with those in position 152 (Asn in human CYP11B1 and Lys in human CYP11B2 and Lys in both baboon CYP11B1wt and CYP11B1a), are located in exon three and is believed to play a vital functional role with regards to interaction with AdX. Thr185 in the human CYP11B enzymes is situated on the surface of these proteins and is essential for binding to AdX. Cape baboon CYP11B1wt and CYP11B1a both have a Thr residue in this position. Human CYP11B1 and CYP11B2, together with baboon CYP11B1wt and CYP11B1a, have a basic residue, Arg, in position 366, which is essential for electrostatic interaction with AdX [10, 114, 115].

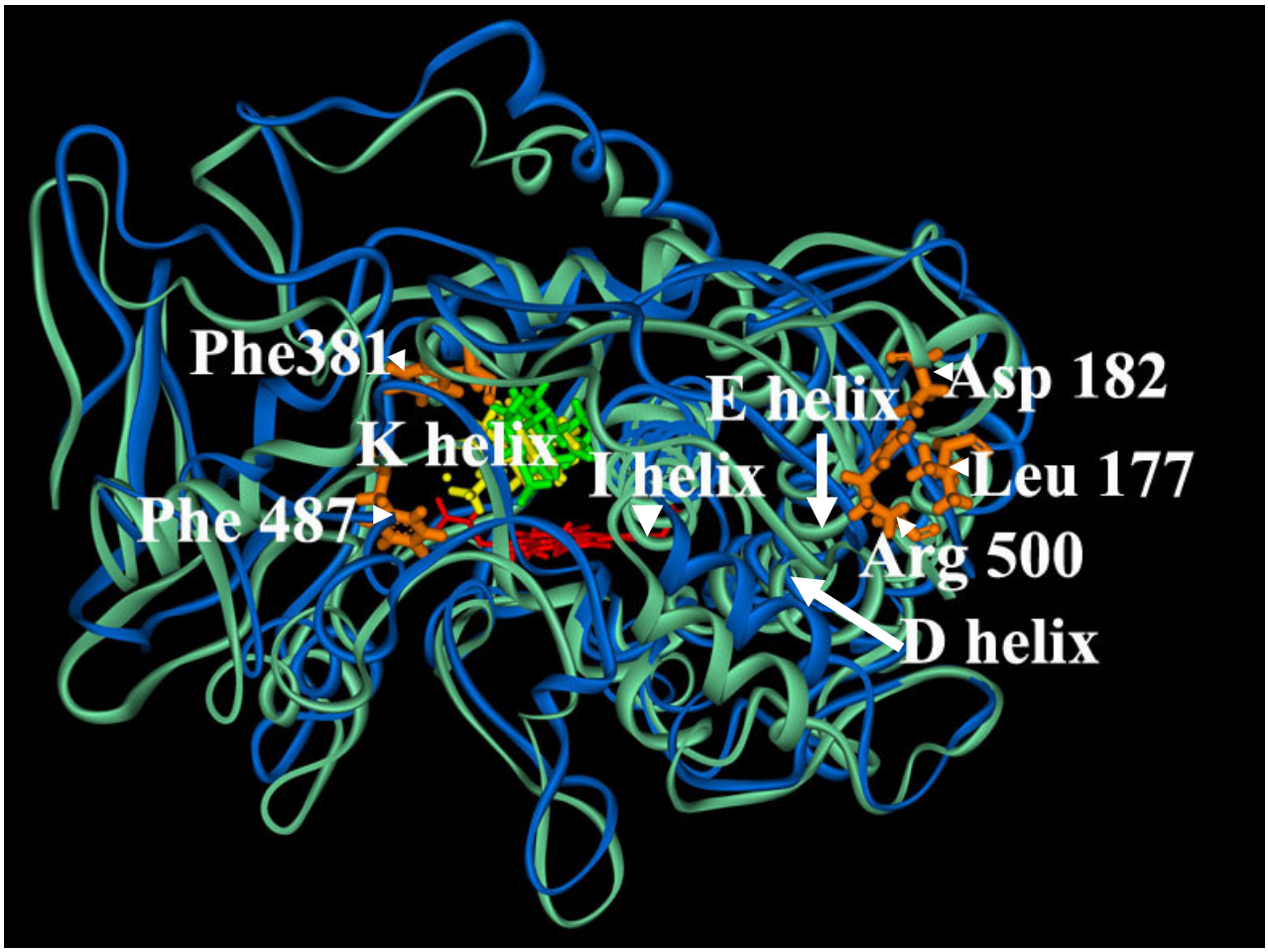

Figure 5.14. Superimposed three-dimensional structures of the Cape baboon CYP11B1 isozymes with 11-DOC as substrate. CYP11B1a is represented in blue with its 11-DOC in green; CYP11B1wt is represented in green with its 11-DOC in yellow. The heme is shown in red.

5.3. DISCUSSION

Sequence analysis showed that CYP11B1a and CYP11B1wt differed by three amino acid substitutions, Val177Leu, Glu182Asp and Ile188Val, in exon three. The modeled 3-dimensional structures of these two isoforms showed that these substitutions lie in the predicted D-E helix region. The models also indicated that there is no direct interaction between the substrates and the three amino acid residues at positions 177, 182 and 188. Although these residues lie distant to the active site they may influence the topology of the substrate-binding pocket (Figures 5.12, 5.13).

As previously mentioned, the amino acid residue at position 177 is situated on the border between helices D and E of CYP11B1a and CYP11B1wt, respectively. The model in Figure

5.12 shows the docked 11-DOC substrate in the active site. It is possible that the longer side-chain of the Leu residue at this position in CYP11B1wt may push against the I-helix, shifting this helix and consequently affecting the topology of the substrate binding pocket. The side-chain of Val is shorter than that of Leu and therefore should not affect the I-helix. As mentioned previously, the I-helix plays an important role in substrate recognition and substrate binding in P450 enzymes.

A comparative enzymatic study of Cape baboon CYP11B1a and CYP11B1wt, using 11-DOC and 11-deoxycortisol as substrates, revealed a distinct difference in the catalytic activities of the two isoforms towards 11-DOC. CYP11B1a was identified as the high affinity isoform with a Km of 0.48 μM, as compared to CYP11B1wt (Km: 0.74 μM). The model shows that the charged residue at position 182 forms a salt bridge with Arg500 in β-sheet 3. When 11-DOC is docked in the active site of CYP11B1wt, the shorter side-chain length of Asp182 may cause the loop between β-sheet 3 and β-sheet 4 to be pulled away from the active site, increasing the size of the active pocket. This larger active pocket of CYP11B1wt causes the bound substrate to be less constricted and may cause a decrease in the affinity of the enzyme for 11-DOC. When 11-DOC binds in the active site of CYP11B1a, the longer side-chain of the Glu residue may cause this same loop to push into the active site, causing a tighter binding of the substrate to the enzyme — hence the higher 11 β-hydroxylase activity of CYP11B1a towards 11-DOC.

As mentioned previously, studies with Dahl rat CYP11B2 and human CYP11B1 and CYP11B2 showed that a Glu to Asp mutation, located at the interface between the D- and E-helices, may affect the enzyme activity considerably [79, 80]. A Glu to Asp mutation in Dahl rat CYP11B2 resulted in an increased rate of 11-DOC conversion to aldosterone [79]. A Glu147Asp mutation in the human CYP11B enzymes resulting in a decrease in the affinity of CYP11B1 for 11-DOC in the human wild type, but did not affect the 11β-hydroxylation of 11-deoxycortisol to cortisol by human CYP11B1. The Asp147Glu mutation in human CYP11B2 enhanced the conversion of 11-DOC to corticosterone, but did not change the conversion of 11-deoxycortisol to cortisol. The influence of residue 147 in the human CYP11B enzymes on catalysis depends on the type of substrate presented to the enzyme. The 17α-hydroxyl group of 11-deoxycortisol, for instance, obviates the role of this amino acid in the formation of cortisol [80].

It is probable that residue 182 in Cape baboon CYP11B1a and CYP11B1wt may interact in some way with the substrate and heme-binding domain regions to maintain the correct orientation of the substrate within the active site.

CYP11B1a and CYP11B1wt showed comparable 11β-hydroxylase activities towards 11-deoxycortisol, with Km-values of 0.76 μM and 0.99 μM, respectively. This may be explained by the fact that 11-deoxycortisol is larger than 11-DOC due to the additional 17-hydroxy group at C17. This larger molecule may stabilize the enzyme-substrate complex by fitting tightly in the active site of both CYP11B1 isoforms, whereby the substrate is converted to cortisol with similar efficiencies.

Molecular modeling is a useful tool for understanding and visualizing possible changes in a protein and the interactions of a protein with its specific substrate. As in the case of the Cape baboon CYP11B1 isoforms, the data presented in Chapter 4 showed that these enzymes have different substrate affinities towards 11-DOC and 11-deoxycortisol. Amino acid residue substitutions in the predicted D-E helix, which lie near the surface of the proteins and may have a few effects on the catalytic activities of the enzymes on its substrates, was identified using homology modeling. The side-chains of these amino acids point inwards towards other structural elements and therefore may have an effect on the topology of the active site. The molecular modeling of the two isoforms of Cape Baboon CYP11B1 presented some evidence that these changes can affect the substrate turnover and substrate affinity.

CHAPTER SIX

DISCUSSION

Immunohistochemical and *in situ* hybridization experiments, carried out in our laboratory demonstrated that Cape baboon CYP11B1 is present in the histologically distinct zones of the adrenal cortex and in the medulla. Three genes encoding this enzyme were also cloned from Cape baboon adrenals.

In this study, Cape baboon CYP11B1 was characterized in terms of its tissue distribution in the adrenal gland, 11β-hydroxylase activities in adrenal cortical- and medullary tissue homogenates, 11β-hydroxylase activities and kinetics of the recombinant CYP11B1 genes expressed in non-steroidogenic COS-1 cells and the structural and functional implication of three amino acid substitutions in these isoforms using homology modeling.

The localization of Cape baboon CYP11B1, AdR, AdX, CYP11A1 and CYP21 were investigated in baboon adrenal cortical- and medullary tissue homogenates using Western blot analyses. CYP11B1 was located in the cortical tissue homogenate as a single protein band, corresponding to an apparent molecular mass of ~54 kDa. In the medullary tissue homogenate, however, two distinct bands with respective apparent molecular masses of ~51 kDa and ~54 kDa were observed. It is possible that CYP11B2 may be present in the adrenal cortex, but that the protein levels were too low to be detected. AdR was tentatively indicated in the cortical- and medullary tissue homogenates as a single band with an apparent Mr of 54 kDa. It is, however, unfeasible to unequivocally assign this protein band to AdR as the precipitation band was not in alignment with that of purified sheep AdR. AdX was only detected in the cortical tissue homogenate as a single band of approximately 14 kDa. Human AdR and AdX have apparent molecular masses of 51 kDa and 14 kDa, respectively. CYP11A1 was indicated as a single band in the cortical tissue homogenate only, with an apparent molecular mass of 52 kDa. CYP21 was detected as three bands; with a prominent band corresponding to an apparent molecular weight of 47 kDa, in the cortical tissue homogenate only. Human CYP11A1 and CYP21 both have molecular weights of 56 kDa.

Investigations into the catalytic activity of baboon CYP11B1 in adrenal cortical- and medullary- tissue homogenates showed that CYP11B1 in the cortical tissue homogenate catalyzed the 11β-hydroxylation of 11-DOC, yielding considerable amounts of corticosterone only, with no detectable 18-hydroxy-corticosterone and aldosterone being formed. The conversion of corticosterone to 18-hydroxycorticosterone and aldosterone was negligible. The CYP11B proteins in the medullary tissue homogenate catalyzed the 11β-hydroxylation of 11-DOC to corticosterone, however, with less efficiency than the isoform in the cortical tissue homogenate. A CYP11B isoform also catalyzed the 18-hydroxylation and 18-oxidation of corticosterone to form 18-hydroxy-corticosterone and aldosterone, respectively. The formation of aldosterone in the adrenal medullary tissue homogenates was confirmed using an APcI-MS method, developed in our department, for identification of steroid metabolites. This method would be useful when investigating the multiple steps in the production of aldosterone from 11-DOC or corticosterone in future studies.

The results obtained from this investigation demonstrate that more than one isoform of CYP11B1, exhibiting different catalytic activities toward 11-DOC, exist in the Cape baboon. The CYP11B1 isoform in the adrenal cortical tissue homogenates seems to have a higher catalytic activity towards 11-DOC than that found in the adrenal medullary tissue homogenates. In the medullary tissue homogenates, another CYP11B isoform, believed to be CYP11B2, exhibited 18-hydroxylase and 18-oxidase activities towards corticosterone, but no 11β-hydroxylase activity towards 11-DOC. This may be because the corticosterone levels produced from 11-DOC in the medullary tissue homogenate were too low and could therefore not be converted to 18-hydroxycorticosterone and aldosterone. If this is the case it would seem as if the 18-hydroxylase and 18-oxidase activities of CYP11B2 towards corticosterone in the medulla, is concentration dependent. It is also possible that the Cape baboon adrenal could express a chimeric CYP11B1/CYP11B2 enzyme, which only exhibits the 18-hydroxylase and 18-oxidase activities and that this chimeric gene may carry a mutation, which results in the loss of the 11β-hydroxylase activity. The function of aldosterone synthesis in the medulla is still unclear, but may be of physiological importance. Cape baboon CYP11B1 could also exhibit 19-hydroxylase activity towards 11-DOC to produce 19-hydroxy-DOC, the precursor of a very potent mineralocorticoid, 19-nor-DOC. Should this be the case, it may be possible that the Cape baboon uses 19-nor-DOC as its primary

mineralocorticoid. The inability of Cape baboon to produce aldosterone in the adrenal cortex may be due to low expression levels of CYP11B2.

The presence of AdR in the medullary tissue homogenates demonstrates that the redox protein system, which is important for mitochondrial steroidogenesis is present in the medulla. The reduced 11β-hydroxylase activity towards 11-DOC in the adrenal medullary tissue homogenate may be due to the absence of AdX in the medulla. Research demonstrated that the 18-hydroxylase- and 18-oxidase activity of CYP11B2 is highly reliant on the presence of high levels of reducing equivalents [68]. A CYP11B isoform in the medullary tissue homogenates exhibited these activities towards corticosterone and therefore it is possible that a protein other than AdX may function as a redox partner in transferring electrons from AdR to CYP11B isozymes in the medulla. This may contribute to the tissue specific regulation of aldosterone synthesis in the Cape baboon adrenal.

The results obtained in this study also present evidence that cells in the medulla have steroidogenic activity. The control mechanisms, regulating the expression of the CYP11B isoforms in the medulla, may differ from that in the cortex and should be investigated.

The 11β-hydroxylase activities of three recombinant Cape baboon CYP11B1 genes, CYP11B1a, CYP11B1wt and CYP11B1S, were studied in COS-1 cells. This investigation revealed contrasting catalytic activities of CYP11B1a and CYP11B1wt towards 11-DOC and comparable activities towards 11-deoxycortisol. No activity was observed with CYP11B1S, which is believed to be a pseudogene due to a termination codon in exon one. CYP11B1a demonstrated a greater 11β-hydroxylase activity towards 11-DOC than for 11-deoxycortisol and also showed that it 11β-hydroxylates 11-DOC more efficiently than CYP11B1wt. Both isoforms exhibited comparable 11β-hydroxylase activities towards 11-deoxycortisol. These CYP11B1 isoforms did not demonstrate 18-hydroxylase or 18-oxidase activities towards 11-DOC.

Kinetic studies with both recombinant baboon CYP11B1 genes revealed that COS-1 cells, transfected with CYP11B1a and human AdX, expressed a high affinity enzyme with an apparent Km of 0.48 μM and *V*-value of 10.35 nmol/hr/mg protein for 11-DOC metabolism. In contrast, COS-1 cells, transfected with CYP11B1wt and human AdX, expressed a low

affinity CYP11B1 isoform (Km: 0.74 μM and *V*-value: 6.62 nmol/hr/mg protein) for 11-DOC metabolism. The formation of steroid metabolites was measured using a corticosterone ELISA kit. For the kinetic analysis for 11-deoxycortisol metabolism by the two isoforms, steroid metabolites were measured using a LC-MS method, which was developed in our department. The *K*m- and *V*-values for 11-deoxycortisol metabolism by CYP11B1a were 0.80 μM and 7.40 nmol/hr/mg protein, respectively, whilst CYP11B1wt demonstrated values of 1.07 μM and 7.10 nmol/hr/mg protein, respectively.

It could be that CYP11B1a, which has a higher affinity for 11-DOC than CYP11B1wt, is the isoform present in the baboon adrenal cortex, while CYP11B1wt might be the isoform responsible for the lower 11β-hydroxylase activity towards 11-DOC in the adrenal medulla.

Nucleotide sequence analysis of the Cape baboon CYP11B1 cDNAs revealed that CYP11B1a has only one Sma1 site, located in the same position as human CYP11B2 (539-544 bp), while CYP11B1wt contains two Sma1 sites in the same location as human CYP11B1 (86-91 bp and 539-544 bp). 11-Deoxycortisol has been identified as the natural substrate for human CYP11B1, and therefore, when CYP11B1a displayed a greater affinity for 11-DOC, which is the natural substrate for human CYP11B2, *in vitro* experiments, using androstenedione and corticosterone as substrates, were performed in our laboratory to establish if CYP11B1a is a true 11β-hydroxylase. Both baboon CYP11B1 cDNAs exhibited only 11β-hydroxylase activity towards androstenedione and corticosterone.

In the studies with Cape baboon adrenal medullary tissue homogenates the possibility of another accessory protein, important to deliver electrons from AdR to the CYP11B isoforms, was mentioned since no AdX was detected in the medullary tissue homogenate. Research showed that basic levels of reducing equivalents are adequate for 11β-hydroxylase activity of CYP11B1, which may be the case with the Cape baboon CYP11B1 cDNAs, which were cotransfected with human AdX in COS-1 cells [68]. It is also possible that CYP11B1wt, which may be the isoform found in the medulla, could not exhibit 18-hydroxylase- and 18-oxidase activities, which requires high levels of reducing equivalents, towards corticosterone produced from 11-DOC, due to the absence of this putative accessory protein, present in the medulla.

Sequence analysis of Cape baboon CYP11B1a and CYP11B1wt showed that nucleotide changes in exon three resulted in the amino acid changes Val177Leu, Glu182Asp and Ile188Val. Cover *et al.* and Fisher *et al.* showed that a Glu to Asp mutation in exon three, which lie in the D-E helices, in Dahl rat CYP11B2 and human CYP11B1 and CYP11B2 substantially affected the enzyme activity [79, 80]. Dahl rat CYP11B2, with a Glu136Asp mutation in exon three, encoded an enzyme with a higher apparent maximum velocity and a lower apparent *K*m, resulting in an increased rate of 11-DOC conversion to aldosterone [79]. The Glu147Asp mutation in the human CYP11B enzymes resulted in a decreased affinity of CYP11B1 for 11-DOC as shown by an increase in the apparent *K*m of the mutant enzyme, 7.5 μM as compared to 2.5 μM in the human wild type. This mutation did not affect the 11-deoxycortisol conversions to cortisol by human CYP11B1. The Asp147Glu mutation in human CYP11B2 enhanced the conversion of 11-DOC to corticosterone, but it did not alter the conversion of 11-deoxycortisol to cortisol. The *K*m-values for the wild type and mutant CYP11B2 were 5 μM and 1.4 μM, respectively [80].

The differences observed, with regards to the catalytic activities of the recombinant baboon CYP11B1 isoforms towards 11-DOC and 11-deoxycortisol, may be due to the differences in their amino acid sequences. It is possible that the conservative change, Glu182Asp in exon three, of these two enzymes can affect the steroid metabolism considerably.

The influence of the amino acid changes in exon three of the two Cape Baboon CYP11B1 isoforms, on the activity of the recombinant enzymes was investigated using homology modeling. The three-dimensional structures of both CYP11B1 isoforms were constructed, using CYP102 and CYP2C5 as templates, in order to identify the residues affecting substrate specificity. Homology modeling of Cape baboon CYP11B1a and CYP11B1wt showed that the amino acid changes lie in the predicted D-E helix near the surface of the proteins. These structures of CYP11B1a and CYP11B1wt also showed that there was no direct interaction between the three amino acid residues at positions 177, 182 and 188, and substrate binding to the enzymes. The side-chains of these amino acids point inwards towards other structural elements and therefore may affect the topology of the active sites of these enzymes. The longer side-chain of Leu177 in CYP11B1wt may cause a shift of the I-helix, which plays an important role in substrate recognition and substrate binding in P450 enzymes, by pushing against the helix, affecting the topology of the substrate binding pocket. The side-chain of Val177 in CYP11B1a is shorter than that of Leu and does not affect the position of the I-

helix. The amino acid residue at position 182 forms a salt bridge with Arg500 in β-sheet 3, which, together with β-sheet 4, forms a loop with the β-turn, lying between β4-1 and β4-2, in the active site. Phe487, which is situated in the β-4 turn, is stacked on top of Phe381 in the K-helix and protrudes into the active site. The Glu to Asp substitution may reposition the β-sheet 3 and β-sheet 4, causing a shift of Phe487, which could in turn affect Phe 381, thus altering the active pocket. When 11-DOC is docked into the active site of CYP11B1wt, the shorter side-chain of Asp182 causes the loop between β-sheet 3 and β-sheet 4 to be pulled away from the active site, thereby increasing the size of the active pocket of the enzyme. This loosening of the active pocket may cause space for movement of the substrate in the active site therefore decreasing the affinity of the enzyme for 11-DOC. When 11-DOC binds in the active site of CYP11B1a, the longer side-chain of Glu182 can cause the loop between β-sheet 3 and β-sheet 4 to push on the K-helix into the direction of the β1-4 region, affecting the active pocket subtly. This might cause a tighter binding of the substrate to the enzyme - hence the higher 11β-hydroxylase activity of CYP11B1a towards 11-DOC. As in the case of Dahl rat and human CYP11B isozymes, the Asp and Glu residues in exon three of Cape baboon CYP11B1 isoforms may interact in some way with the substrate and heme-binding domain regions where it possibly maintains the correct orientation of the substrate within the active site. Therefore, the Asp-Glu residue changes in the two Cape baboon CYP11B1 isoforms might have an influence on enzyme activity towards 11-DOC and 11-deoxycortisol. Residue 188 appears to have little effect on the substrate specificity of the two enzymes.

Cape baboon CYP11B1a and CYP11B1wt expressed in COS-1 cells, respectively, showed comparable 11β-hydroxylase activities towards 11-deoxycortisol, which is larger than 11-DOC due to an additional 17-hydroxy group at C17. This larger molecule may stabilize the enzyme-substrate complex by fitting tightly in the active site of both CYP11B1 isoforms, whereby the substrate is converted to cortisol.

Molecular modeling of Cape baboon CYP11B1 isoforms has been a useful tool for understanding and visualizing possible changes, caused by amino acid substitutions at positions 177, 182 and 188, that can affect substrate affinity and substrate turnover.

Sequence alignment of Cape baboon CYP11B1a and CYP11B1wt showed that these isoforms are more closely related to human CYP11B1 than CYP11B2. Cape baboon CYP11B1a,

CYP11B1wt and CYP11B1S contain six amino acid residues, Ser112, Ser288, Pro301, Asp302, Val320 and Asn335, which are essential for 11β-hydroxylase activity of human CYP11B1 and only two amino acid residues, Asp147 and Val386, which are important for aldosterone synthase activity of human CYP11B1. Leu301 in CYP11B2 is vital for 18-oxidase activity. Cape baboon CYP11B1 isoforms has a Pro in this position. Taking this, and the 11β-hydroxylase activity exhibited by the Cape baboon CYP11B1 cDNAs, into consideration it can be established that these isoforms are expressed by CYP11B1 genes.

To date, only two CYP11B genes, encoding CYP11B1 and CYP11B2, have been isolated from humans. Normally, CYP11B1 exhibits 11β-hydroxylase activity and is expressed in the zF/R of adrenal cortex, while CYP11B2 has, in addition to the 11β-hydroxylase activity, 18-hydroxylase and 18-oxidase activities and is expressed in the zG of the adrenal cortex. Genetic disorders results in malfunctions of these isozymes and have severe consequences in humans. Some mutations, i.e. nonsense mutations: Trp116End, Lys174End, Gln338End and Gln356End; and frameshift mutations, in CYP11B1 can prevent the synthesis of the enzyme, while missense mutations such as Arg448His are located in regions of known functional importance and abolish enzyme activity. Another type of mutation, where a chromosome carries three CYP11B genes instead of the normal two, is caused by unequal crossing-over. This chimeric gene is regulated like CYP11B1, but exhibit enzymatic activity like CYP11B2 [48]. The results presented in this thesis give evidence that suggest the existence of three genes encoding CYP11B1 and two functional isoforms in the Cape baboon. Previously, CYP11B genes were cloned from Cape baboon blood [1]. Investigations into the nucleotide sequence revealed that two CYP11B genes were isolated from Cape baboon of which one was approximately 400 bp longer in intron five. Since human CYP11B2 is 440 bp longer in intron five than the corresponding intron in CYP11B1; it is believed that CYP11B2 is present in the Cape baboon. These genomic studies only revealed the presence of one CYP11B1 gene in the Cape baboon. The CYP11B1 promoter was also isolated and showed a similarity of 90% to the human CYP11B1 promoter [1]. Genomic studies, performed in our laboratory, also revealed two Sma1 sites in baboon CYP11B1 that are located in the corresponding positions in human CYP11B1. The CYP11B2 promoter has also been isolated and sequence analysis shows a marked difference between the two CYP11B promoters [personal communication with Dr Amanda Swart, Stellenbosch University]. This unpublished data shows that the Cape baboon definitely has two genes encoding CYP11B1 and CYP11B2, respectively. The

recombinant CYP11B1 cDNAs, which was used in this study, was cloned from baboon adrenals. Since only one CYP11B1 gene has been cloned from baboon blood [1], uncertainty was raised as to whether the Cape baboon has three genes encoding CYP11B1 or not. It is possible that, like in humans where certain mutations determine the number of CYP11B genes present, not all baboons have three genes encoding CYP11B1. It may be that the presence of these three genes is due to various mutations and that only one gene encoding CYP11B1 is present in other baboons. The adrenals, which were used in this study was obtained from healthy baboons.

ABSTRACT

This study describes the characterization of two CYP11B1 isoforms in the Cape baboon.

Intracellular localization of Cape baboon CYP11B1 in the adrenal gland using Western blot analyses indicated CYP11B1 as a single band, with an apparent molecular mass of 54 kDa, in the cortical tissue homogenate and as two distinct bands in the medullary tissue homogenate. The first band in the medullary tissue homogenate corresponded to a similar molecular mass as the protein found in the cortical tissue homogenate, while the second band corresponded to an apparent molecular mass of ~51 kDa. These results prompted further investigations into the localization of the mitochondrial CYP11A1, AdR and AdX and the microsomal CYP21 in the baboon adrenal tissue. Cape baboon CYP11A1 was identified as a single band in the cortical tissue homogenate only and corresponded to an apparent molecular weight of 52 kDa. AdR was present in both the cortical- and medullary tissue homogenates and AdX was detected in the cortical tissue homogenate only. CYP21 was identified as three bands, with a prominent band corresponding to an apparent molecular mass of 47 kDa, in the cortical tissue homogenate only.

The catalytic activity of Cape baboon CYP11B1 towards 11-DOC and corticosterone was subsequently studied in adrenal cortical- and medullary tissue homogenates. CYP11B1 exhibited 11β-hydroxylase activity towards 11-DOC, yielding corticosterone, in both tissue homogenates. However, the 11β-hydroxylase activity in the cortical tissue homogenate was higher than the activity in the medullary tissue homogenate. CYP11B1 exhibited no 18-hydroxylase and 18-oxidase activity towards corticosterone in the cortical tissue homogenate, while in the medullary tissue homogenate, a CYP11B isoform exhibited both 18-hydroxylase and 18-oxidase activity towards corticosterone yielding 18-hydroxycorticosterone and aldosterone, respectively.

Previously, three genes encoding CYP11B1, *viz.* CYP11B1a, CYP11B1wt and CYP11B1s, was cloned from Cape baboon adrenals. Sequence analysis showed that these baboon CYP11B cDNAs are 96.5% homologous to human CYP11B1 and 94.6% homologous to human CYP11B2. The baboon cDNAs were expressed in non-steroidogenic COS-1 cells and their catalytic activity towards 11-DOC and 11-deoxycortisol assayed. Only CYP11B1a and CYP11B1wt were shown to be functional enzymes. CYP11B1a and CYP11B1wt catalyzed

the conversion of 11-DOC to corticosterone at different rates, while both cDNAs exhibited comparable 11β-hydroxylase activities towards 11-deoxycortisol.

To further understand the differences in the 11β-hydroxylation of 11-DOC and 11-deoxycortisol by CYP11B1a and CYP11B1wt, respectively, three-dimensional structures of both CYP11B1 isoforms were obtained by homology modeling. Amino acid sequence analyses showed changes of three residues in exon three.

The results presented in this thesis give evidence of the existence of two CYP11B1 isoforms, exhibiting different substrate affinity towards 11-DOC and 11-deoxycortisol, in the Cape baboon. The different efficiency and selectivity whereby the two CYP11B1 isoforms metabolize 11-DOC and 11-deoxycortisol, respectively, may be due to indirect involvement of three amino acid substitutions at positions 177, 182 and 188.

An interesting finding in this study is the synthesis of aldosterone in the medulla and the possibility of a novel redox-partner, which might facilitate electron transfer between AdR and CYP11B. It is established that the medulla contains areas of cortical cells, which surround some of the medullary vessels. These cortical cells have not been studied in detail yet, but are believed to contain both zG and zF cells [76]. The work presented in this study may be the first to suggest that cortical cells in the medulla express CYP11B activity. This study on Cape baboon CYP11B1 further provide a solid foundation for future studies, which could allow for the cloning of the CYP11B2 gene.

The findings in Chapter three was published in *Endocrine Research* (2002) **28(4)**, 477-484 [69; see Appendix E]. A part of the results presented in Chapter four was published in *Endocrine Research* (2000) **26(4)**, 1011-1018 [2].

REFERENCES

1. Hampf, M., Swart, A. C., Swart, P. (1996) *Endocrine Research* **22(4)**, 495-499.
2. Swart, A. C., Brown, N., Kolar, N, Swart, P. (2000) *Endocrine Research* **26(4)**, 1011-1018.
3. O'Malley B. W. and Strott C. A. (1991) Steroid Hormones. In: Reproductive Endocrinology (Edited by S. S. C. Yen and R. B. Jaffe). W. B. Saunders Co., Philadelphia, 3rd ed., pp. 156-180.
4. Hanukoglu I. (1992) *Journal of Steroid Biochemistry and Molecular Biology* **43**:779-804.
5. Jefcoate C. R., McNamara B. C., Artemenko I. and Yamazaki T. J. (1992) *Journal of Steroid Biochemistry and Molecular Biology* **43**, 751-767.
6. Garfinkel, D. (1958) *Archives of Biochemistry and Biophysics* **77**, 493.
7. Klingelberg, M. (1958) *Archives of Biochemistry and Biophysics* **75**, 376-386.
8. Omura, T. & Sato, R. (1964) *Journal of Biological Chemistry* **239**, 2370.
9. Porter, T. D & Coon, M. J. (1991) *Journal of Biological Chemistry* **266(21)**, 13469-13472.
10. Bureik, M., Lisurek, M., Bernhardt, R. (2002) *Biological Chemistry* **383**, 1537-1551.
11. Werck-Reichhart, D. & Feyereisen, R. (2000) *Genome Biology* **1(6)**, 3003.1-3003.9.
12. Sakaki, T. & Inouye, K. (2000) *Journal of Bioscience and Bioengineering* **90(6)**, 583-590.
13. Roberts, G. A., Grogan, G., Greter, A., Flitsch, S. L, Turner, N. J. (2002) *Journal of Bacteriology* **184 (14)**, 3898-3908.
14. Muller, J. J., Lapko, A., Bourenkov, G., Ruckpaul, K., Heinemann, U. (2001) *Journal of Biological Chemistry* **276(4)**, 2786-2789.
15. Beckert, V. & Bernhardt, R. (1997) *Journal of Biological Chemistry* **272(8)**, 4883-4888.
16. Hanukoglu I. (1996) *Advances in Molecular and Cellular Biology* **14**, 29-55.
17. Hlavica, P., Lewis, D. F. V. (2001) *European Journal of Biochemistry* **268**, 4817-4832.
18. Payne, A. H. & Hales, D. B. (2004) *Endocrine Review* **25(6)**, 947-970.
19. Belkina, N. V., Lisurek, M., Ivanov, A. S., Bernhardt, R. (2001) *Journal of Inorganic Biochemistry* **87**, 197-207.

20. Hasemann, C. A., Ravichandran, K. G., Peterson, J. A., Deisenhofer, J. (1994) *Journal of Molecular Biology* **236**, 1169-1185.
21. Poulos, T. L. (1995) *Current Opinion in Structural Biology* **5**, 767-774.
22. Stocco, D. M. (2000) *Journal of Endocrinology* **164**, 247-253.
23. Connel, J. M. C. & Davies, E. (2005) *Journal of Endocrinology* **186**, 1-20.
24. Morohashi, K., Fujii-Kuriyama, Y., Okada, Y., Sogawa, K., Hirose, T., Inayama, S., Omura, T. (1984) *Proceedings of the National Academy of Sciences, USA* **81**, 4647-4651.
25. John, M. E., John, M. C., Ashley, P., MacDonald, R. J., Simpson, E. R., Waterman, W. R. (1984) *Proceedings of the National Academy of Sciences, USA* **81**, 5628-5632.
26. Chung, B.-C., Matteson, K. J., Voutilainen, R., Mohandas, T. K., Miller, W. L. (1986) *Proceedings of the National Academy of Sciences, USA* **83**, 8962-8966.
27. Morohashi, K., Sogawa, K., Omura, T., Fujii-Kuriyama, Y. (1987) *Journal of Biochemistry* **101**, 879-887.
28. Sparkes, R. S., Klisak, I., Miller, W. L. (1991) *DNA and Cell Biology* **10**, 359-356.
29. Storbeck, K-H., Swart, P., Graham, S., Swart, A. C. (2004) *Endocrine Research* **30(4)**, 761-767.
30. Storbeck, K-H., Swart, P., Graham, S., Swart, A. C. (2007) *Molecular and Cellular Endocrinology* doi: 10.1016/j.mce.2006.12.005.
31. Hall, P. F. (1985) *Steroids* **47**, 133-196.
32. Sheets, J. J. & Vickery, L. E. (1982) *Proceedings of the National Academy of Sciences* **79**, 5773-5777.
33. Matocha, M. F. & Waterman, M. R. (1985) *Journal of Biological Chemistry* **260(22)**, 12259-12265.
34. Picado-Leonard, J. & Miller, W. L. (1987) *DNA* **6**, 439-448.
35. Swart, A. C., Kolar, N. W., Lombard, N., Mason, I. J., Swart, P. (2002) *European Journal of Biochemistry* **269**, 5608-5616.
36. White, P. C., New, M. I., Dupont, B. (1987) *New England Journal of Medicine* **316**, 1580-1586.
37. Chua, S. C., Szabo, P., Vitek, A., Grzeschik, K.-H., John, M., White, P. C. (1987) *Proceedings of the National Academy of Sciences USA* **84**, 7193-7197.
38. Wagner, M. J., Ge, Y., Siciliano, M., Wells, D. E. (1991) *Genomics* **10**, 114-115.

39. Mornet, E., Dupont, J., Vitek, A., White, P. C. (1989) *Journal of Biological Chemistry* **264**, 20961-20967.
40. Ogishima, T, Shibata, H., Shimada, H., Mitani, F., Suzuki, H., Saruta, T., Ishimura, Y. (1991) *Journal of Biological Chemistry* **266**, 10731-10734.
41. Bulow, H. E. & Bernhardt, R. (2002) *European Journal of Biochemistry* **269**, 3838-3846.
42. Lisurek, M., Bernhardt, R. (2004) *Molecular and Cellular Endocrinology* **215**, 149-159.
43. Rainey, W. E. (1999) *Molecular and Cellular Endocrinoly* **151**, 151-160.
44. Véronneau, S., Bernard, H., Cloutier, M., Courtemanche, J., Ducharme, L., Lefebvre, A., Mason, J. I., LeHoux, J. G. (1996) *Journal of Steroid Biochemistry and Molecular Biology* **57(1/2)**, 125-139.
45. Hakki, T., Bernhardt, R. (2006) *Pharmacology and Therapeutics* **111**, 27-52.
46. White, P. C., Rainey, W. E. (2005) *Journal of Clinical Endocrinology and Metabolism* **90(2)**, 1252-1255.
47. Stratakis, C. A., Bossi, I. (2004) *Reviews in Endocrine and Metabolic Disorders* **5**, 53-68.
48. White, P. C., Curnow, K. M., Pascoe, L. (1994) *Endocrine reviews* **15(4)**, 421-438.
49. Boon, W. C., Coghlan, J. P, Curnow, K. M., McDougall, J. G. (1997) *Trends in Endocrinology and Metabolism* **8**, 346-354.
50. http://www.yourdictionary.com.
51. Pascoe, L., Curnow, K. M., Slutsker, L., Rosler, A., White, P. C. (1992) *Proceedings of the National Academy of Sciences USA* **89**, 4996-5000.
52. Coulter, C. L. & Jaffe, R. B. (1998) *Endocrinology* **139(12)**, 5144-5150.
53. Pattison, J. C., Abbott, D. H., Saltzman, W. Nguyen, A. D., Henderson, G., Jing, H., Pryce, C. R., Allen, A. J., Conley, A. J., Bird, I. M. (2005) *Endocrinology* **146(1)**, 365-374.
54. Stocco, D. M. & Clark, B. J. (1996) *Endocrine Review* **17**, 221-244.
55. Lin, D., Sugawara, T., Strauss, J. F., Clark, B. J., Stocco, D. M., Saenger, P., Rogol, A., Miller, W. L. (1995) *Science* **267**, 1828-1831.
56. Carlone, D. L., Richards, J. A. S. (1997) *Molecular Endocrinology* **11 (3)**, 292-304.
57. **Stocco, D. M. (1999)** *BioEssays* **21,** 768-775.
58. Rainey, W. E., Saner, K., Schimmer, B. P. (2004) *Molecular and Cellular Endocrinology* **228**, 23-38.

59. Stocco, D. M., Wang, X. J., Jo, Y., Manna, P. R. (2005) Molecular Endocrinology, **19 (11)**, 2647-2659.

60. John, M. E., John, M. C., Boggaram, V., Simpson, E. R., Waterman, M. R. (1986) *Proceedings of the National Academy of Sciences USA* **83**, 4715-4719.

61. DiBlasio, A. M., Voutilainen, R., Jaffe, R. B., Miller, W. L. (1988) *Journal of Clinical Endocrinology and Metabolism* **65**, 170-175.

62. Wang, X. L., Bassett, M., Zhang, Y., Yin, S., Clyne, C., White, P. C., Rainey, W. E. (2000) *Endocrinology* **141(10)**, 3587-3594.

63. Bassett, M. H., Suzuki, T., Sasano, H, White, P. C. Rainey, W. E. (2004) *Molecular Endocrinology* **18(2)**, 279-290.

64. Boon, W. C., Roche, P. J., Hammond, V. E., Jeyaseelan, K., Crawford, R. J. Coghlan, J. P. (1995) *Biochimica et Biophysica Acta* **1260(1)**, 109-112.

65. LeHoux, J. G., Mason, J. I., Bernard, H., Ducharme, L., LeHoux, J., Véronneau, S., Lefebvre, A. (1994) *Journal of Steroid Biochemistry and Molecular Biology* **49(2/3)**, 131-137.

66. Ogishima, T., Suzuki, H., Hata, J. C., Mitani, F., Ishimura, Y. (1992) *Endocrinology* **130(5)**, 2971-2977.

67. Zhou, M. Y., Gomez-Sanchez, E. P., Foecking, M. F., Gomez-Sanchez, C. E. (1995) *Molecular and Cellular Endocrinology* **114**, 137-145.

68. Bulow, H, Bernhardt, R. (2001) *European Journal of Biochemistry* **269**, 3838-3846.

69. Brown, N., Swart, P., Fenhalls, G., Stevens, L., Kolar, N. W., Swart, A. C. (2002) *Endocrine Research* **28(4)**, 477-484.

70. MacKenzie, S. M., Clark, C. J., Fraser, R., Gomez-Sanchez, C. E., Connell, J. M. C., Davies, E. (2000) *Journal of Molecular Endocrinology* **24**, 321-328.

71. Erdman, B., Denner, K., Gerst, H., Lenz, D., Bernhardt, R. (1995) *Endocrine Research* **21**, 425-435.

72. Peters, B., Clausmeyer, P. T., Obermuller, N., Kranzlin, B., Gretz, N., Inagami, T., Peters, J. (2001) *The Journal of Histochemistry and Cytochemistry* **49(5)**, 649-656.

73. Sato, R. & Omura, T. (1978) In Cytochrome P450, 1-35. Kodansha Ltd. And Academic Press Inc. Tokyo, New York, San Francisco, London.

74. Kawamoto, T., Mitsuuchi, Y., Toda, K., Yokoyama, Y., Miyahara, K., Miura, S., Ohnishi, T., Ichikawa, Y., Nakao, K., Imura, H., Ulick, S., Shizuta, Y. (1992) *Proceedings of the National Academy of Sciences* **89**, 1458-1462.

75. Weder, N., "A spectral and immunological study of two adrenal mitochondrial cytochrome P-450's" (MSc thesis, University of Stellenbosch, Stellenbosch, 1989), 121.

76. Mapes, S., Corbin, C. J., Tarantal, A., Conley, A. (1999) *Journal of Clinical Endocrinology & Metabolism* **84(9)**, 3382-3385.

77. Dowd, J. E., Riggs, D. S. (1964) *Journal of Biological Chemistry* **240(2)**, 863, 869.

78. Cornish-Bowden, A. (1995) In Fundamentals of Enzyme Kinetics, Revised Edition, 30-37.

79. Cover, C. M., Wang, J. M., St. Lezin, E., Kurtz, T. W., Mellon, S. H. (1995) *Journal of Biological Chemistry* **270(28)**, 16555-16560.

80. Fisher, A., Fraser, R., McConnel, J., Davies, E. (2000) *Journal of Clinical Endocrinology and Metabolism* **85(3)**, 1261-1266.

81. Nelson, D. R., Koymans, L., Kamataki, T., Stegeman, J. J., Feyereisen, R., Waxman, D. J, Waterman, M. R , Gotoh, O., Coon, M. J, Estabrook, R. W. (1996) *Pharmacogenetics* **6**, 1-42.

82. Liu, J., Ericksen, S. S., Besspiata, D., Fisher, C. W., Szklarz, G. D. (2003) *Drug metabolism and Disposition* **31(4)**, 412-420.

83. Yano, K. J., Blasco, F., Li, H., Schmid, R. D., Henne, A., Poulos, T. L. (2003) *Journal of Biological Chemistry* **278(1)**, 608-616.

84. Szklarz, G. D. & Halpert, J. R. (1998) *Drug Metabolism and Disposition* **26(12)**, 1179-1184.

85. Krone, N., Riepe, F. G., Gotze, D., Korsch, E., Rister, M., Commentz, J., Partsch, C. J., Grotzinger, J., Peter, M., Sippell, W. G. (2005) *Journal of Clinical Endocrinology & Metabolism* **90**, 3724-3730.

86. Poulos, T. L. (1991) *Methods in Enzymology* **206**, 11-30.

87. Poulos, T. L., Finzel, B. C., Howards, A. J. (1987) *Journal of Molecular Biology* **195**, 687-700.

88. Hasemann, C. A., Kurumbail, R. G., Boddupalli, S. S., Peterson, J. A., Deisenhoff, J. (1995) *Structure* **2**, 41-62.

89. Schiffler, B. & Bernhardt, R. (2003) *Biochemical and Biophysical Research Communications* **312**, 223-228.

90. Miguel, R. N., Chen, S., Nikfarjam, L., Kominami, S., Carpenter, B., Pra, C. D., Betterle, C., Zanchetta, R., Nakamatsu, T., Powell, M., Hewer, R., Blundell, T.,

Smith, B. R., Furmaniak, J. (2005) *European Journal of Endocrinology* **153**, 949-961.

91. Ravichandran, K. G., Boddupalli, S. S., Hasemann, C. A., Peterson, J. A., Deisenhofer, J. (1993) *Science* **261**, 731-736.
92. Cup-Vickery, J. R. & Poulos, T. L. (1995) *Nature Structural Biology* **2**, 144-153.
93. Kellner, D. G., Maves, S. A., Sligar, S. G. (1997) *Current Opinion in Biotechnology* **8**, 274-278.
94. Peterson, J. A., Graham, S. E. (1998) *Structure* **6(9)**, 1079-1085.
95. Robins, T., Carlsson, J., Sunnerhagen, M., Wedell, A., Persson, B. (2006) *Molecular Endocrinology* **281(12)**, 8051-8061.
96. Graham-Lorence, S., Amarneh, B., White, R. E., Peterson, J. A., Simpson, E. R. (1995) *Protein Science* **4**, 1065-1080.
97. Gotoh, O. (1992) *Journal of Biological Chemistry* **267(1)**, 83-90.
98. Williams, P. A., Cosme, J., Sridhar, V., Johnson, E. F., McRee, D. E. (2000) *Molecular Cell* **5**, 121-131.
99. Williams, P. A., Cosme, J., Sridhar, V., Johnson, E. F., McRee, D. E. (2000) *Journal of Inorganic Biochemistry* **81**, 183-190.
100. Loge, C., Le Borgne, M, Marchand, P., Robert, J. M., Baut, G., Palzer, M., Hartmann, R. W. (2005) *Journal of Enzyme Inhibition and Medicinal Chemistry* **20(6)**, 581-585.
101. William, P. A., Cosme, J., Ward, A., Angove, H. C., Vinkovic, D. M., Jhoti, H. (2003) *Nature* **424**, 464-468.
102. Wester, M. R., Yano, J. K., Schoch, G. A., Yang, C., Griffin, K. J., Stout, C. D., Johnson, E. F. (2004) *Journal of Biological Chemistry* **279**, 35630-35637.
103. Schoch, G. A., Yano, J. K., Wester, M. R., Griffin, K. J., Stout, C. D., Johnson, E. F. (2004) *The Journal of Biological Chemistry* **279(10)**, 9497-9503.
104. William, P. A., Cosme, J., Vinkovic, D. M., Ward, A., Angove, H. C., Day, P. J., Vonrhein, C., Tickle, I. J., Jhoti, H. (2004) *Science* **305**, 683-686.
105. Yano, J. K., Wester, M. R., Schoch, G. A., Griffin, K. J., Stout, C. D., Johnson, E. F. (2004) *Journal of Biological Chemistry* **279**, 38091-38094.
106. Yano, J. K., Hsu, M.-H., Griffin, K. J., Stout, C. D., Johnson, E. F. (2005) *Nature Structural and Molecular Biology* **12**, 822-832.

107. Rowland, P., Blaney, F. E., Smyth, M. G., Jones, J. J., Leydon, V. L, Oxbrow, A. K., Lewis, C. J., Tennant, M. G., Modi, S., Eggleston, D. S., Chenery, R. J., Bridges, A. M. (2006) *Journal of Biological Chemistry* **281(11)**, 7614-7622.

108. Rainey, W. E., Carr, B. R., Sasano, H., Suzuki, T., Mason, J. I. (2002) *TRENDS in Endocrinology and Metabolism* **13(6)**, 234-239.

109. Szklarz, G. D., Graham, S. E., Paulsen, M. D. (2000) *Vitamins and Hormones* **58**, 53-86.

110. Ziegler, G. A., Vonrhein, C., Hanukoglu, I., Schulz, G. E. (1999) *Journal of Molecular Biology* **289**, 981-990.

111. Muller, E. C., Lapko, A., Otto, A., Muller, J. J., Ruckpaul, K., Heinemann, U. (2001) *European Journal of Biochemistry* **268**, 1837-1843.

112. Hlavica, P., Schulze, J., Lewis, D. F. V. (2003) *Journal of Inorganic Biochemistry* **96**, 279-297.

113. Lewis, D. F. V., Lee-Robischaud, P. (1998) *Journal of Steroid Biochemistry and Molecular Biology* **66(4)** 217-233.

114. Bechtel, S., Belkina, N., Bernhardt, R. (2002) *European Journal of Biochemistry* **269**, 1118-1127.

115. Muller, A., Muller, J. J., Muller, Y. A., Uhlmann, H., Bernhardt, R., Heinemann, U. (1998) *Structure* **6**, 269-280.

Appendix A

Nucleotide sequence alignment of Cape baboon CYP11B1a, CYP11B1wt and CYP11B1S with human CYP11B1 and CYP11B2. Red letters indicate the nucleotide differences. Green blocks indicate the Sma1 sites. The red block indicates the stop codon in baboon CYP11B1s.

```
                                                                                                    81
CYP11B1a    ATG GCA CTG AGA GCA AAG GCA GAG GTG TGC ATG GCA GTG CCC TGG CTG GCC CTA CAA AGG GCA CGG GCA CTG GGC ACC AGA
CYP11B1wt   ATG GCA CTG AGA GCA AAG GCA GAG GTG TGC ATG GCA GTG CCC TGG CTG GCC CTA CAA AGG GCA CGG GCA CTG GGC ACC AGA
CYP11B1S    ATG GCA CTG AGA GCA AAG GCA GAG GTG TGC ATG GCA GCG CCC TGG CTG TCC CTA CAA AGG GCA CGG GCA CTG GGC ACC AGA
Hum CYP11B1 ATG GCA CTC AGG GCA AAG GCA GAG GTG TGC ATG GCA GTG CCC TGG CTG TCC CTG CAA AGG GCA CAG GCA CTG GGC ACG AGA
Hum CYP11B2 ATG GCA CTC AGG GCA AAG GCA GAG GTG TGC GTG GCA GCG CCC TGG CTG TGC CTG CAA AGG GCA CGG GCA CTG GGC ACG AGA
                                                                                                    162
CYP11B1a    GCC ACC CGG GTC CCC AGG ACA GTG CTG CCC TTT GAA GCC ATG CCC CGG CGT CCA GGC AAC AGG TGG CTG AGG CTG CTG CAG
CYP11B1wt   GCC ACC CGG GTC CCC AGG ACA GTG CTG CCC TTT GAA GCC ATG CCC CGG CGT CCA GGC AAC AGG TGG CTG AGG CTG CTG CAG
CYP11B1S    GCC ACC CGG GTC CCC AGG ACA GTG CTG CCC TTT GAA GCC ATG CCC CGG CGT CCA GGC AAC AGG TGG CTG AGG CTG CTG CAG
Hum CYP11B1 GCC GCC CGG GTC CCC AGG ACA GTG CTG CCC TTT GAA GCC ATG CCC CGT CGT CCA GGC AAC AGG TGG CTG AGG CTG CTG CAG
Hum CYP11B2 GCC GCC CGA GCC CCC CAG CAT GTG CTG CCC TTT GAA GCC ATG CCC CAG CAT CCA GGC AAC AGG TGG CTG AGG CTG CTG CAG
                                                                                                    243
CYP11B1a    ATC TGG AGG GAG CAG GGT TAT GAG CAC CTG CAC CTG GAG GTG CAC CAG ACC TTC CAG GAA CTG GGG CCC ATT TTC AGG TAT
CYP11B1wt   ATC TGG AGG GAG CAG GGT TAT GAG CAC CTG CAC CTG GAG GTG CAC CAG ACC TTC CAG GAA CTG GGG CCC ATT TTC AGG TAT
CYP11B1S    ATC TAG AGG GAG CAG GGT TAT GAG CAC CTG CAC CTG GAG GTG CAC CAG ACC TTC CAG GAA CTG GGG CCC ATT TTC AGG TAT
Hum CYP11B1 ATC TGG AGG GAG CAG GGT TAT GAG GAC CTG CAC CTG GAA GTA CAC CAG ACC TTC CAG GAA CTG GGG CCC ATT TTC AGG TAC
Hum CYP11B2 ATG TGG AGG GAG CAG GGT TAT GAG CAC CTG CAC CTG GAA ATG CAC CAG ACC TTC CAG GAA CTG GGG CCC ATT TTC AGG TAC
                                                                                                    324
CYP11B1a    GAC TTG GGA GGA GCA GGC ATG GTG TGT GTG ATG CTG CCA GAG GAC GTG GAG AAG CTG CAG CAG GTG GAC AGC CTG AAC CCA
CYP11B1wt   GAC TTG GGA GGA GCA GGC ATG GTG TGT GTG ATG CTG CCA GAG GAC GTG GAG AAG CTG CAG CAG GTG GAC AGC CTG AAC CCA
CYP11B1S    GAC TTG GGA GGA GCA GGC ATG GTG TGT GTG ATG CTG CCA GAG GAC GTG GAG AAG CTG CAG CAG GTG GAC AGC CTG AAC CCA
Hum CYP11B1 GAC TTG GGA GGA GCA GGC ATG GTG TGT GTG ATG CTG CCG GAG GAC GTG GAG AAG CTG CAA CAG GTG GAC AGC CTG CAT CCC
Hum CYP11B2 AAC TTG GGA GGA CCA CGC ATG GTG TGT GTG ATG CTG CCG GAG GAC GTG GAG AAG CTG CAA CAG GTG GAC AGC CTG CAT CCC
                                                                                                    405
CYP11B1a    CGC CGG ATG AGC CTG GAG CCC TGG GTG GCC TAC AGA CAA CAT CGT GGG CAC AAA TGT GGC GTG TTC TTG CTG AAC GGG CCT
CYP11B1wt   CGC CGG ATG AGC CTG GAG CCC TGG GTG GCC TAC AGA CAA CAT CGT GGG CAC AAA TGT GGC GTG TTC TTG CTG AAC GGG CCT
CYP11B1S    CGC CGG ATG AGC CTG GAG CCC TGG GTG GCC TAC AGA CAA CAT CGT GGG CAC AAA TGT GGC GTG TTC TTG CTG AAC GAG CCT
Hum CYP11B1 CAC AGG ATG AGC CTG GAG CCC TGG GTG GCC TAC AGA CAA CAT CGT GGG CAC AAA TGT GGC GTG TTC TTG CTG AAT GGG CCT
Hum CYP11B2 TGC AGG ATG ATC CTG GAG CCC TGG GTG GCC ATC AGA CAA CAT CGT GGG CAC AAA TGT GGC GTG TTC TTG CTG AAT GGG CCT
                                                                                                    486
CYP11B1a    GAA TGG CGC TTC AAT CGA TTG CGG CTG AAC CCA GAT GTG CTG TCG CCC AAG GCT GTG CAG AGG TTT CTC CCG ATG GTG GAT
CYP11B1wt   GAA TGG CGC TTC AAT CGA TTG CGG CTG AAC CCA GAT GTG CTG TCG CCC AAG GCT GTG CAG AGG TTT CTC CCG ATG GTG GAT
CYP11B1S    GAA TGG CGC TTC AAT CGA TTG CGG CTG AAC CCA GAT GTG CTG TCG CCC AAG GCT GTG CAG AGG TTT CTC CCG ATG GTG GAT
Hum CYP11B1 GAA TGG CGC TTC AAC CGA TTG CGG CTG AAT CCA GAA GTG CTG TCG CCC AAC GCT GTG CAG AGG TTC CTC CCG ATG GTG GAT
Hum CYP11B2 GAA TGG CGC TTC AAC CGA TTG CGG CTG AAT CCA GAT GTG CTG TCG CCC AAG GCT GTG CAG AGG TTC CTC CCG ATG GTG GAT
                                                                                                    567
CYP11B1a    GCG GTG GCC AGG GAC TTC TCC CAG GCC CTG AGG AAG AAG GTG GTG CAG AAC GCC CGA GAG AGC GTG ACC CTG GAC ATC CAG
CYP11B1wt   GCG GTG GCC AGG GAC TTC TCC CAG GCC CTG AGG AAG AAG GTG CTG CAG AAC GCC CGG GAC AGC GTG ACC CTG GAC GTC CAG
CYP11B1S    GCG GTG GCC AGG GAC TTC TCC CAG GCC CTG AGG AAG AAG GTG CTG CAG AAC GCC CGG GAG AGC GTG ACC CTG GAC ATC CAG
Hum CYP11B1 GCA GTG GCC AGG GAC TTC TCC CAG GCC CTG AAG AAG AAG GTG CTG CAG AAC GCC CGG GGG AGC CTG ACC CTG GAC GTC CAG
Hum CYP11B2 GCA GTG GCC AGG GAC TTC TCC CAG GCC CTG AGG AAG AAG GTG CTA CAG AAC GCC CGG GGG AGC CTG ACC CTG GAC GTC CAG
                                                                                                    648
CYP11B1a    CCC AGC ATC TTC CAC TAC ACC ATA GAA GCC AGC AAC TTA GCT CTT TTT GGA GAG CGG CTG GGC CTG GTT GGT CAC AGC CCC
CYP11B1wt   CCC AGC ATC TTC CAC TAC ACC ATA GAA GCC AGC AAC TTA GCT CTT TTT GGA GAG CGG CTG GGC CTG GTT GGT CAC AGC CCC
CYP11B1S    CCC AGC ATC TTC CAC TAC ACC ATA GAA GCC AGC AAC TTA GCT CTT TTT GGA GAG CGG CTG GGC CTG GTT GGT CAC AGC CCC
Hum CYP11B1 CCC AGC ATC TTC CAC TAC ACC ATA GAA GCC AGC AAC TTG GCT CTT TTT GGA GAG CGG CTG GGC CTG GTT GGC CAC AGC CCC
Hum CYP11B2 CCC AGC ATC TTC CAC TAC ACC ATA GAA GCC AGC AAC TTG GCT CTT TTT GGA GAG CGG CTG GGC CTG GTT GGC CAC AGC CCC
                                                                                                    729
CYP11B1a    AGC TCT GCC AGC CTG AGC TTC CTC CAT GCC CTG GAG GTC ATG TTC AAA TCC ACC GTC CAG CTC ATG TTC ATG CCC AGG AGC
CYP11B1wt   AGC TCT GCC AGC CTG AGC TTC CTC CAT GCC CTG GAG GTC ATG TTC AAA TCC ACC GTC CAG CTC ATG TTC ATG CCC AGG AGC
CYP11B1S    AGC TCT GCC AGC CTG AGC TTC CTC CAT GCC CTG GAG GTC ATG TTC AAA TCC ACC GTC CAG CTC ATG TTC ATG CCC AGG AGC
Hum CYP11B1 AGT TCT GCC AGC CTG AAC TTC CTC CAT GCC CTG GAG GTC ATG TTC AAA TCC ACC GTC CAG CTC ATG TTC ATG CCC AGG AGC
Hum CYP11B2 AGT TCT GCC AGC CTG AAC TTC CTC CAT GCC CTG GAG GTC ATG TTC AAA TCC ACC GTC CAG CTC ATG TTC ATG CCC AGG AGC
                                                                                                    810
CYP11B1a    CTG TCT CGC TGG ACC AGC CCC AAG GTG TGG AAG GAG CAC TTT GAG GCC TGG GAC TGC ATC TTC CAG TAC GGT GAC AAC TGT
CYP11B1wt   CTG TCT CGC TGG ACC AGC CCC AAG GTG TGG AAG GAG CAC TTT GAG GCC TGG GAC TGC ATC TTC CAG TAC GGT GAC AAC TGT
CYP11B1S    CTG TCT CGC TGG ACC AGC CCC AAG GTG TGG AAG GAG CAC TTT GAG GCC TGG GAC TGC ATC TTC CAG TAC GGT GAC AAC TGT
Hum CYP11B1 CTG TCT CGC TGG ACC AGC CCC AAG GTG TGG AAG GAG CAC TTT GAG GCC TGG GAC TGC ATC TTC CAG TAC GGC GAC AAC TGT
Hum CYP11B2 CTG TCT CGC TGG ATC AGC CCC AAG GTG TGG AAG GAG CAC TTT GAG GCC TGG GAC TGC ATC TTC CAG TAC GGC GAC AAC TGT
                                                                                                    891
CYP11B1a    ATC CAG AAA ATC TAT CAG GAA CTG GCC TTG AGC CGC CCT CAG CAG TAC ACC AGC ATC GTG GCG GAA CTC CTG TTG AAT GCG
CYP11B1wt   ATC CAG AAA ATC TAT CAG GAA CTG GCC TTG AGC CGC CCT CAG CAG TAC ACC AGC ATC GTG GCG GAA CTC CTG TTG AAT GCG
CYP11B1S    ATC CAG AAA ATC TAT CAG GAA CTG GCC TTG AGC CGC CCT CAG CAG TAC ACC AGC ATC GTG GCG GAA CTC CTG TTG AAT GCG
Hum CYP11B1 ATC CAG AAA ATC TAT CAG GAA CTG GCC TTC AGC CGC CCT CAA CAG TAC ACC AGC ATC GTG GCG GAG CTC CTG TTG AAT GCG
Hum CYP11B2 ATC CAG AAA ATC TAT CAG GAA CTG GCC TTC AAC CGC CCT CAA CAC TAC ACC GGC ATC GTG GCG GAG CTC CTG TTG AAG GCG
                                                                                                    972
CYP11B1a    GAA CTG TCG CCA GAT GCC ATC AAG GCC AAC TCT ATG GAA CTC ACT GCA GGG AGC GTG GAC ACG ACT GTG TTT CCC TTG CTG
CYP11B1wt   GAA CTG TCG CCA GAT GCC ATC AAG GCC AAC TCT ATG GAA CTC ACT GCA GGG AGC GTG GAC ACG ACT GTG TTT CCC TTG CTG
CYP11B1S    GAA CTG TCG CCA GAT GCC ATC AAG GCC AAC TCT ATG GAA CTC ACT GCA GGG AGC GTG GAC ACG ACT GTG TTT CCC TTG CTG
Hum CYP11B1 GAA CTG TCG CCA GAT GCC ATC AAG GCC AAC TCT ATG GAA CTC ACT GCA GGG AGC GTG GAC ACG ACG GTG TTT CCC TTG CTG
Hum CYP11B2 GAA CTG TCG CTA GAA GCC ATC AAG GCC AAC TCT ATG GAA CTC ACT GCA GGG AGC GTG GAC ACG ACG GCG TTT CCC TTG CTG
```

```
                                                                                                  1053
CYP11B1a     ATG ACA CTC TTT GAG CTG GCT CGG AAC CCC AAC GTG CAG CAG GCC CTG CGC CAG GAG AGC CTG GCC GCC GCC GCC AGC ATC
CYP11B1wt    ATG ACA CTC TTT GAG CTG GCT CGG AAC CCC AAC GTG CAG CAG GCC CTG CGC CAG GAG AGC CTG GCC GCC GCC GCC AGC ATC
CYP11B1S     ATG ACA CTC TTT GAG CTG GCT CGG AAC CCC AAC GTG CAG CAG GCC CTG CGC CAG GAG AGC CTG GCC GCC GCC GCC AGC ATC
Hum CYP11B1  ATG ACG CTC TTT GAG CTG GCT CGG AAC CCC AAC GTG CAG CAG GCC CTG CGC CAG GAG AGC CTG GCC GCC GCA GCC AGC ATC
Hum CYP11B2  ATG ACG CTC TTT GAG CTG GCT CGG AAC CCC GAC GTG CAG CAG ATC CTG CGC CAG GAG AGC CTG GCC GCC GCA GCC AGC ATC

                                                                                                  1134
CYP11B1a     AGT GAA CAT CCC CAG AAG GCA ACC ACC GAG CTG CCC TTG CTG CGG GCG GCC CTC AAG GAG ACC CTG AGG CTC TAC CCT GTG
CYP11B1wt    AGT GAA CAT CCC CAG AAG GCA ACC ACC GAG CTG CCC TTG CTG CGG GCG GCC CTC AAG GAG ACC CTG AGG CTC TAC CCT GTG
CYP11B1S     AGT GAA CAT CCC CAG AAG GCA ACC ACC GAG CTG CCC TTG CTG CGG GCG GCC CTC AAG GAG GCC CTG AGG CTC TAC CCT GTG
Hum CYP11B1  AGT GAA CAT CCC CAG AAG GCA ACC ACC GAG CTC CCC TTG CTG CGT GCG GCC CTC AAG GAG ACC TTG CGG CTC TAC CCT GTG
Hum CYP11B2  AGT GAA CAT CCC CAG AAG GCA ACC ACC GAG CTC CCC TTG CTG CGT GCG GCC CTC AAG GAG ACC TTG CGG CTC TAC CCT GTG

                                                                                                  1215
CYP11B1a     GGT CTG TTT TTG GAG CGA GTG GTG AGC TCA GAC TTG GTG CTT CAG AAC TAC CAC ATC CCA GCT GGG ACA CTG GTG CGC GTG
CYP11B1wt    GGT CTG TTT TTG GAG CGA GTG GTG AGC TCA GAC TTG GTG CTT CAG AAC TAC CAC ATC CCA GCT GGG ACA CTG GTG CGC GTG
CYP11B1S     GGT CTG TTT TTG GAG CGA GTG GTG AGC TCA GAC TTG GTG CTT CAG AAC TAC CAC ATC CCA GCT GGG ACA CTG GTG CGC GTG
Hum CYP11B1  GGT CTG TTT CTG GAG CGA GTG GCG AGC TCA GAC TTG GTG CTT CAG AAC TAC CAC ATC CCA GCT GGG ACA TTG GTG CGC GTG
Hum CYP11B2  GGT CTG TTT CTG GAG CGA GTG GTG AGC TCA GAC TTG GTG CTT CAG AAC TAC CAC ATC CCA GCT GGG ACA TTG GTG CAG GTG

                                                                                                  1296
CYP11B1a     TTC CTC TAC TCG CTG GGT CGC AAC CCC GCC TTA TTC CCG AGG CCT GAG CGC TAT AAC CCC CAG CGC TGG CTA GAC ATC AGG
CYP11B1wt    TTC CTC TAC TCG CTG GGT CGC AAC CCC GCC TTA TTC CCG AGG CCT GAG CGC TAT AAC CCC CAG CGC TGG CTA GAC ATC AGG
CYP11B1S     TTC CTC TAC TCG CTG GGT CGC AAC CCC GCC TTA TTC CCG AGG CCT GAG CGC TAT AAC CCC CAG CGC TGG CTA GAC ATC AGG
Hum CYP11B1  TTC CTC TAC TCT CTG GGT CGC AAC CCC GCC TTG TTC CCG AGG CCT GAG CGC TAT AAC CCC CAG CGC TGG CTA GAC ATC AAG
Hum CYP11B2  TTC CTC TAC TCT CTG GGT CGC AAC GCC GCC TTG TTC CCG AGG CCT GAG CGC TAT AAC CCC CAG CGC TGG CTA GAC ATC AGG

                                                                                                  1377
CYP11B1a     GGC TCC GGC AGG AAC TTC TAC CAT GTG CCC TTT GGC TTT GGC ATG CGC CAG TGC CTG GGG CGG CGC CTG GCA GAA GCG GAG
CYP11B1wt    GGC TCC GGC AGG AAC TTC TAC CAT GTG CCC TTT GGC TTT GGC ATG CGC CAG TGC CTG GGG CGG CGC CTG GCA GAA GCG GAG
CYP11B1S     GGC TCC GGC AGG AAC TTC TAC CAT GTG CCC TTT GGC TTT GGC ATG CGC CAG TGC CTG GGG CGG CGC CTG GCA GAA GCG GAG
Hum CYP11B1  GGC TCC GGC AGG AAC TTC TAC CAC GTG CCC TTT GGC TTT GGC ATG CGC CAG TGC CTT GGG CGG CGC CTG GCA GAG GCA GAG
Hum CYP11B2  GGC TCC GGC AGG AAC TTC CAC CAC GTG CCC TTT GGC TTT GGC ATG CGC CAG TGC CTT GGG CGG CGC CTG GCA GAG GCC GAG

                                                                                                  1458
CYP11B1a     ATG CTG CTG CTG CTG CAC CAT GTG CTG AAA CAC CTC CAG GTG GAG ACA CTA ACC CAA GAG GAT ATA AAG ATG GTC TAC AGC
CYP11B1wt    ATG CTG CTG CTG CTG CAC CAT GTG CTG AAA CAC CTC CAG GTG GAG ACA CTA ACC CAA GAG GAT ATA AAG ATG GTC TAC AGC
CYP11B1S     ATG CTG CTG CTG CTG CAC CAT GTG CTG AAA CAC CTC CAG GTG GAG ACA CTA ACC CAA GAG GAT ATA AAG ATG GTC TAC AGC
Hum CYP11B1  ATG CTG CTG CTG CTG CAC CAT GTG CTG AAA CAC CTC CAG GTG GAG ACA CTA ACC CAA GAG GAC ATA AAG ATG GTC TAC AGC
Hum CYP11B2  ATG CTG CTG CTG CTG CAC CAT GTG CTG AAA CAC TTC CTG GTG GAG ACA CTA ACC CAA GAG GAC ATA AAG ATG GTC TAC AGC

                                                                  1510
CYP11B1a     TTC ATA TTG AGG CCC AGC ACG TTC CCC CTC CTC ACC TTC AGG GCC ATC AAC TAA
CYP11B1wt    TTC ATA TTG AGG CCC AGC ACG TTC CCC CTC CTC ACC TTC AGG GCC ATC AAC TAA
CYP11B1S     TTC ATA TTG AGG CCC AGC ACG TTC CCC CTC CTC ACC TTC AGG GCC ATC AAC TAA
Hum CYP11B1  TTC ATA TTG AGG CCC AGC ATG TGC CCC CTC CTC ACC TTC AGA GCC ATC AAC TAA
Hum CYP11B2  TTC ATA TTG AGG CCC GGC ACG TCC CCC CTC CTC ACC TTC AGA GCC ATC AAC TAA
```

Appendix B

Amino acid sequence alignment of Cape baboon CYP11B1a, CYP11B1wt and CYP11B1S with human CYP11B1 and CYP11B2. Differences are indicated by yellow blocks.

```
babCYP11B1a   MALRAKAEVC MAVPWLALQR ARALGTRATR VPRTVLPFEA MPRRPGNRWL RLLQIWREQG 60
babCYP11B1wt  MALRAKAEVC MAVPWLALQR ARALGTRATR VPRTVLPFEA MPRRPGNRWL RLLQIWREQG
bCYP11B1S     MALRAKAEVC MAAPWLSLQR ARALGTRATR VPRTVLPFEA MPRRPGNRWL RLLQI*REQG
hCYP11B1      MALRAKAEVC MAVPWLSLQR AQALGTRAAR VPRTVLPFEA MPRRPGNRWL RLLQIWREQG
hCYP11B2      MALRAKAEVC VAAPWLCLQR ARALGTRAAR APRTVLPFEA MPQHPGNRWL RLLQMWREQG

babCYP11B1a   YEHLHLEVHQ TFQELGPIFR YDLGGAGMVC VMLPEDVEKL QQVDSLNPRR MSLEPWVAYR 120
babCYP11B1wt  YEHLHLEVHQ TFQELGPIFR YDLGGAGMVC VMLPEDVEKL QQVDSLNPRR MSLEPWVAYR
bCYP11B1S     YEHLHLEVHQ TFQELGPIFR YDLGGAGMVC VMLPEDVEKL QQVDSLNPRR MSLEPWVAYR
hCYP11B1      YEDLHLEVHQ TFQELGPIFR YDLGGAGMVC VMLPEDVEKL QQVDSLHPHR MSLEPWVAYR
hCYP11B2      YEHLHLEMHQ TFQELGPIFR YNLGGPRMVC VMLPEDVEKL QQVDSLHPCR MILEPWVAIR

babCYP11B1a   QHRGHKCGVF LLNGPEWRFN RLRLNPDVLS PKAVQRFLPM VDAVARDFSQ ALRKKVVQNA 180
babCYP11B1wt  QHRGHKCGVF LLNGPEWRFN RLRLNPDVLS PKAVQRFLPM VDAVARDFSQ ALRKKVLQNA
bCYP11B1S     QHRGHKCGVF LLNEPEWRFN RLRLNPDVLS PKAVQRFLPM VDAVARDFSQ ALRKKVLQNA
hCYP11B1      QHRGHKCGVF LLNGPEWRFN RLRLNPEVLS PNAVQRFLPM VDAVARDFSQ ALKKKVLQNA
hCYP11B2      QHRGHKCGVF LLNGPEWRFN RLRLNPDVLS PKAVQRFLPM VDAVARDFSQ ALRKKVLQNA

babCYP11B1a   RESVTLDIQP SIFHYTIEAS NLALFGERLG LVGHSPSSAS LSFLHALEVM FKSTVQLMFM 240
babCYP11B1wt  RDSVTLDVQP SIFHYTIEAS NLALFGERLG LVGHSPSSAS LSFLHALEVM FKSTVQLMFM
bCYP11B1S     RDSVTLDIQP SIFHYTIEAS NLALFGERLG LVGHSPSSAS LSFLHALEVM FKSTVQLMFM
hCYP11B1      RGSLTLDVQP SIFHYTIEAS NLALFGERLG LVGHSPSSAS LNFLHALEVM FKSTVQLMFM
hCYP11B2      RGSLTLDVQP SIFHYTIEAS NLALFGERLG LVGHSPSSAS LNFLHALEVM FKSTVQLMFM

babCYP11B1a   PRSLSRWTSP KVWKEHFEAW DCIFQYGDNC IQKIYQELAL SRPQQYTSIV AELLLNAELS 300
babCYP11B1wt  PRSLSRWTSP KVWKEHFEAW DCIFQYGDNC IQKIYQELAL SRPQQYTSIV AELLLNAELS
bCYP11B1S     PRSLSRWTSP KVWKEHFEAW DCIFQYGDNC IQKIYQELAL SRPQQYTSIV AELLLNAELS
hCYP11B1      PRSLSRWTSP KVWKEHFEAW DCIFQYGDNC IQKIYQELAF SRPQQYTSIV AELLLNAELS
hCYP11B2      PRSLSRWISP KVWKEHFEAW DCIFQYGDNC IQKIYQELAF NRPQHYTGIV AELLLKAELS

babCYP11B1a   PDAIKANSME LTAGSVDTTV FPLLMTLFEL ARNPNVQQAL RQESLAAAAS ISEHPQKATT 360
babCYP11B1wt  PDAIKANSME LTAGSVDTTV FPLLMTLFEL ARNPNVQQAL RQESLAAAAS ISEHPQKATT
bCYP11B1S     PDAIKANSME LTAGSVDTTV FPLLMTLFEL ARNPNVQQAL RQESLAAAAS ISEHPQKATT
hCYP11B1      PDAIKANSME LTAGSVDTTV FPLLMTLFEL ARNPNVQQAL RQESLAAAAS ISEHPQKATT
hCYP11B2      LEAIKANSME LTAGSVDTTA FPLLMTLFEL ARNPDVQQIL RQESLAAAAS ISEHPQKATT

babCYP11B1a   ELPLLRAALK ETLRLYPVGL FLERVVSSDL VLQNYHIPAG TLVRVFLYSL GRNPALFPRP 420
babCYP11B1wt  ELPLLRAALK ETLRLYPVGL FLERVVSSDL VLQNYHIPAG TLVRVFLYSL GRNPALFPRP
bCYP11B1S     ELPLLRAALK EALRLYPVGL FLERVVSSDL VLQNYHIPAG TLVRVFLYSL GRNPALFPRP
hCYP11B1      ELPLLRAALK ETLRLYPVGL FLERVASSDL VLQNYHIPAG TLVRVFLYSL GRNPALFPRP
hCYP11B2      ELPLLRAALK ETLRLYPVGL FLERVVSSDL VLQNYHIPAG TLVQVFLYSL GRNAALFPRP

babCYP11B1a   ERYNPQRWLD IRGSGRNFYH VPFGFGMRQC LGRRLAEAEM LLLLHHVLKH LQVETLTQED 480
babCYP11B1wt  ERYNPQRWLD IRGSGRNFYH VPFGFGMRQC LGRRLAEAEM LLLLHHVLKH LQVETLTQED
bCYP11B1S     ERYNPQRWLD IRGSGRNFYH VPFGFGMRQC LGRRLAEAEM LLLLHHVLKH LQVETLTQED
hCYP11B1      ERYNPQRWLD IKGSGRNFYH VPFGFGMRQC LGRRLAEVEM LLLLHHVLKH LQVETLTQED
hCYP11B2      ERYNPQRWLD IRGSGRNFHH VPFGFGMRQC LGRRLAEAEM LLLLHHVLKH FLVETLTQED

babCYP11B1a   IKMVYSFILR PSTFPLLTFR AIN                                        503
babCYP11B1wt  IKMVYSFILR PSTFPLLTFR AIN
bCYP11B1S     IKMVYSFILR PSTFPLLTFR AIN
hCYP11B1      IKMVYSFILR PSMCPLLTFR AIN
hCYP11B2      IKMVYSFILR PGTSPLLTFR AIN
```

Amino acid residue differences between Cape baboon CYP11B1a, CYP11B1wt and CYP11B1S and human CYP11B1 and CYP11B2.

POSITION	Bab CYP11B1a	Bab CYP11B1wt	Bab CYP11B1S	Hum CYP11B1	Hum CYP11B2
13	V	V	A	V	A
17	A	A	S	S	C
56	W	W	STOP	W	W
177	V	L	L	V	L
182	E	D	D	G	G
188	I	V	I	V	V
372	T	T	A	T	T

Appendix C

Amino acid sequence alignment of human CYP11B1 and CYP11B2. Differences are indicated by yellow blocks.

```
hCYP11B1      MALRAKAEVC MAVPWLSLQR AQALGTRAAR VPRTVLPFEA MPRRPGNRWL RLLQIWREQG 60
hCYP11B2      MALRAKAEVC VAAPWLCLQR ARALGTRAAR APRTVLPFEA MPQHPGNRWL RLLQMWREQG

hCYP11B1      YEDLHLEVHQ TFQELGPIFR YDLGGAGMVC VMLPEDVEKL QQVDSLHPHR MSLEPWVAYR 120
hCYP11B2      YEHLHLEMHQ TFQELGPIFR YNLGGPRMVC VMLPEDVEKL QQVDSLHPCR MILEPWVAIR

hCYP11B1      QHRGHKCGVF LLNGPEWRFN RLRLNPEVLS PNAVQRFLPM VDAVARDFSQ ALKKKVLQNA 180
hCYP11B2      QHRGHKCGVF LLNGPEWRFN RLRLNPDVLS PKAVQRFLPM VDAVARDFSQ ALRKKVLQNA

hCYP11B1      RGSLTLDVQP SIFHYTIEAS NLALFGERLG LVGHSPSSAS LNFLHALEVM FKSTVQLMFM 240
hCYP11B2      RGSLTLDVQP SIFHYTIEAS NLALFGERLG LVGHSPSSAS LNFLHALEVM FKSTVQLMFM


hCYP11B1      PRSLSRWTSP KVWKEHFEAW DCIFQYGDNC IQKIYQELAF SRPQQYTSIV AELLLNAELS 300
hCYP11B2      PRSLSRWISP KVWKEHFEAW DCIFQYGDNC IQKIYQELAF NRPQHYTGIV AELLLKAELS

hCYP11B1      PDAIKANSME LTAGSVDTTV FPLLMTLFEL ARNPNVQQAL RQESLAAAAS ISEHPQKATT 360
hCYP11B2      LEAIKANSME LTAGSVDTTA FPLLMTLFEL ARNPDVQQIL RQESLAAAAS ISEHPQKATT

hCYP11B1      ELPLLRAALK ETLRLYPVGL FLERVASSDL VLQNYHIPAG TLVRVFLYSL GRNPALFPRP 420
hCYP11B2      ELPLLRAALK ETLRLYPVGL FLERVVSSDL VLQNYHIPAG TLVQVFLYSL GRNAALFPRP

hCYP11B1      ERYNPQRWLD IKGSGRNFYH VPFGFGMRQC LGRRLAEVEM LLLLHHVLKH LQVETLTQED 480
hCYP11B2      ERYNPQRWLD IRGSGRNFHH VPFGFGMRQC LGRRLAEAEM LLLLHHVLKH FLVETLTQED

hCYP11B1      IKMVYSFILR PSMCPLLTFR AIN 503
hCYP11B2      IKMVYSFILR PGTSPLLTFR AIN
```

Amino acid residue differences between human CYP11B1 and CYP11B2.

POSITION	Hum CYP11B1	Hum CYP11B2
11	M	V
13	V	A
17	S	C
22	Q	R
31	V	A
33	R	Q
34	R	H
43	R	Q
44	R	H
55	I	M
56	W	W
63	D	H
68	V	M
82	V	N
86	A	P
87	G	R
109	H	C
112	S	I
119	Y	I
134	G	G
147	E	D
152	N	K
173	K	R
177	V	L
248	T	I
280	F	F
281	S	N
285	Q	H
288	S	G
296	N	K
301	P	L
302	D	E
320	V	A
335	N	D
339	A	I
372	T	T
386	A	V
404	R	Q
414	P	A
432	K	R
439	Y	H
458	V	A
471	L	F
472	Q	L
492	S	G
493	M	T
494	C	S

Appendix D

Baboon CYP11B1 isoform structural alignment with bacterial CYP102 and microsomal CYP2C5.

```
CYP102          TIKEMPQPKT F.GELKNLPL LNTDKPVQAL MKIA.DELGE IFKFEAPGRV TRYLSSQRLI KEACD.ES..
CYP2C5          .GKLPPGPTP F.PIIGNILQ IDAKDISKSL TKFS.ECYGP VFTVYLGMKP TVVLHGYEAV KEALV.DL..
CYP11B1a        ....PRRPGN RWLRLLQIWR EQGYEHLHLE VHQTFQELGP IFRYDLGGAG MVCVMLPEDV EKLQQVDSLN
CYP11Bwt        ....PRRPGN RWLRLLQIWR EQGYEHLHLE VHQTFQELGP IFRYDLGGAG MVCVMLPEDV EKLQQVDSLN
                                          A Helix       β1-1     β1-2   B Helix

CYP102          ..RFDKNLSQ ALKFVRDFA. GDGLFTSWTH EKNWKKAHNI LLPSF....S QQAMK.GYHA MMVDIAVQLV
CYP2C5          GEEFAGRGSV PI..LEKVSK GLGIAFSN.. AKTWKEMRRF SLMTLR..NF GMGKR.SIED RIQEEARCLV
CYP11B1a        PRRMSLEPWV AYRQHRGHKC GVFLL....N GPEWRFNRLR LNPDVLSPKA VQRFLPMVDA VARDFSQALR
CYP11B1wt       PRRMSLEPWV AYRQHRGHKC GVFLL....N GPEWRFNRLR LNPDVLSPKA VQRFLPMVDA VARDFSQALR
                   β1-5     B' Helix                C Helix                        D Helix

CYP102          QKWERL.NAD EHIEVPEDMT RLTLDTIGLC GFNYRFNSFY RDQ..PHPFI TSMVRALDEA MNK.LQRANP
CYP2C5          EELRKT.NAS .PCDPTFILG CAPCNVICSV IFHNRFD..Y KDE.EFLKLM ESLHENVELL GTPWLQVYNN
CYP11B1a        KKVVQNAREŠ VTLDIQPSIF HYTIEASNLA LFGERLGLVG HSPSSASLSF LHALEVMFKS TVQLMFMPRS
CYP11B1wt       KKVLQNARDS VTLDVQPSIF HYTIEASNLA LFGERLGLVG HSPSSASLSF LHALEVMFKS TVQLMFMPRS
              D Helix               E Helix                          F Helix

CYP102          DD....PAYD ENKRQFQEDI KVMNDLVDKI IADRKAS... GEQS..DDLL THMLNGKDPE TGEPLDDENI
CYP2C5          F....PALLD YFPGIHKTLL KNADYIKNFI MEKVKEHQKL LDVNNPRDFI DCFLIKMEQE NNLEFTLESL
CYP11B1a        LSRWTSPKVW KEHFEAWDCI FQYGDNCIQK IYQELALSR. PQQY.TSIVA ELLLNAEL.. .....SPDAI
CYP11B1wt       LSRWTSPKVW KEHFEAWDCI FQYGDNCIQK IYQELALSR. PQQY.TSIVA ELLLNAEL.. .....SPDAI
                              G Helix                          H Helix           I Helix

CYP102          RYQIITFLIA GHETTSGLLS FALYFLVKNP HVLQKAAEEA ARV.LVDPVP SYKQVK.QLK YVGMVLNEAL
CYP2C5          VIAVSDLFGA GTETTSTTLR YSLLLLLKHP EVAARVQEEI ERV.IGRHRS PCMQDRSRMP YTDAVIHEIQ
CYP11B1a        KANSMELTAG SVDTTVFPLL MTLFELARNP NVQQALRQES LAAAASISEH PQKATTEL.P LLRAALKETL
CYP11B1wt       KANSMELTAG SVDTTVFPLL MTLFELARNP NVQQALRQES LAAAASISEH PQKATTEL.P LLRAALKETL
                        I Helix                 J Helix          J' Helix     K Helix

CYP102          RLWPTAPA.F SRYAKEDTVL GGEYPLEKGD ELMVLIPQLH RDKTIWGDDV EEFRPERF.. ENPSAIP...
CYP2C5          RFIDLLPTNL PHAVTRDVRF RNYFIPKGTD IITSLTSVLH DEKAFPNPKV FDPGHFLDES GNFKKSDYFM
CYP11B1a        RLYPVGLFLE RVVSSDLVLQ NYHIPAGTLV RVFLYSLGRN PALFPRPERY NPQRWLDIRG KSGRNFYHVP
CYP11B1wt       RLYPVGLFLE RVVSSDLVLQ NYHIPAGTLV RVFLYSLGRN PALFPRPERY NPQRWLDIRG KSGRNFYHVP
              K Helix    β1-4   β2-1     β2-2  β1-3    K' Helix       Meander

CYP102          .QHFFKPFGN GQRACIGQQF ALHEATLVLG MMLKHFDF.. .EDHTNYELD IKET...LTL KPE.GFVVKA
CYP2C5          PFSAGKRMCV GEGLAEMLFL FLTSILQNFK LQSLVEPKDL DITAVVNGFV S...VPPSYQ LCFIPI....
CYP11B1a        FGFGMRQCLG RRLAEAEMLL LLHHVLKHLQ VETLTQEDIK MVYSFILRPS TFPLLTFRAI N.........
CYP11B1wt       FGFGMRQCLG RRLAEAEMLL LLHHVLKHLQ VETLTQEDIK MVYSFILRPS TFPLLTFRAI N.........
                                  L Helix       β3-3             β4-2      β4-2 β3-2

CYP102          KSKKIPLGGI PSPST
CYP2C5          .......... .....
CYP11B1a        .......... .....
CYP11B1wt       .......... .....
              β3-2
```

MARCEL DEKKER, INC. • 270 MADISON AVENUE • NEW YORK, NY 10016

ENDOCRINE RESEARCH
Vol. 28, No. 4, pp. 477–484, 2002

BABOON CYP11B1: THE LOCALIZATION AND CATALYTIC ACTIVITY IN BABOON ADRENAL TISSUE

N. Brown,[1] P. Swart,[1] G. Fenhalls,[2] L. Stevens,[2] N. W. Kolar,[1] and A. C. Swart[1,*]

[1]Dept. of Biochemistry, University of Stellenbosch, Stellenbosch 7602, South Africa
[2]Dept. of Medical Biochemistry, University of Stellenbosch, Tygerberg, South Africa

ABSTRACT

A third gene encoding baboon CYP11B1 was isolated and was shown to catalyze only the metabolism of deoxycorticosterone (DOC) to corticosterone. The investigation into the localization of CYP11B1 in the baboon adrenal tissue, using in situ hybridization, showed that mRNA transcripts were predominantly present in the zona reticularis (ZR) and zona fasciculata (ZF). Signal was also observed in the zona glomerulosa (ZG) and scattered within the medulla. Immunohistochemical studies, using rabbit anti-sheep CYP11B1 IgG, indicated that CYP11B1 was expressed only in the zona fasciculata, zona reticularis and in the medulla. CYP11B1 was not detected in the zona glomerulosa. Subsequent Western Blot investigations into the presence of CYP11B1 in baboon adrenal cortex and medullary homogenates indicated CYP11B1 as a single band in the cortex and as two distinct bands in the medulla. CYP11A was present only in the baboon adrenal cortex. The metabolism of deoxycorticosterone and corticosterone was subsequently investigated in the baboon adrenal cortex and medulla. In cortex homogenates, deoxycorticosterone was converted to corticosterone, and neither 18-hydroxycorticosterone nor aldosterone was detected. In medulla homogenates, however, corticosterone was metabolized to aldosterone, as confirmed by APcI-MS.

*Corresponding author: E-mail: acswart@sun.ac.za

DOI: 10.1081/ERC-120016826 0743-5800 (Print); 1532-4206 (Online)

MARCEL DEKKER, INC. • 270 MADISON AVENUE • NEW YORK, NY 10016

INTRODUCTION

Significant differences exist between species in the number of genes that encode the CYP11B-related enzymes involved in the terminal steps of glucocorticoid and mineralocorticoid synthesis. In some species i.e., humans, rats, mice, and hamsters, two isoforms of CYP11B, CYP11B1, and CYP11B2, are present which catalyse glucocorticoid and mineralocorticoid synthesis, respectively. In other species a single enzyme catalyzes the formation of both glucocorticoids and mineralocorticoids. In cattle, pig, sheep, and bullfrogs these corticoids are produced via a single enzyme catalyzing the 11β-hydroxylation, 18-hydroxylation, and 18-oxidation of 11-deoxycorticosterone (DOC) to aldosterone.[1] In humans CYP11B1 catalyses the 11β-hydroxylation of DOC and 11-deoxycortisol yielding corticosterone and cortisol, respectively. CYP11B2 catalyses the consecutive 11β-hydroxylation, 18-hydroxylation, and 18-oxidation of DOC to aldosterone.[2] CYP11B isozyme activities are zone-specific i.e., the CYP11B2 activity is restricted to the zona glomerulosa (ZG) of the adrenal cortex and CYP11B1 activity to the zona fasciculata (ZF) and zona reticularis (ZR).[3]

Three genes encoding baboon CYP11B1 were cloned from adrenal cortex using RT-PCR and expressed in COS1 cells. The catalytic activity was investigated using both DOC and corticosterone as substrates. The presence of baboon CYP11B1 mRNA transcripts in the adrenal gland was determined using baboon specific DIG-labelled riboprobes. Immunohistochemistry was carried out using rabbit anti-sheep CYP11B1 IgG to determine the intracellular localisation of baboon CYP11B1 at protein level. The localization of CYP11B1 was subsequently investigated in baboon adrenal medulla and cortex tissue homogenates using Western blot analysis. The catalytic activity of baboon CYP11B1 was investigated in these adrenal homogenates. The conversion of DOC and corticosterone was assayed and the products formed were analysed by TLC, HPLC and atmospheric pressure chemical ionisation mass spectrometry (APcI-MS).

MATERIALS AND METHODS

Functional Expression of Baboon CYP11B1 cDNA in COS1 Cells

Baboon mRNA was isolated from baboon adrenal cortex and the cDNA amplified by RT-PCR as previously described.[4] In addition to two CYP11B1 genes previously cloned (babc11 and babc11S), a third gene encoding baboon CYP11B1, babc11a, was identified. The recombinant cDNA (5 μg/mL) was expressed in COS1 cells and co-transfected with human pCD-ADX (5 μg/mL) using the DEAE-Dextran method as previously published.[4] Enzyme activity was determined by following DOC metabolism, using [^{3}H]DOC (Amersham, Bucks, UK) as tracer. The products formed were analysed by TLC (CH_2Cl_2/MeOH,

98 : 2). Studies comparing the activity of the expressed gene with previously isolated genes, babc11S and babc11, were also conducted.

In Situ Hybridization and Immunolocalization

In situ hybridization was performed to determine mRNA localization in baboon adrenal tissue as described.[5] Digoxigenin-UTP labelled RNA probes were synthesized using baboon CYP11B1 cDNA template and confirmed by Northern blot analysis. Immunohistochemistry was subsequently carried out as described.[5] Non-specific proteins were blocked using donkey anti-rabbit IgG. Tissue sections were probed with rabbit anti-sheep P450 CYP11B1 IgG (1 : 200). The slides were viewed and the images were captured using a Zeiss light microscope (Axioskop 2) fitted with a Sony 3CCV video camera.

Western Blot

Baboon adrenal cortex and medulla tissue were homogenized separately in 0.25 M sucrose buffer, 1% BSA, subjected to SDS-PAGE (12.5%), 20 μg protein per lane, and transferred onto a nitrocellulose membrane. Western blot analysis was carried out using rabbit anti-sheep CYP11B1 (1 : 1000) and CYP11A (1 : 1000) IgG. Immunoreacting proteins were detected using SuperSignal® West Pico Chemiluminescent Substrate (Pierce Chemical Company, Rockford, USA), according to manufacturer's instructions.

Determination of CYP11B1 Activity in Baboon Adrenal Homogenates

The metabolism of DOC and corticosterone was assayed in adrenal cortex and medulla tissue homogenates as previously described.[6] Tissue homogenates (160 μg protein) were preincubated with steroid substrate (10 μM) in a total volume of 500 μL for 5 min at 37°C. The reaction mixture contained the following: isocitrate (420 nmol), isocitrate dehydrogenase (0.398 U), $MgCl_2$ (0.44 mmol), and 50 mM *Tris*-HCl, pH 7.4 (containing 1% BSA and 50 mM NaCl). The reaction was initiated by the addition of NADPH (0.44 mmol). Aliquots (50 μL) of the reaction mixture were removed prior to the addition of NADPH and subsequently at 10 min intervals. Steroids were extracted with dichloromethane, dried and redissolved in methanol. HPLC analysis was performed on a Waters (Milford, MA) high performance liquid chromatograph coupled to a WISP™ automatic injector (Waters). Metabolites were separated on a Novapak® C_{18} column at a flow rate of 1 mL/min. The mobile phase consisted of solvent A (water) and solvent B (100% methanol). Steroids were eluted using a linear gradient from 100% A to 100% B in 40 min.

MARCEL DEKKER, INC. • 270 MADISON AVENUE • NEW YORK, NY 10016

RESULTS AND DISCUSSION

CYP11B1 Activity in COS1 Cells Transfected with Baboon CYP11B1 cDNA

Baboon CYP11B1 was expressed in COS1 cells and incubated with DOC (1 μM). After 16 hours babc11a converted 30% of the DOC to corticosterone, with negligible amounts of 18-hydroxycorticosterone and aldosterone being synthesized, indicating that the gene encodes CYP11B1 and has little or no aldosterone synthase activity. Studies were conducted comparing the activity of babc11 and babc11S (previously isolated) to babc11a. Babc11S contained a termination codon in exon one resulting from the nucleotide change at 168 A/G and babc11 exhibited only 11β-hydroxylase activity towards DOC. Babc11 and babc11a differed in exon three with three amino acid substitutions viz Val/Leu, Glu/Asp, and Ile/Val respectively, lying in the predicted E-helix. Babc11 and babc11a showed a marked difference in catalytic activity towards DOC (Fig. 1). Both genes metabolized only DOC and exhibited no aldosterone synthase activity suggesting that both isoforms (CYP11B1 and CYP11B2) could occur in the Cape baboon.

In Situ- and Immunolocalization of Baboon CYP11B1

The intracellular localization of baboon CYP11B1 in the adrenal tissue was investigated using DIG-labelled riboprobes. mRNA transcripts were present in the nuclei of the ZG, ZF, and ZR cells and in the medullary cell nuclei [Fig. 2A(i) and (iii)]. However, CYP11B1 was not detected in the ZG with rabbit anti-sheep

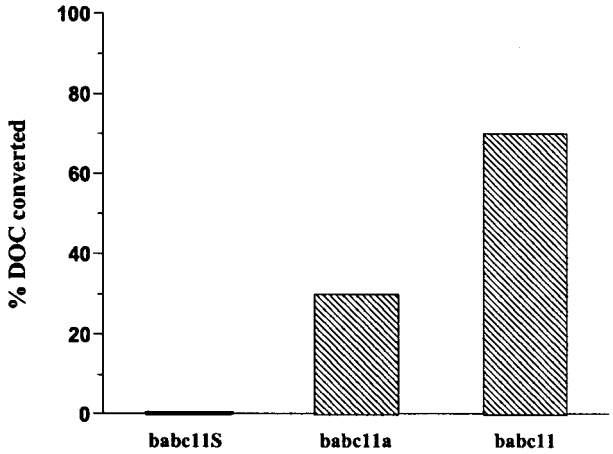

Figure 1. Metabolism of DOC (1 μM) by baboon CYP11B1: babc11S, gene containing a termination codon in exon one; babc11a showing 30% metabolism of DOC, and babc11 showing 70% metabolism of DOC.

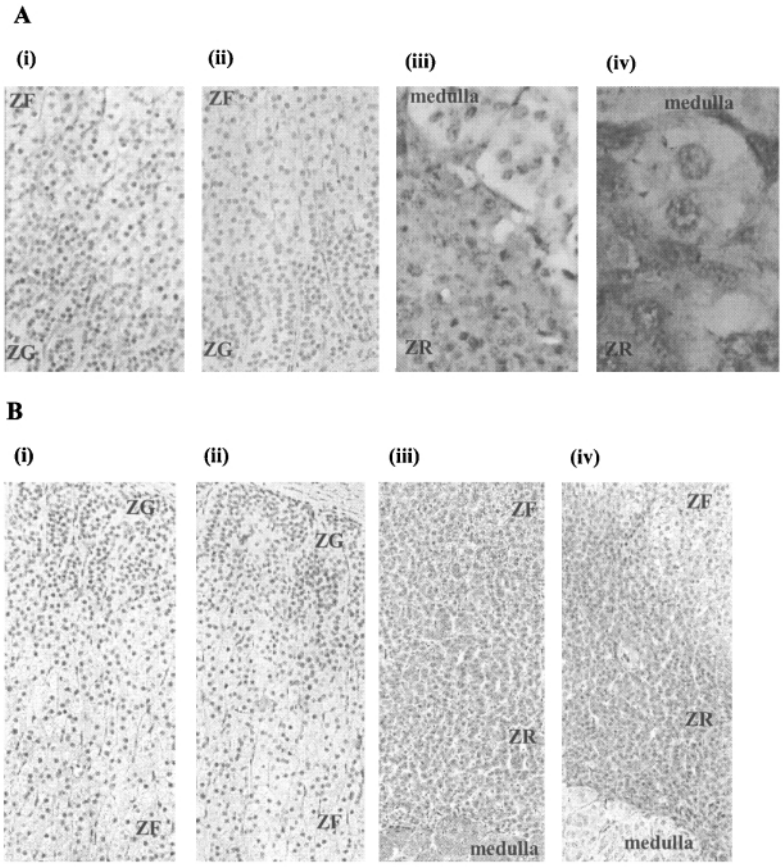

Figure 2. A: Localization of CYP11B1 by in situ hybridization. The presence of mRNA transcripts is determined by a positive color reaction indicated by the brown color in (i) the ZG and the ZF and in (iii) ZR and in cell nuclei in the medulla. No signal was obtained with the sense probe in (ii) the ZG and the ZF and in (iv) the ZR and medulla. Magnification: (i) and (iii): 200×; (ii): 400×; (iv): 1000×. B: Immunolocalization of CYP11B1 using rabbit anti-sheep CYP11B1 IgG: (i) and (iii) brown color shows the presence of CYP11B1 in the ZF, ZR and medulla. No staining was observed in the ZG; (ii) and (iv) no signal was obtained using donkey anti-rabbit IgG. Magnification: (i)–(iv): 200×. (for color photos please see http://www.sun.ac.za/biochem/swart/CYP11B1Loc).

CYP11B1 IgG, as shown in Fig. 2B(i). CYP11B1 was detected in the ZF/ZR and in cells in the medulla, Fig. 2B(iii). The signal obtained with the mRNA probe in the ZG could be attributed to sequence similarity between baboon CYP11B1 and CYP11B2. The presence of CYP11B1 in the medulla has been reported by others[7,8] In humans adrenal cortical and medullary cells are closely interwoven and CYP11B1 mRNA transcripts have been detected in the medulla of the human adrenal gland as hybridization signals were detected in clusters of cortical cells lying within the medulla.

MARCEL DEKKER, INC. • 270 MADISON AVENUE • NEW YORK, NY 10016

Western Blot Analyses

The localization of CYP11B1 and CYP11A was subsequently investigated in baboon adrenal medulla and cortex tissue homogenates using Western blot analysis. A single protein band corresponding to a Mr of approximately 50 kDa was identified in the adrenal cortex homogenate using a rabbit anti-sheep CYP11B1 antibody (Fig. 3). A band indicating a protein of similar mass was identified in the medullary homogenate as well as a second smaller protein band, corresponding to a Mr of approximately 48 kDa. Protein bands indicating the presence of CYP11A were detected in the cortex homogenate only, suggesting that the cells in the medulla synthesizing CYP11B1 do not synthesize CYP11A.

CYP11B1 Activity in Baboon Adrenal Homogenates

The metabolism of DOC and corticosterone was assayed in the baboon adrenal cortex and medulla homogenates, respectively. HPLC analyses (Fig. 4) showed that in the cortex DOC was metabolized to corticosterone only. No 18-hydroxycorticosterone or aldosterone was detected. In addition, no aldosterone was detected when corticosterone metabolism was assayed in the cortex. Analyses of the metabolic conversion of DOC in the medulla showed negligible amounts of corticosterone being formed. However, corticosterone metabolism in the medulla yielded 18-hydroxycorticosterone and aldosterone metabolites. The presence of aldosterone was confirmed by APcI-MS.

In this study we demonstrated the existence of two genes encoding CYP11B1 in the Cape Baboon. Two functional genes were isolated from baboon adrenal

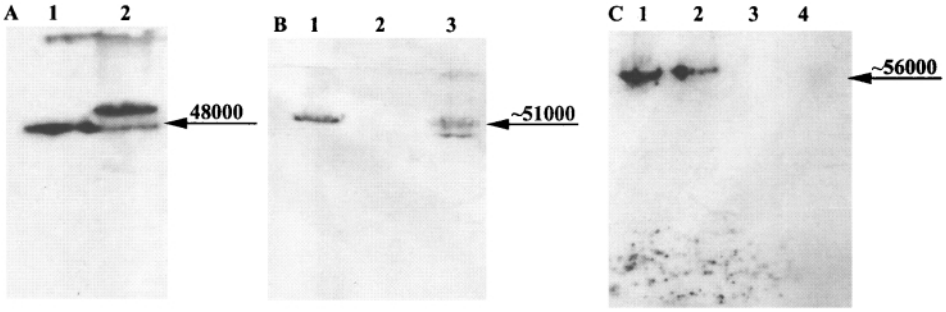

Figure 3. Immunoblot of baboon adrenal cortex, adrenal medulla homogenate and testes microsomes with rabbit anti-sheep CYP11B1 IgG. Tissue homogenates and testes microsomes (20 μg protein/lane) were separated on 12.5% SDS-PAGE. Proteins were detected using: CYP11B1 IgG. A: Lane 1, purified sheep CYP11B1 (48 kDa); and lane 2, medulla homogenate (48 kDa and ~50 kDa); B: Lane 1, cortex homogenate; lane 2, testes microsomes; and lane 3, medulla homogenate; C: Lane 1, purified sheep CYP11A (56 kD); lane 2, cortex homogenate; lane 3, medulla homogenate; and lane 4, testes microsomes.

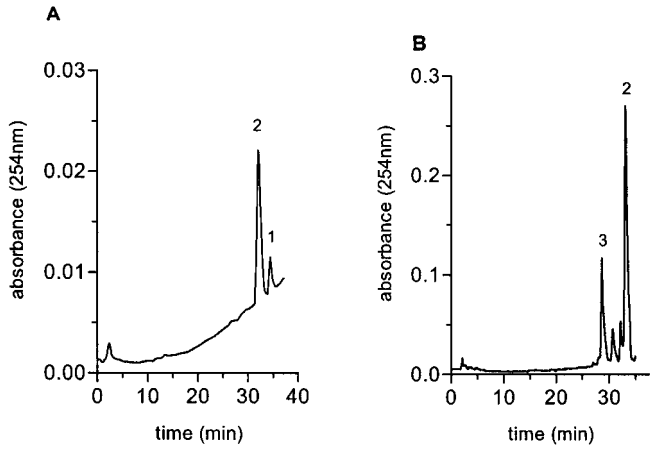

Figure 4. A: HPLC analysis of products of DOC (10 μM) metabolism in the baboon adrenal cortex at 40 min. Peaks on the chromatogram are 1, DOC (34.5 min); and 2, corticosterone (32 min). B: HPLC analysis of products of corticosterone (10 μM) metabolism in the baboon adrenal medulla. Peaks on the chromatogram are 2, corticosterone (32.4 min); and 3, aldosterone (28.5 min).

cortex and the recombinant cDNAs were expressed in COS 1 cells. Both catalyzed the formation of corticosterone when the cells were incubated with DOC. Negligible amounts of 18-hydroxycorticosterone and aldosterone were detected. The expressed CYP11B1 did not catalyze the conversion of corticosterone to aldosterone. CYP11B1 was localized in the ZF and ZR and in cells in the medulla of baboon adrenal. A single protein fraction, with an apparent molecular mass of ~50 kDa, was identified in the cortex using rabbit anti-sheep CYP11B1 IgG and it would seem that this isoform catalyzes only the metabolism of DOC to corticosterone with no detectable 18-hydroxycorticosterone and aldosterone being formed. It is possible that CYP11B2 is present in the cortex but that protein levels and catalytic activity were too low to be detected. Two protein fractions were identified in the medulla using the same CYP11B1 antibody—a protein of similar mass and a second protein with an apparent molecular mass of ~48 kDa. These proteins catalyzed the hydroxylation and oxidation of corticosterone to aldosterone, the conversion of DOC to corticosterone being negligible. These results suggest the possible existence of the two isoforms, CYP11B1 and CYP11B2, in the Cape Baboon.

ACKNOWLEDGMENTS

The authors wish to thank the NRF,d the University of Stellenbosch for financial support and Mr. M. J. van der Merwe for APcl-MS analyses.

REFERENCES

1. Ohnishi, T.; Wada, A.; Lauber, M.; Yamano, T.; Okamoto, M. Aldosterone Biosynthesis in Mitochondria of Isolated Zones of Adrenal Cortex. J. Steroid. Biochem. **1988**, *31*, 73–81.
2. Erdmann, B.; Gerst, H.; Bulow, H.E.; Lenz, D.; Bahr, V.; Bernhardt, R. Zone-Specific Localization of Cytochrome P45011B1 in Human Adrenal Tissue by PCR-Derived Riboprobes. Histochem. Cell Biol. **1995**, *104*, 301–307.
3. Pascoe, L.; Jeunemaitre, X.; Lebrethon, M.C. Glucocorticoid-Suppressible Hyperaldosteronism and Adrenal Tumors Occurring in a Single French Pedigree. J. Clin. Invest. **1995**, *96*, 2236–2246.
4. Swart, A.C.; Brown, N.; Kolar, N.; Swart, P. Baboon Cytochrome P450c11 is Encoded by More Than One Gene. Endocrine Res. **2000**, *26* (4), 1011–1018.
5. Fenhalls, G.; Wong, A.; Bezuidenhout, J.; Van Helden, P.; Bardin, P.; Lukey, P.T. In Situ Production of Gamma Interferon, Interleukin-4, and Tumor Necrosis Factor Alpha mRNA in Human Lung Tuberculous Granulomas. Infection and Immunity **2000**, *68*, 2827–2836.
6. Swart, P.; Engelbrecht, Y.; Bellstedt, D.U.; De Villiers, C.A.; Dreesbeimdieke, C. The Effect of Cytochrome b5 on Progesterone Metabolism in the Ovine Adrenal. Endocrine Res. **1995**, *21* (1&2), 297–306.
7. MacKenzie, S.M.; Clark, C.J.; Fraser, R.; Gómez-Sanchez, C.E.; Connell, J.M.C.; Davies, E. Expression of 11β-Hydroxylase and Aldosterone Synthase Genes in the Rat Brain. J. Mol. Endocr. **2000**, *24*, 321–328.
8. Erdman, B.; Denner, K.; Gerst, H.; Lenz, D.; Bernhardt, R. Localisation by In Situ Hybridisation and Functional Expression in Cell Cultures. Endocrine Res. **1995**, *21*, 425–435.